Charge of water droplets in non-polar oils

Schoeler, Andreas Martin

Awarding institution:
King's College London

KING'S College LONDON

Charge of water droplets in non-polar oils

by
Andreas Martin Schoeler

A thesis submitted in partial fulfilment of the requirements for the degree of Doctor of Philosophy in Mechanical Engineering

to

King's College London
University of London
School of Natural & Mathematical Sciences
Department of Physics
Experimental Biophysics & Nanotechnology Research Group

01.01.2015

I confirm that the following thesis does not exceed the word limit prescribed in the College regulations. I further confirm that the work presented in the thesis is my own and all references are cited accordingly. The copyright of this thesis rests with the author and no quotation from it or information derived from it may be published without proper acknowledgement.

Acknowledgments

This thesis would not have been possible without the help and guidance from a number of individuals or the financial support from the Engineering and Physical Sciences Research Council (EPSRC) through a DTA studentship (EPSRC 2009 DTA – Grant Ref: EP/P504961/1).

My immense gratitude must go to both my supervisors, Dr. Patrick Mesquida and Dr. Shahriar Sajjadi. Without their guidance, support and encouragement when needed, I don't think I would have been able to come this far. I value the time you have invested in me, whether it would be reading my work or being available for discussions.

Of course none of the experimental work would have been possible, were it not for Julian Greenberg and Jim Trotter and their ability to make any experimental problem or shortage of lab supplies disappear.

I also doubt I would have ever started a PhD were it not for the care, reassurance and safety offered to me by my family, especially from my parents.

I often wonder if I could have made it to this stage were it not for the distractions in the name of science offered to me by Dimitris and Greg. Many late nights were spent working in the lab investigating the possibilities ultrasonic probes or high speed cameras. I strongly believe that everything that we discovered furthered my work in one way or another.

I also must not forget to thank my colleagues in the ECLAT office: Angela, Ankur, Hugo, Joao, Neil and Vahid. Were it not for you, I don't think I would have enjoyed coming to the office as much as I did, nor would I have ever been able to gain such

great understanding of Portuguese politics. I also valued our collaborative scientific discussions and Joao, the Truth, Bimbo's guidance with regards to Matlab.

No PhD can ever be written without the support from your friends. The gang has provided me with much needed distractions and was able to pick me up when I was feeling discouraged.

Last, but in no way least, I want to thank my beloved wife, Tish. In truth I would not be where I am today were it not for your love, affection, your delicious kitchen treats and your ever so subtle reminders that I should be doing some work.

Abstract

Water-in-oil microdroplets are an attractive “tool” in lab-on-a-chip devices, as they offer simple compartmentalisation, constitute tiny reaction chambers and can be used to perform “digital” operations. One of the many benefits they offer is the ability to manipulate droplets by electric fields, which can be implemented on-chip, using electrodes and suitable wiring. Water droplets dispersed in a non-polar oil are manipulated by exploiting the fundamental phenomenon of electrophoretic motion, i.e. motion in response to an external, electric field.

There are surprisingly little data regarding the electrophoretic mobility of water droplets dispersed in a non-polar oil and this work aims to elucidate some of the properties of droplet charge from measurements of the electrophoretic mobility of individual water droplets in two different, non-polar oils of similar, physical fluid properties: silicone and paraffin oil.

Single droplets of varying pH and ion concentrations were investigated and it was found that the effective initial droplet charge (i.e. the charge a water droplet has before making contact with a biased electrode) is always positive and independent of pH and ion concentration. When the anionic surfactant SDS (Sodium Dodecyl Sulfate) was dispersed in the water phase, the initial droplet charge could be altered from positive to negative at concentrations greater than 1 g/l. However, using cationic surfactant CTAB (Hexadecyltrimethyl Ammonium Bromide) had no impact on droplet surface charge. Once the droplet touches a biased electrode, the droplet charge in increased by a factor of 10 and any surfactant charge effects are overridden.

Lastly, complex oil-in-water-in-oil and water-in-oil-in-water-in-oil droplets were created and their electrophoretic mobility was studied. It was found that the inner

droplet does not affect electrophoretic motion of the core shell drop, regardless of size and composition, nor does it experience the same (if any) electric field strength the outer water shell is subjected to. This is advantageous in a variety of applications. For example, oil droplets of varying types and sizes could accurately be transported and manipulated at the same speed using monodisperse water shells, which can be either thick or ultrathin. This could also be used for the manipulation of materials that would otherwise be damaged by an electrical field.

Zusammenfassung

Wasser in Öl Mikrotropfen sind ein attraktives "Werkzeug" für Lab on a Chip Geräte, da sie zur Kompartimentierung dienen, als winzige Reaktionskammern verwendet werden können und weil man mit ihnen "digitale" Operationen durchzuführen kann. Einer der vielen Vorteile ist die Fähigkeit, Tropfen durch elektrische Felder manipulieren zu können, in dem man Elektroden auf einem Chip implementiert. Wassertropfen werden durch das Phänomen der elektrophoretischen Bewegung, also eine Bewegung in Reaktion auf ein externes, elektrisches Feld, in einem nicht-polaren Öl, bewegt.

Es ist überraschend wie wenig Daten zur der elektrophoretischen Mobilität von Wassertropfen in einem nicht-polaren Öl momentan in der Literatur zu finden sind. Ziel dieser Arbeit ist einige der Eigenschaften der Tropfenladung zu untersuchen, in dem man die elektrophoretische Mobilität der einzelnen Wassertropfen, die in zwei ähnliche, nicht-polare Öle (Silikon und Paraffinöl) gespritzt werden, misst.

Einzelne Tröpfchen mit unterschiedlichem pH-Wert und Ionenkonzentrationen wurden untersucht und es wurde festgestellt, dass die effektive Tropfenladung (d.h. die Ladung eines Wassertropfens, bevor er in Kontakt mit einer geladenen Elektrode kommt) ist immer positiv und unabhängig vom pH-Wert und Ionenkonzentration. Wenn das anionische Tensid SDS (Natriumdodecylsulfat) in der Wasserphase aufgelöst wird, dann verändert sich die Tropfenladung, vor dem Kontakt mit einer Elektrode, bei einer Konzentration von mehr als 1 g/l, von positiv zu negativ. Das kationische Tensid CTAB (Hexadecyltrimethylammoniumbromid) hatte dagegen keinen Einfluss auf die Tropfenoberfläche. Sobald der Tropfen eine geladene Elektrode berührt, erhöht sich die

Tropfenladung um einen Faktor von 10 und jegliche Tensidladungseffekte werden außer Kraft gesetzt.

Zuletzt wurden komplexe Öl in Wasser in Öl und Wasser in Öl in Wasser in Öl Tropfen hergestellt und ihre elektrophoretische Beweglichkeit untersucht. Es wurde festgestellt, dass die inneren Tropfen keinen Einfluss auf die elektrophoretische Bewegung der Kern-Schale Tropfen (Core-Shell droplets) haben, unabhängig von ihrer Größe oder Zusammensetzung. Ausserdem erfährt der innere Kerntropfen nicht die gleiche, elektrische Feldstärke (wenn überhaupt) wie der äußere Schalen-Wassertropfen. Dies ist in einer Vielzahl von Anwendungen von Vorteil. Beispielsweise können Öltropfen unterschiedlicher Art und Größe mit der gleichen Geschwindigkeit transportiert werden, indem man sie durch monodisperse Wasserschalen (entweder dick oder sehr dünn) extrem genau manipuliert. Dies könnte auch für die Handhabung von Materialien, die ansonsten von einem elektrischen Feld beschädigt werden, verwenden werden.

Contents

List of Figures xi

List of Tables xiii

Nomenclature xiv

Chapter 1 Motivation and Background 1
1.1 Motivation for the thesis 1
1.2 Background 5
1.2.1 Emulsions 5
1.2.1.1 Types of Emulsification 9
1.2.2 Electrokinetics 10
1.2.2.1 Electrical Double Layer 11
1.2.2.2 Zeta Potential 14
1.2.2.3 Electrowetting 14
1.2.2.4 Types of Electrokinetics 15
1.2.2.5 Electrokinetic Applications 17
1.3 Water Droplet Electrophoresis 21
1.4 Summary 25
1.5 References 26
Chapter 2 Methodology 32
2.1 Chapter Abstract 32
2.2 Multiple Droplet Electrophoresis 32
2.2.1 Multiple Droplet Electrophoresis – Experimental Set-Up 36
2.2.2 Effects of Ultrasonic Amplitude on Droplet Size 37
2.2.3 Additional Experimental Complications 40
2.2.4 Multiple Droplet Electrophoresis – Conclusion 41
2.3 Single Droplet Electrophoresis 42
2.3.1 Experimental Apparatus 43
2.3.2 General Measurement Principle 45
2.3.3 Wall Effect and Slip Correction 46
2.3.4 Determination of Drag Correction Function C(R) 48
2.4 Estimation of Droplet Deformation 52
2.5 Droplet Tracking (Matlab) 53
2.6 Charge v. Applied voltage 56
2.6.1 Impact of electric field on oil viscosity 57
2.6.2 Solder Flux Complications 58
2.7 References 60

Chapter 3 Charge of Water Droplets in Non-Polar Oils 64
3.1 Chapter Abstract 64
3.2 Introduction 64
3.3 Experimental Set-Up 66
3.4 Results 67
3.4.1 Electrophoretic experiments: General droplet behaviour 67
3.4.2 Influence of Ions on Droplet Charge 69
3.4.3 Influence of Chaotropic Agent 71
3.4.4 Molecular dynamics simulations 72
3.5 Discussion 78
3.5.1 The native charge 78
3.6 Conclusion 80
3.7 References 82
Chapter 4 Controlling the surface charge of water droplets in non-polar oils 85
4.1 Chapter Abstract 85
4.2 Introduction 85
4.3 Experimental Set-Up 86
4.4 Results and discussion 87
4.4.1 Influence of surfactants on the initial charge of droplets 90
4.4.2 Effect of direct, physical contact-charging of droplets 93
4.5 Conclusion 94
4.6 References 96
Chapter 5 Electrophoretic Manipulation of multiple emulsion droplets 98
5.1 Chapter Abstract 98
5.2 Introduction 98
5.3 Experimental Set-Up 99
5.4 Results 100
5.4.1 General Behaviour of (O/W)/O Droplets 100
5.4.2 Influence of the Oil Core Size of (O/W)/O Droplets on the Electrophoretic Mobility 102
5.4.3 Deflection of the Oil Core against the Direction of Motion in Electrostatic Fields 105
5.4.4 Droplet deformation 107
5.4.5 More complex (W/O/W)/O droplets 108
5.5 Discussion 109
5.6 Conclusion 110
5.7 References 112
Chapter 6 Conclusions, Limitations and Future Work 114
6.1 References 119

Chapter 7 List of publications arisen from this thesis 121
Chapter 8 Fluid Properties 122
Chapter 9 Appendix 123
9.1 Appendix A 123
9.2 Appendix B 136
9.3 Appendix C 138
9.4 Appendix D 141
9.5 Appendix E 142

List of Figures

Figure 1.1 Schematic representation of long-range structuring of water molecules at the oil-water interface. 2
Figure 1.2 Examples of a polydisperse (a) and monodisperse (b) emulsion. 5
Figure 1.3 Different methods of stabilising a water (blue circles) in oil (orange) emulsion. 8
Figure 1.4 Schematic of a T-Junction microchannel emulsification device 10
Figure 1.5 Schematic of an electrical double layer and zeta potential. 13
Figure 1.6 Schematic of the principle of electrowetting on dielectrics 15
Figure 1.7 Schematic of electroosmotic flow. 16
Figure 1.8 Schematic illustration of electrophoretic motion of a particle 16
Figure 1.9 The four typical types of free-flow electrophoresis 18
Figure 1.10 EDL process principle 20
Figure 2.1 Ultrasonic emulsion creation 33
Figure 2.2 Two-step droplet formation 34
Figure 2.3 Schematic image of the multiple droplet electrophoretic cell design 35
Figure 2.4 Example of 1% water dispersed in FC-77 36
Figure 2.5 1% water in n-heptane without surfactant 38
Figure 2.6 Average droplet diameter versus viscosity ratio 39
Figure 2.7 Two droplets of opposite charge coalescing 41
Figure 2.8 Block Diagram of a typical SDE experimental set up 43
Figure 2.9 a) Vertical set-up for electrophoretic measurements 44
Figure 2.10 Horizontal set-up for drag force calibration 49
Figure 2.11 Dependence of terminal velocity, v_g, on droplet radius 51
Figure 2.12 Matlab graphical user interface 55
Figure 2.13 Dependence of initial water droplet charge on applied voltage 56
Figure 2.14 a) Solder (dark grey schlieren, highlighted lines) dissolving in Paraffin 59
Figure 3.1 Experimental set-up for electrophoretic experiments 66
Figure 3.2 Dependence of native droplet charge on oil type 67
Figure 3.3 Influence of KCl concentration on droplet surface charge density 70
Figure 3.4 Influence of pH on droplet surface charge density 71
Figure 3.5 Influence of Urea concentration on droplet surface charge density 72
Figure 3.6 Cumulative surface charge density 74

Figure 3.7 Probability that a water molecule is oriented 77
Figure 4.1 Experimental set-up for electrophoretic measurements 87
Figure 4.2 Magnitudes of surface charge density after a droplet is charged on a biased electrode 89
Figure 4.3 Influence of ionic surfactant on initial droplet surface charge 92
Figure 4.4 Surface charge density of droplets with surfactant 93
Figure 5.1 (a) Amended experimental set-up 100
Figure 5.2 (a) and (b) Electrophoretic droplet velocity 104
Figure 5.3 Difference in horizontal position of the core relative to the shell 105
Figure 5.4 Difference in oil core position within the outer water shell between a stationary core-shell and a moving core-shell droplet 106
Figure 5.5 Droplet deformation of the outer water droplet with of 2.30 g/l SDS 108
Figure 5.6 Difference in horizontal droplet position within an (W/O/W)/O droplet 109

List of Tables

Table 2.1 Settling velocities of water droplets in silicone oil 57
Table 2.2 Settling velocities of water droplets in paraffin oil 58

Nomenclature

Symbol	Meaning
$\vec{E}$	External electric field
$\vec{P}$	Dipole moment
$\vec{\tau}$	Torque
μ_{oil}	Dynamic viscosity of oil
A	Surface area
d	Displacement vector
D	Distance between electrodes
E	Electric field magnitude
$f(ka)$	Henry function
F_{Coul}	Coulomb force
F_e	Electric force
F_{HB}	Happel and Bart drag force
F_{HR}	Hadamard and Rybczynski drag force
F_S	Stokes' Drag Force
G	Gravitational acceleration
$h_{cylinder}$	Cylinder height
L	Half width of a square duct
Q	charge
q_0	Test charge
Q_{Sphere}	Charge of solid spheres
R	Particle/droplet radius
$r_{cylinder}$	Cylinder radius

s	Magnitude of droplet displacement
PE	Potential energy
V	Electric potential
v	Velocity of sphere
v_{∞}	Velocity in an infinite medium
v_{CTV}	Combined terminal velocity
v_{em}	Electrophoretic mobility
v_{HR}	Hadamard and Rybczynski terminal velocity
$v_{observed}$	Observed velocity
$v_{terminal}$	Terminal velocity of sphere
W	Energy required to increase interfacial area
γ	Interfacial tension
ΔA	Interfacial area
Δp	Laplace pressure
ΔV	Potential difference
ε	Relative permittivity
ζ	Zeta potential
η	Kinematic viscosity
ρ_{charge}	Volume Charge Density
ρ_{oil}	Density of oil
ρ_{water}	Density of water
σ	Surface charge density
θ	Contact angle
t	Thickness of the dielectric layer
κ	Debye screening length

Chapter 1 Motivation and Background

1.1 Motivation for the thesis

In the last decade, microfluidics has emerged as an attractive research subject due to the various opportunities it presents in the field of colloid science. The small length scales make it possible to create stable emulsions with uniform droplet sizes [1, 2]. In most cases, oil-in-water emulsions are investigated [3-5]. However, with the advent of digital microfluidics [6, 7], that is, the use of water droplets as tiny compartments inside microfluidic, lab-on-a-chip devices [8-11], it has become more important to have information about the charge of water droplets. This is because, often, electrostatic fields are used to manipulate droplets and because repulsion or attraction between droplets can affect the performance of microfluidic devices [12]. One such device has recently been presented by Im et al., whereby the motion of water droplets was controlled by an array of electrodes [13].

The aim of this thesis is to elucidate some of the properties of droplet charge from measurements of the electrophoretic mobility of individual water droplets in two different, non-polar oils of similar, physical fluid properties: silicone and paraffin oil. Although the electrophoretic mobility of a water droplet once it has made contact with a biased electrode has been investigated in the literature [6, 13-18], little attention has been given to the inherent droplet charge, that is, the charge of a water droplet before contact with an electrode and results are contradictive [14, 15, 17, 19].

Charges at the water–hydrophobic medium (oil or air) interface have been the subject of considerable scientific interest and debate, due to their significance for emulsion stability and in various applications in the field of colloid science [3, 4, 20-26] and microfluidics [8-11] and are well understood for droplets, particles or molecules

dispersed in water [27-31]. However, surprisingly little data can be found for liquid-liquid interfaces, especially in the case of the continuous phase being a non-polar oil (such as silicone or paraffin oil), where the solubility for ions is limited and the dispersed phase consists of liquid water droplets. Here, the whole concept of preferential adsorption and double-layer formation is not applicable, meaning that theories such as DLVO theory (named after Derjaguin and Landau, Verwey and Overbeek) or electrical double layer theory can no longer explain the electrostatic interactions within the emulsion system. In one of the few examples in the literature, Marinova et al. [4] considered a simple liquid-liquid interface and investigated the electrophoretic mobility of oil droplets dispersed in water, without any separate ions or surfactant in the continuous water phase. They suggested long-range structuring of water molecules close to the oil-water-interface, as depicted in Figure 1.1, which could produce an electrical potential due to the molecular dipole moment. They also found that the oil droplet charge depended on the pH of the continuous water phase and proposed that this was due to Hydroxyl ions adsorbing at the oil-water interface.

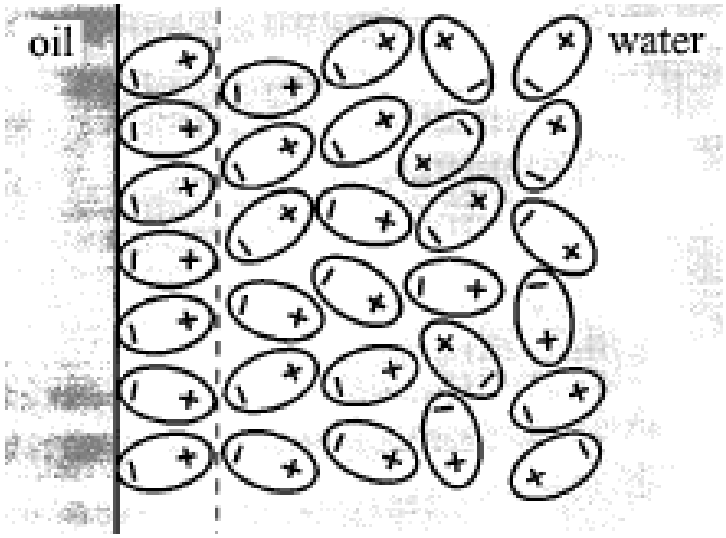

Figure 1.1 Schematic representation of long-range structuring of water molecules at the oil-water interface. Image taken from [4]

However, in the case of the continuous phase being a non-polar oil (in this case, a silicone and a paraffin oil) with no significant solubility for ions and the dispersed particles being liquid water droplets, the whole concept of preferential adsorption and double-layer formation is not applicable. An important question that needs to be addressed is the dependence of droplet charge on ion type and concentration in the dispersed aqueous phase, which could provide some indications as to the nature of interface charge. Marinova et al. [4] have shown that changing the electrolyte concentration of the continuous water phase can influence the electrophoretic motion of the dispersed oil droplets, as ions adsorb at the interface. However, no details can be found for the inverse emulsion, which is why this area deserves further study.

Sometimes droplets are given a charge through direct, physical contact with an electrode. An alternative method to the direct charging method is through chemical additives, such as ionic surfactant. It is well established that use of surfactant facilitates droplet rupture and aids the reduction of droplet size. The literature has shown that the addition of ionic surfactant to a continuous aqueous phase can change the electrophoretic mobility of silicone oil droplets dispersed in it [5, 32]. However, the inverse emulsion (W/O emulsions) has not yet been explored. It remains to be investigated if the addition of surfactant has any effect on the electrophoretic mobility of water droplets dispersed in oil.

Lastly, double emulsions, water-in-oil-in-water ((W/O)/W) and oil-in-water-in-oil ((O/W)/O), are an attractive tool in biomedical engineering as they offer liposome delivery vehicles [33], microcapsules [34], controlled content release [35] or living cell encapsulation [36]. As previously discussed, Im et al. [18] have performed a feasibility study to test the influence of an electric field on living cells and did not observe any noticeable change in viability and proliferation of living cells. Cell manipulation often

requires sterile techniques, for example laminar flow cabinets that prevent the contamination of biological samples or other kinds of particle sensitive devices. Electrophoresis offers a new technique for high precision manipulation of droplets and could replace such large bench designs with smaller lab-on-a-chip devices. Choi et al. recently presented a droplet manipulation technique, whereby a water droplet is given a charge from an electrode and is then driven by electric fields [6]. Apart from carrying a native charge, water-in-oil droplets can also be deliberately charged through direct contact with a voltage-biased electrode [37]. The great advantage it offers is the degree of control with respect to sign and magnitude of the charge. It needs to be assessed whether the addition of oil droplets within water droplets would change the electrophoretic mobility of the latter, which, in turn, would have implications on the design of (O/W)/O droplet manipulation procedures.

1.2 Background

1.2.1 Emulsions

The term ‘colloid’ describes a type of mixture whereby a substance (liquid or solid, which can range from a few nm to a few μm in size) is dispersed inside another. A specific type of colloid is an emulsion, which is a liquid-in-liquid dispersion of two or more immiscible liquids (in most cases water and oil), where one is dispersed as small droplets in the other [29]. They can be further divided into monodisperse and polydisperse emulsions – polydispersity simply means that droplets are of different sizes (Figure 1.2a), whereas monodispersity means that all droplets have the same size, within a specific margin of error (Figure 1.2b).

(a) (b)

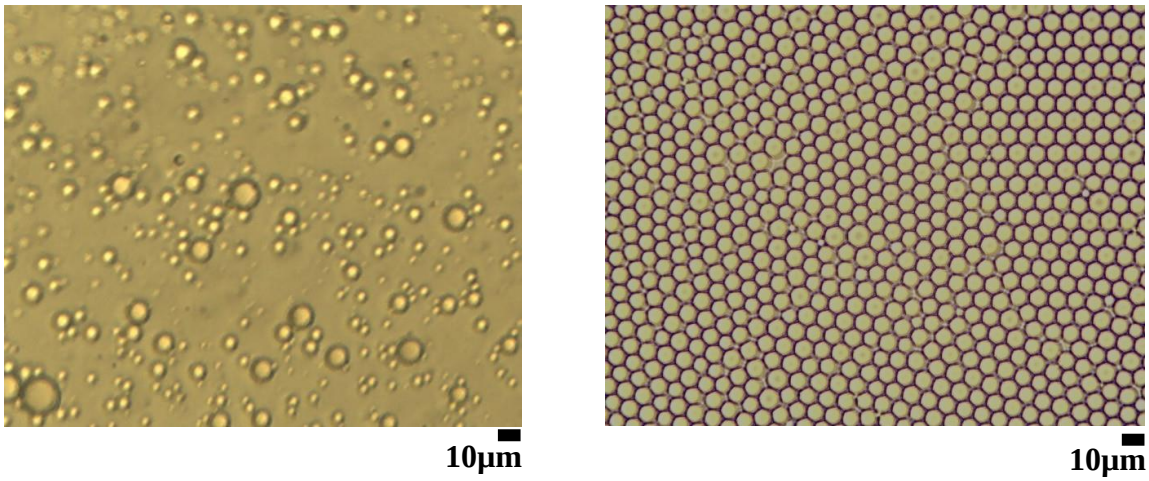

Figure 1.2 Examples of a polydisperse (a) and monodisperse (b) emulsion. a) Water droplets dispersed in FC-77 after being sonified for 30s. (b) Silicone oil droplets dispersed in an alginate solution, created via constant shear stress

Emulsions are used in a variety of different industries, such as food, pharmaceuticals, agriculture and cosmetics, due to their ability to transport solubilised hydrophobic substances in a water continuous phase [38-40]. Common emulsions are inherently unstable and do not form spontaneously. They require input energy (such as shaking,

homogenising, ultrasonication) but will eventually separate if left long enough. There are various different ways in which the two fluids can separate. The main four are:

Coalescence: the most common emulsion instability, in which droplets merge together to form larger droplets. Extensive droplet coalescence eventually leads to the formation of a separate layer of one liquid on top of the other.

Ostwald ripening: a process by which small droplets are dissolved and redeposited onto larger droplets [41, 42], i.e. smaller droplets become smaller, whilst larger droplets become larger. It is a result of the chemical potential differences between the different sized droplets and can be observed in systems where the two liquids have a finite mutual solubility. A typical example of Ostwald ripening is the crystallisation of water during ice cream production. As the mixture is churned, water crystals at the wall are dispersed within the emulsion and over time (typically minutes) larger crystals grow at the expense of smaller ones. The final average size of the crystals determines the texture of the ice cream [43].

Flocculation: individual droplets aggregate together, leading to large clusters of droplets within the continuous phase.

Creaming: droplets float to the top or bottom of the continuous phase due to density differences.

Emulsion stability can be achieved by balancing the input energy of mixing the two liquids and the interfacial energy associated with the boundaries [44]. For example, microemulsions are thermodynamically stable mixtures of water, oil and surfactant that form upon simple mixing.

An emulsion is usually achieved by applying a mechanical shear force to two immiscible liquids. In 1930, Taylor investigated droplet formation [45, 46] and concluded that the final droplet size depends on balancing droplet breakup and the coalescence processes. The energy (W) required to increase the interfacial area between the two liquids, ΔA, is defined as [47]:

$$W = \Delta A \gamma, \qquad \text{Equation 1-1}$$

where γ is the interfacial tension between the two liquids.

This means that in order to reduce droplet size (i.e. increasing ΔA), greater amounts of work are required. Generally, at least one more component, known as a surfactant, is added to the mixture to aid emulsification. Surfactants reduce the interfacial tension between the two phases and aid rupture. According to Bancroft's Rule, the phase in which most of the surfactant is dissolved becomes the continuous phase [48, 49].

Emulsions can be stabilised in various ways using materials such as surfactants, polymers, solid particles or proteins. Exploiting the electric double layer [50] or steric interactions [51] near the interface (Figure 1.3) can further improve stability, as they prevent droplets from coalescing with each other.

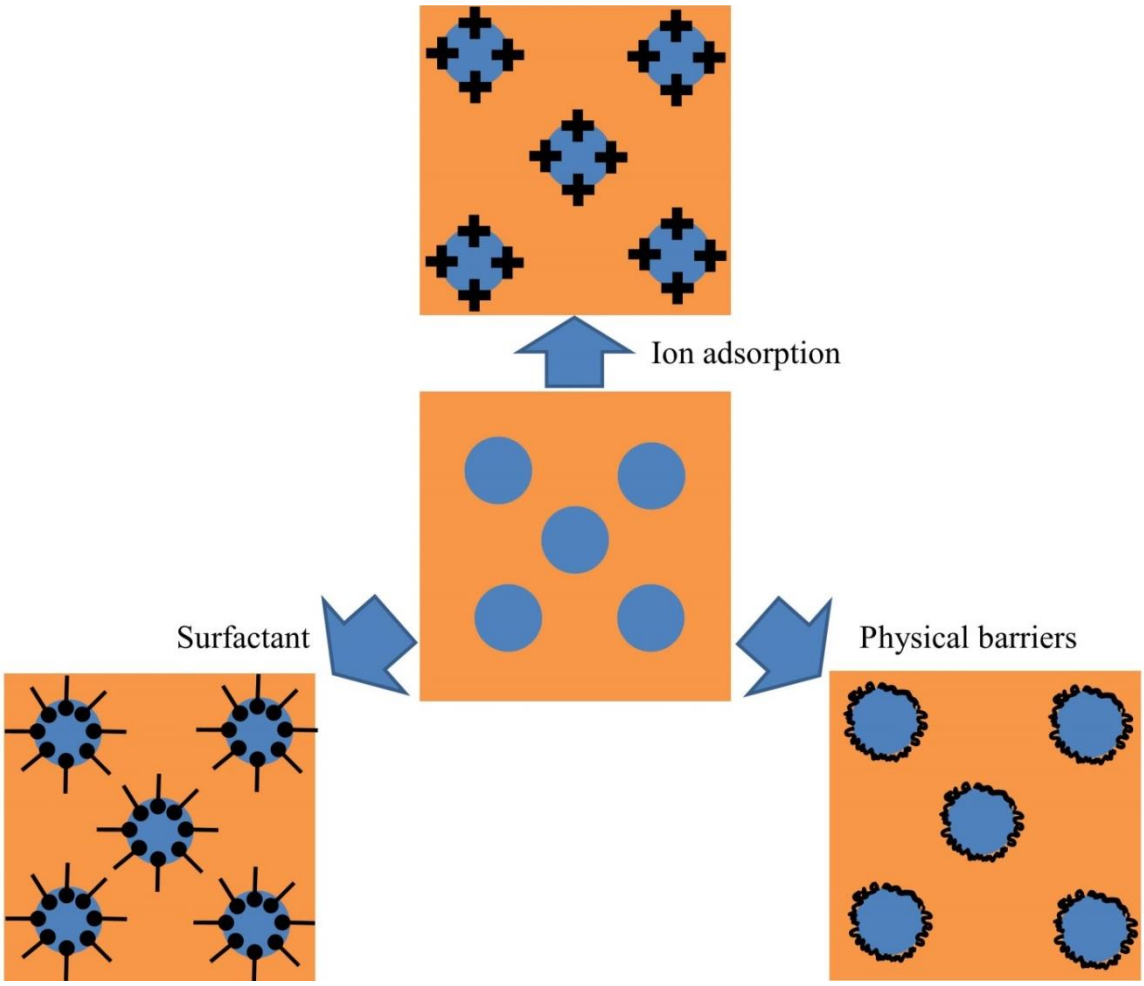

Figure 1.3 Different methods of stabilising a water (blue circles) in oil (orange) emulsion. Clockwise from top: emulsion is electrically stabilised, as droplets of the same charge repel each other; physical barriers such as proteins or solid particles stop droplets from coalescing; surfactants with a hydrophobic head and hydrophilic tail repel each other.

The general chemical structure of a surfactant is such that it possesses a hydrophilic head (black circles) and a hydrophobic tail (black lines), which are absorbed by the relevant phase (Figure 1.3). Surfactants can be further classified into three groups: anionic, cationic and non-ionic [52]. An anionic surfactant has an anionic (i.e. negative) functional head group; the cationic surfactant has a cationic (i.e. positive) head group, whilst the non-ionic surfactant has no charge groups in its head at all.

The effectiveness of polymers is usually limited and so they are mainly used for stabilising oil-in-oil emulsions or increasing the viscosity of the continuous phase [53]. Emulsions stabilised by solid particles are called Pickering emulsions [54]. The scientist, Pickering, observed that water-wetted particles can act as a surfactant for oil-in-water emulsions.

1.2.1.1 Types of Emulsification

In order to generate an emulsion, a liquid needs to be ruptured so that its drops are dispersed in the continuous phase liquid. There are many different methods of creating an emulsion [55], which include: micro-fluidic devices [56-58], dripping drop technique [59-61], ultrasonication [62, 63] and stirring [42].

Emulsions are the product of the rupture and coalescence processes competing against one another simultaneously. In order to deform and rupture a droplet, one must apply sufficient energy to overcome the Laplace pressure (Δp). The Laplace pressure acts across the water-oil interface towards the centre of a large water drop, which means that there is a larger pressure inside the drop than outside.

$$\Delta p = \frac{2\gamma}{R}, \qquad \text{Equation 1-2}$$

where γ= interfacial tension and R = radius of droplet.

Ultrasonication

To rupture the droplet into smaller droplets, it is necessary to apply an external force that is significantly larger than the interfacial tension [40]. An ultrasonic homogeniser has three main components: an electronic generator, a transducer and a horn or probe. The electrical generator, which is connected to the mains, converts the input electricity into an alternating electrical signal (ranging from 20 kHz to tens of MHz), which drives

the transducer [64-66]. A transducer contains piezoelectric crystals, which, upon receiving the electrical signal, start to oscillate, causing the horn or probe to longitudinally expand and contract. Emulsification occurs because these pressure waves lead to the creation of voids within the continuous phase, which implode violently when they have reached a critical size [67]. This is known as transient cavitation. When this occurs, large amounts of energy are released, generating high temperature, shear rates, shockwaves and pressure differences, rupturing drops and creating micro/nano-dispersions. Ultrasonication is covered in more detail in the Methodology chapter.

Microfluidisation

Microfluidisation is a recent technique of creating emulsions with uniform droplet sizes [1, 2]. Two or more fluids are forced through a system of channels (usually using a pumping device and with at least one channel of dimensions < 1 mm [40, 68]) and droplets are formed at the tip of a capillary tube (Figure 1.4), when they reach a size where the co-flowing liquid drag exceeds the interfacial tension [69]. This technique is widely used for creating monodisperse emulsions. More detail on microfluidisation can be found in Chapter 2.

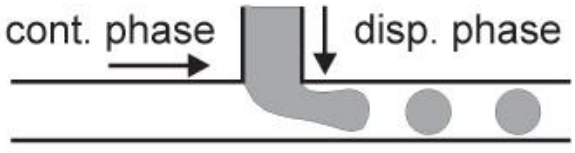

Figure 1.4 Schematic of a T-Junction microchannel emulsification device [70]

1.2.2 Electrokinetics

Electrokinetic motion of droplets is defined as the migration of droplets under the influence of an externally-applied electric field (usually between two electrodes immersed in the continuous phase) in a liquid emulsion or solution and originates from

the charge separation at the interface between the two different phases [71]. Surfaces, when in contact with a polar medium, will acquire an electric charge by dissociation of surface groups or by adsorption of charged molecules [72]. Different charge mechanisms operate, such as ionisation, ion dissolution and ion adsorption [31]. Charges at the oil-water interface are of great interest to the colloid research community, although the topic is still under some debate [4, 20, 21, 73].

Ionisation is the process of either adding or removing ions or electrons from an interface, so that its net charge is not equal to zero. There are two types of ionisation (positive or negative), which are defined by the electric charge that is being produced [74].

When an electrolyte material (solid, liquid or gas that ionises when dissolved in a suitable substance, e.g. salt in water) is added to a solvent, the dissolved ions diffuse within the solution and become surrounded by the solvent molecules, thus creating an ionic solution. For example, when dissolved in water, the ionic compound sodium chloride (NaCl) will separate into sodium ions and chloride ions, which become surrounded by the water molecules. During the process of ion adsorption, ions (from a gas, liquid or solid) adhere to a surface but are not dissolved into the bulk. It is a surface-based process which alters the surface charge density [40, 75].

1.2.2.1 Electrical Double Layer

Interfacial charges are well understood for droplets, particles or molecules dispersed in water [27-31]. The object's surface gains a charge due to ions in the continuous phase adsorbing at the interface, a process that is described by the electrical double layer theory (Figure 1.5). The electrical double layer is a region close to the object's surface, where a layer of positive/negative ions is adsorbed onto the surface of the object due to

a host of chemical interactions (Stern layer, Figure 1.5). The surface charges then attract counter ions to the interface via the Coulomb force, whilst the ionic composition of the liquid governs the thickness of the diffuse layer (Figure 1.5) [40].

To mathematically predict the distribution of ions near the interface, the Poisson-Boltzmann equation is used, which describes the distribution of an electrical potential near a charged surface. It combines the electrical properties of the surface (i.e. surface charge density and electrical surface potential) and the solution (i.e. ion type, ion concentration and dielectric constant) as follows [40]:

$$\frac{d^2\psi(x)}{dx^2} = -\frac{e}{\epsilon_0\epsilon_R}\sum_i z_i n_{0i} exp\left(\frac{-z_i e\psi(x)}{kT}\right), \qquad \text{Equation 1-3}$$

where n_{0i} is the concentration of ionic species of type i in the bulk solution, z_i is their valency, e is the elementary charge, ε_0 is the dielectric constant in a vacuum, ε_R is the relative dielectric constant of the solution, $\psi(x)$ is the electrical potential at a distance x from the charged surface, k is the Boltzmann constant and T is the temperature [40].

In colloidal systems, this equation is frequently used to calculate the electrostatic interactions within the emulsions and suspensions (i.e. the surface charge of the suspended particles); the presence of an electrical double layer is often the cause for kinetically stable emulsions, as it reduces the likelihood of coalescence between particles [74]. Forces acting at the interface are described by the DLVO theory, which is used to predict if a colloidal system is stable or not [30, 76]. In general, the DLVO theory takes into account two long-range forces, which determine the proximity of two particles dispersed in an emulsion undergoing Brownian motion: the van der Waals' force of attraction (i.e. the sum of the attractive forces that exists between like molecules) and the electrostatic repulsion of the electrical double layer [72].

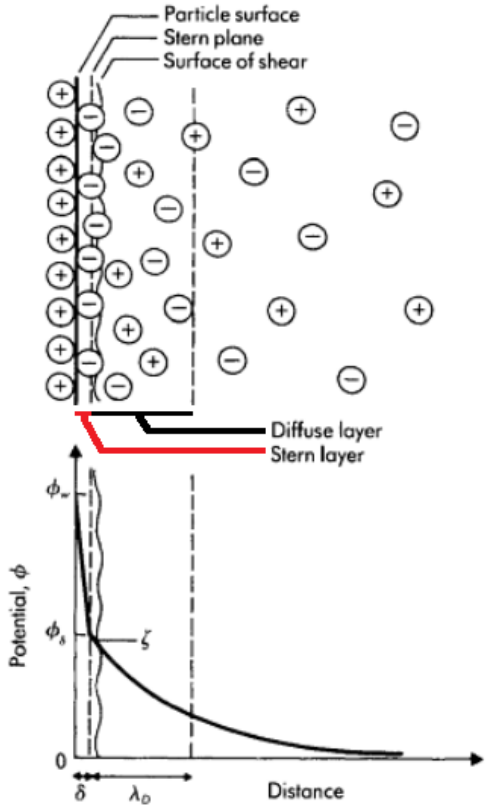

Figure 1.5 Schematic of an electrical double layer and zeta potential. Image taken from [31], where φ_w is the wall potential, φ_δ is the potential of the Stern layer, δ is the thickness of the Stern layer**,** ζ is the zeta potential and λ_D is the Debye length.

Although these theories are well understood, surprisingly few data can be found for liquid-liquid interfaces, especially in the case of the continuous phase being a non-polar oil (such as silicone or paraffin oil), where the solubility for ions is limited and the dispersed phase consists of liquid water droplets. Here, the whole concept of preferential adsorption and double-layer formation is not applicable, meaning that theories such as DLVO theory or electrical double layer theory can no longer explain the electrostatic interactions within the emulsion system.

1.2.2.2 Zeta Potential

The potential difference between the dispersion medium and the stationary layer of fluid attached to the dispersed particle is known as zeta potential (Figure 1.5). The value of the zeta potential is related to the stability of the emulsion. A high zeta potential (more than ±30 mV) leads to stable emulsions, as they are electrostatically stabilised, whilst a low zeta potential means that there is a greater chance for the emulsion to flocculate or coalesce [77]. The zeta potential can be calculated using the Henry equation [77]:

$$v_{em} = \frac{2\varepsilon\zeta f(ka)}{3\eta}, \qquad \text{Equation 1-4}$$

where ε is the relative permittivity, ζ is the zeta potential, η is the kinematic viscosity of the continuous phase, v_{em} the electrophoretic mobility of the droplet and *f(ka)* is the Henry's function.

Two values are generally used as approximations for *f(ka)*; 1.5 or 1. For an aqueous solution of moderate electrolyte concentration, a value of 1.5 is used, which is also known as the Smolichowski approximation [78]. To calculate the zeta potential in a non-polar liquid, Huckel's approximation is used and *f(ka)* becomes equal to 1 [79].

1.2.2.3 Electrowetting

Electrowetting on a dielectric-coated surface (otherwise known as electrowetting on dielectric, EWOD) is an electrical method of controlling the contact angle between a water droplet and a substrate [80] and is used in the microactuation of droplets in digital microfluidics [81, 82]. The typical configuration of the EWOD actuation method is illustrated in Figure 1.6 [83]: a water droplet is placed on a hydrophobic, insulating layer, which covers a planar electrode below. A second wire electrode, connected to the counterelectrode underneath is used to penetrate the droplet, thus closing the electric

circuit. Increasing the electrical potential, ΔV, parabolically decreases the contact angle, θ, a reversible process that is described by the Lippmann Young equation [83]:

$$cos\theta = cos\theta_0 + \frac{\varepsilon \Delta V^2}{2\gamma_{lg} t} = cos\theta_0 + \tau, \qquad \text{Equation 1-5}$$

where θ_0 is the initial contact angle, ε the permittivity of the dielectric layer, γ_{lg} the liquid-air interfacial tension, t the thickness of the dielectric layer and τ the electrowetting number, a dimensionless number, which represents the strength of the EWOD.

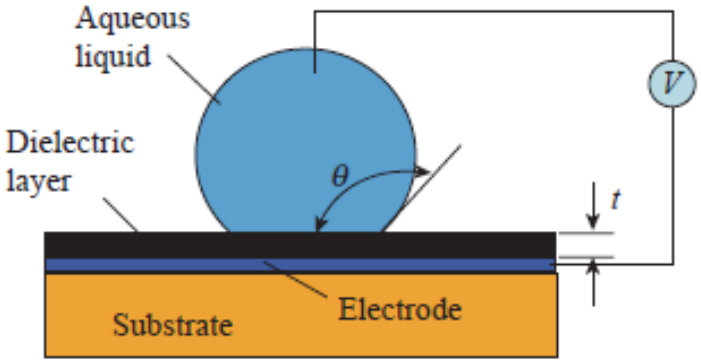

Figure 1.6 Schematic of the principle of electrowetting on dielectrics (EWOD) [83]

1.2.2.4 Types of Electrokinetics

Electroosmosis

Electroosmosis describes the movement of a liquid, induced by an applied electric field, relative to a stationary charged surface (e.g. a capillary). The cause of the migration is the Coulomb force acting on the mobile counter ions within the electrical double layer, which forms at the interface between the solid surface and the liquid (Figure 1.7). Electroosmosis can be used to dewater solids in the construction industry or to remove contaminants from soils [31].

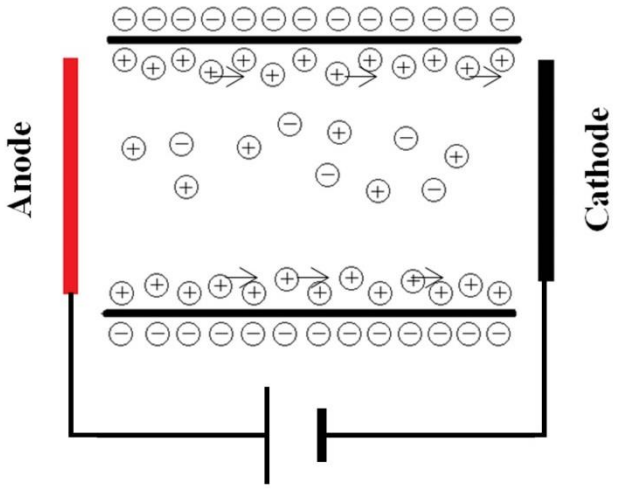

Figure 1.7 Schematic of electroosmotic flow. Liquid is moving due to the net migration of the mobile ions in the diffuse layer

Electrophoresis

When an electric field is applied to a liquid in which a particle is freely suspended, the Coulomb force acts on the net surface charge causing the migration of the particle. This is known as electrophoresis (Figure 1.8).

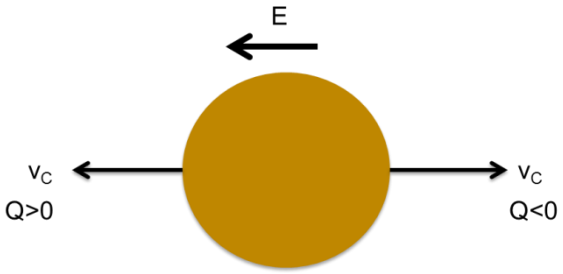

Figure 1.8 Schematic illustration of electrophoretic motion of a particle,where E is the electric field, v_c is the droplet's velocity due to the Coulomb force and Q is the charge of the droplet.

The electrophoretic movement of particles larger than the wavelength of light in an externally applied electric field can be observed under a light microscope and hence

their charge, *Q*, can be determined [84]. However, the manner in which the charge can be calculated heavily depends on the hydrodynamic drag force coefficients (Ladenburg, Hadamard−Rybczynski, etc.) considered and can differ by as much as 33% [85]. This will be discussed in more detail in the Methodology chapter.

1.2.2.5 Electrokinetic Applications

All electrokinetic applications use the particle's charge to manipulate a sample, a small selection of which are described below.

Microcapillary Electrophoresis

Capillary electrophoresis or capillary zone electrophoresis is a common and well-established method used to separate distinct analytes by their charge and frictional forces. It is commonly used for single cell analysis [71]. For example, Reichmuth et al [86] presented a microfluidic chip of electrophoretic immunoassay, which was used to detect and concentrate viruses simultaneously. In their work, electrophoresis was used to separate and remove excessive antibodies from the antibody virus complexes.

Microfluidic Free-Flow Electrophoresis

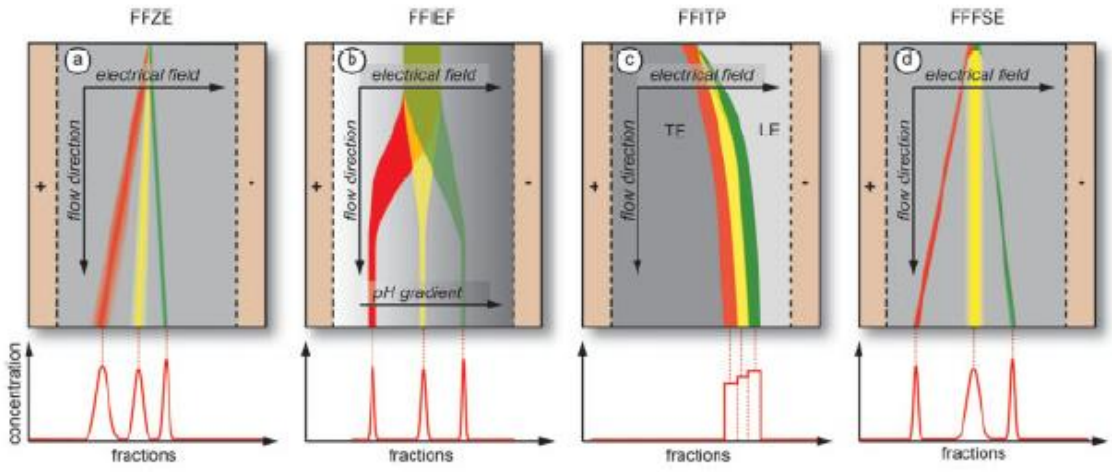

Figure 1.9 The four typical types of free-flow electrophoresis, a) free-flow zone electrophoresis, b) free-flow isoelectric focusing, c) free-flow isotachophoresis and d) free-flow field step electrophoresis [87]

Microfluidic free-flow electrophoresis is a separation method, which can be divided into four different modes, according to their operation principles (Figure 1.9) [87]. In free-flow zone electrophoresis (FFZE), particles are separated on the basis of their electrophoretic mobility using an electrolyte carrier with homogenous pH and electrical conductivity (Figure 1.9a). Free-flow isoelectric focusing (FFIEF) describes a process where particles migrate through a pH gradient, which is formed perpendicular to the flow using a mixture of ampholytes. Components migrate up until the point where their isoelectric point is equal to the pH value of the buffer, i.e. the particle carries no more net electric charge (Figure 1.9b). In free-flow isotachophoresis (FFITP), the sample is suspended in between a leading electrolyte (LE) and a terminating electrolyte (TE). An electrophoretic mobility exists between the sample ions and the electrolytes. After applying an electric field for a period of time, discrete solute zones are formed in order of their distinct electrophoretic mobility (Figure 1.9c). Free-flow field step

electrophoresis uses a less conductive buffer within the centre of the separation zone and a more conductive buffer near the boundary. This builds up an electric field step gradient where the centre zone experiences significantly high field strength and causes the particles that are to be separated to move faster in the centre zone. Separated components are then found at the boundary zone, as the electric field strength and electrophoretic velocity are drastically reduced (Figure 1.9d).

Electrostatic Atomisation

Electrostatic atomisation is a phenomenon used for generating water-in-oil emulsions. A wire is inserted into a microchannel as a ground electrode and the channel is then placed near a container and a high voltage electrode. When a voltage is applied, μm-sized droplets are 'sprayed' from the boundary layer as the electrostatic force becomes greater than the surface tension. Using this method, monodisperse droplets smaller than the inner diameter of the channel are generated [88].

Electrocoalescence

This technique is most commonly used in the petroleum industry following the crude oil extraction stage, as crude oil naturally occurs as a water-in-oil emulsion. During the electrostatic demulsification process, water-in-crude-oil dispersions are separated by applying a high electric field to the emulsion to accelerate the natural process of flocculation and coalescence [89].

Electric Droplet Lithography

Electric Droplet Lithography (EDL) is method for micro/nanopatterning soft, biological materials on a solid surface. For the EDL process, electrical charges are injected onto a substrate using a moveable needle and a surface charge pattern is created. Water

droplets (which can contain nanoparticles or antibodies) dispersed in oil are then attracted to the substrate [84]. On hitting the solid surface, the droplets deposit the particles onto the plate, creating a quasi 2D structure (Figure 1.10) [90-92]. Naujoks et al. [90] observed that nanoparticles can be deposited onto a defined geometric pattern on a substrate via electrostatic interaction but the precise nature of the effective water charge was not discussed.

Dispersions can be created in various ways, e.g. by ultrasound or using microchannels, and the resolution of the surface charge pattern depends on the size and uniformity of drops.

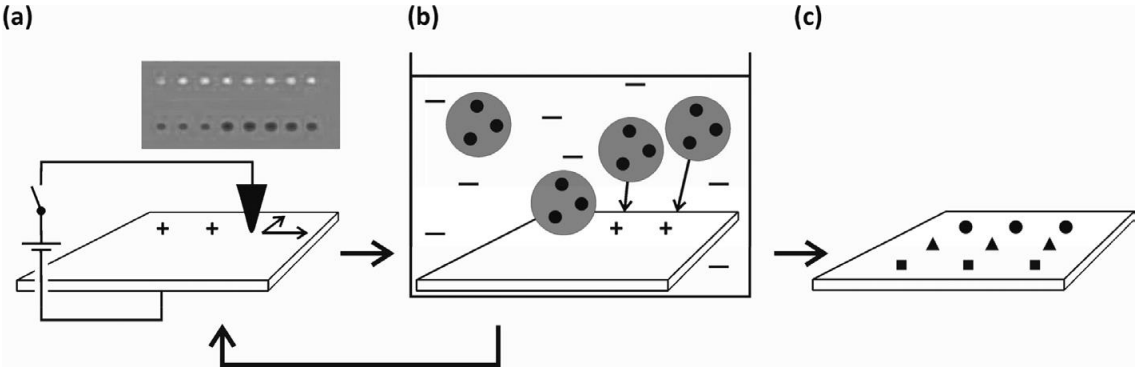

Figure 1.10 EDL process principle (a) Step 1, pre-patterning (b) Step 2, deposition (c) Repetition of step 2 in order to deposit different materials, as indicated by the different geometric symbols, on the same surface [93].

In order to prevent the charge pattern from decaying, oils with a high electrical resistivity (e.g. fluorocarbon or hydrocarbon oils [94]) are used. As the water droplets contain the material to be patterned, steps 1 (Figure 1.10a) and 2 (Figure 1.10b) can be repeated, whilst varying the material to be deposited and thus creating a more complex structure. After each deposition, the excess water droplets and oil are washed away with pure oil, leaving only the attached material (Figure 1.10c). The fact that water and other

organic/inorganic materials have a very low solubility in the fluorocarbon oil has additional benefits, as no residue is left on the samples, which avoids sample contamination [94].

Another advantage of the EDL process is that the deposition times normally range from a few seconds to a few minutes [95, 96], which makes emulsion stability less of a crucial requirement. In fact, rapid agglomeration and/or creaming might even have a beneficial effect on the EDL process once deposition has occurred, as it is easier to wash away.

1.3 Water Droplet Electrophoresis

Recently water droplet electrophoresis has become the subject of intense research in the field of digital microfluidics and lab-on-a-chip devices [14, 15, 17-19, 37, 97, 98]. Khayari et al. [37] examined the dynamics and deformation of a "bouncing" water drop (droplet radius = 1.4 mm) dispersed in corn oil under the influence of an electric field. The droplet was placed on a horizontally-aligned electrode and two critical voltages were identified, the first one being the initial lift-off voltage necessary to overcome the adhesion force and gravitational force. The second is the voltage at which the droplet returns to the electrode, without detaching again – the latter being considerably less than the former. The governing parameters of the adhesion force were identified as the contact area and contact angle; the smaller the contact area and the larger the contact angle the smaller the adhesion force becomes. Khayari also found that the material of which the electrode is made greatly influences droplet behaviour. For some materials, such as titanium, the contact area becomes so large that the adhesion force prevents droplet lift-off.

Jung et al. [97] studied the electrical charging of a water droplet at a copper electrode in silicone oil and considered the effects of the electric field, viscosity of the oil and the droplet size. Rhythmic motion of water droplets was observed and it was reported that the amount of electrical charging increased with the electric field strength and the droplet size. During the experiments, they observed that charging occurred between the electrode and the droplet and referred to it as a contact charging process. Jung found that, when summarising the results in the form of a scaling law, the water droplet charge was proportional to 1.59 times the droplet radius and the electric field strength to the power of 1.33. However, the viscosity of the medium did have a significant effect on droplet charge. On the other hand, Khayari et al. [37] claimed that there was no contact between the water droplet and the electrode and explained it by the fact that the electrical breakdown, which produces an electrical conducting path that charges the droplet, occured before the droplet touched the electrode.

Holto et al. [98] observed the electrocoalescence of water droplets in naphthenic oil in a bipolar square AC voltage system. Droplet sizes ranged from 5-100 μm and the electric field ranged from 1.3 to 5 kV/cm. At high voltages and high frequencies, little droplet agitation and a high coalescences rate were observed. However, it was also frequently observed that droplets would collide with one another and not coalesce, but instead an exchange of charge would occur and the droplets would start to repel each other – a finding that would suggest that droplet charge occurs at the droplet's surface. High voltages also caused larger droplets to elongate and break-up, resulting in smaller droplets.

In 2000, Bailes et al. [14] experimentally investigated the motion of a single deionised water droplet in n-dodecane (with varying droplet diameter between 100 μm and 400 μm) in a pulsed DC electric field (field strength 1.5 kV/cm). It was observed that

deionised water droplets, when placed between a pair of parallel electrodes (the positive being insulated), have an inherent positive charge. It was also found that droplet mobility decreased with an increasing conductivity of the continuous oil phase.

Hase et al. [15] investigated the motion of a water droplet (100 µm diameter) in rapeseed oil under the influence of a DC electric field. A single droplet was placed between a pair of gold rods, which were 400 µm apart and a voltage was applied. They found that water droplets exhibited repetitive translational motion between the electrodes. A critical field strength was determined experimentally after which droplets started oscillating. For 0-0.5 kV/cm, water droplets were attracted to either electrode and attached to the electrode surface. At fields above 0.5 kV/cm, droplets touched the electrode and were repelled towards the oppositely-charged electrode, thus oscillating between the electrodes, whilst slowly falling under gravity. The greater the field strength (up to 2.5kV/cm), the faster the droplets oscillated. Hase observed that an uncharged, deionised water droplet was initially attracted to the nearest electrode (regardless of the electrode's polarity), suggesting that the initial charge of a water droplet could be either positive or negative.

This stands in contrast to what has been observed by Bailes or Im, who both observed that a water droplet had an inherent positive charge [14, 17, 18]. Lee et al. [19], on the other hand, reported that a deionised water dispersed in silicone oil would initially travel towards the positive electrode, implying that negative charges at the oil/water interface were responsible for this native, negative charge. However, the experimental specifications (such as droplet size, continuous oil phase, types of electrode) all differ, which makes direct comparison difficult.

Im et al. experimentally investigated the electrophoretic mobility of charged water droplet in silicone oil and the influence an electric field has on living cells in a charged water-in-silicone oil droplet [17, 18]. It was observed that a deionised water droplet had an inherent positive charge and underwent electrophoretic oscillating motion under a strong electric field (1.3-5 kV/cm). Four different parameters were considered: droplet size, electrolyte ion species, electrolyte ion concentration and the electric field strength [17]. Contrary to common expectation, Im found that charging of an electrolyte droplet is more limited than a deionised water droplet, which means that the conductivity of water is not the major factor that governs droplet charge (after contact with a biased electrode). This implies that complex electrochemical reactions are involved during the transfer of charge at the water/electrode interface. Experiments showed that larger droplets moved more rapidly, meaning that they attained a greater charge than smaller droplets when in contact with a biased electrode [17]. It was also observed that a strong electric field did not influence the viability or proliferation of cells, which makes electrophoresis a safe manipulation method for droplets containing living biological systems [18].

1.4 Summary

The main findings of the above background theory can be summarised as follows:

- Emulsions are a colloidal system that can be used in a variety of applications. In order to create an emulsion, a mechanical force needs to be applied to overcome the interfacial tension between two immiscible liquids. The two types of emulsification processes used in this thesis are ultrasonication and microfluidisation.
- When an electric field is applied to a liquid in which a droplet is freely suspended, the Coulomb force acts on the net surface charge causing the migration of the droplet. Known as electrophoresis, this method is used in a variety of applications, including electrocoalescence and electric droplet lithography.
- Theories regarding interfacial charges for particles dispersed in water are well understood. However, very few data can be found for water-in-oil systems.

1.5 References

[1] S. M. Jafari, Y. He, and B. Bhandari, "Optimization of nano-emulsions production by microfluidization," *European Food Research and Technology,* vol. 225, pp. 733-741, Sep 2007.

[2] S. M. Jafari, Y. H. He, and B. Bhandari, "Nano-emulsion production by sonication and microfluidization - A comparison," *International Journal of Food Properties,* vol. 9, pp. 475-485, 2006.

[3] J. K. Beattie and A. M. Djerdjev, "The pristine oil/water interface: Surfactant-free hydroxide-charged emulsions," *Angewandte Chemie-International Edition,* vol. 43, pp. 3568-3571, 2004.

[4] K. G. Marinova, R. G. Alargova, N. D. Denkov, O. D. Velev, D. N. Petsev, I. B. Ivanov, and R. P. Borwankar, "Charging of oil-water interfaces due to spontaneous adsorption of hydroxyl ions," *Langmuir,* vol. 12, pp. 2045-2051, Apr 17 1996.

[5] Y. G. Gu and D. Q. Li, "Electric charge on small silicone oil droplets dispersed in ionic surfactant solutions," *Colloids and Surfaces a-Physicochemical and Engineering Aspects,* vol. 139, pp. 213-225, Aug 10 1998.

[6] K. Choi, M. Im, J. M. Choi, and Y. K. Choi, "Droplet transportation using a pre-charging method for digital microfluidics," *Microfluidics and Nanofluidics,* vol. 12, pp. 821-827, Mar 2012.

[7] M. J. Jebrail, M. S. Bartsch, and K. D. Patel, "Digital microfluidics: a versatile tool for applications in chemistry, biology and medicine," *Lab on a Chip,* vol. 12, pp. 2452-2463, 2012.

[8] A. D. Griffiths and D. S. Tawfik, "Miniaturising the laboratory in emulsion droplets," *Trends in Biotechnology,* vol. 24, pp. 395-402, 2006.

[9] A. Huebner, S. Sharma, M. Srisa-Art, F. Hollfelder, J. B. Edel, and A. J. deMello, "Microdroplets: A sea of applications?," *Lab on a Chip,* vol. 8, pp. 1244-1254, 2008.

[10] S. Y. Teh, R. Lin, L. H. Hung, and A. P. Lee, "Droplet microfluidics," *Lab on a Chip,* vol. 8, pp. 198-220, 2008.

[11] G. S. Fiorini and D. T. Chiu, "Disposable microfluidic devices: fabrication, function, and application," *Biotechniques,* vol. 38, pp. 429-446, Mar 2005.

[12] J. R. Millman, K. H. Bhatt, B. G. Prevo, and O. D. Velev, "Anisotropic particle synthesis in dielectrophoretically controlled microdroplet reactors," *Nature Materials,* vol. 4, pp. 98-102, Jan 2005.

[13] D. J. Im, B. S. Yoo, M. M. Ahn, D. Moon, and I. S. Kang, "Digital Electrophoresis of Charged Droplets," *Analytical Chemistry,* vol. 85, pp. 4038-4044, Apr 16 2013.

[14] P. J. Bailes, J. G. M. Lee, and A. R. Parsons, "An experimental investigation into the motion of a single drop in a pulsed DC electric field," *Chemical Engineering Research & Design,* vol. 78, pp. 499-505, Apr 2000.

[15] M. Hase, S. N. Watanabe, and K. Yoshikawa, "Rhythmic motion of a droplet under a DC electric field," *Physical Review E,* vol. 74, p. 046301, Oct 2006.

[16] M. Takinoue, Y. Atsumi, and K. Yoshikawa, "Rotary motion driven by a direct current electric field," *Applied Physics Letters,* vol. 96, p. 104105, Mar 2010.

[17] D. J. Im, J. Noh, D. Moon, and I. S. Kang, "Electrophoresis of a Charged Droplet in a Dielectric Liquid for Droplet Actuation," *Analytical Chemistry,* vol. 83, pp. 5168-5174, Jul 1 2011.

[18] D. J. Im, J. Noh, N. W. Yi, J. Park, and I. S. Kang, "Influences of electric field on living cells in a charged water-in-oil droplet under electrophoretic actuation," *Biomicrofluidics,* vol. 5, Dec 2011.
[19] C. P. Lee, H. C. Chang, and Z. H. Wei, "Charged droplet transportation under direct current electric fields as a cell carrier," *Applied Physics Letters,* vol. 101, p. 014103, Jul 2 2012.
[20] J. C. Carruthers, "The electrophoresis of certain hydrocarbons and their simple derivatives as a function of ph," *Transactions of the Faraday Society,* vol. 34, pp. 300-307, 1938.
[21] B. W. DICKINSON, "The effect of PH upon the electrophoretic mobility of emulsions of certain hydrocarbons and aliphatic halides," *Transactions of the Faraday Society,* vol. 37, pp. 140-148, 1941.
[22] A. J. Taylor and F. W. Wood, "The Electrophoresis of Hydrocarbon Droplets in Dilute Solutions of Electrolytes," *Transactions of the Faraday Society,* vol. 53, pp. 523-529, 1957.
[23] G. V. Franks, A. M. Djerdjev, and J. K. Beattie, "Absence of specific cation or anion effects at low salt concentrations on the charge at the oil/water interface," *Langmuir,* vol. 21, pp. 8670-8674, Sep 13 2005.
[24] J. K. Beattie, A. N. Djerdjev, and G. G. Warr, "The surface of neat water is basic," *Faraday Discussions,* vol. 141, pp. 31-39, 2009.
[25] V. Knecht, H. J. Risselada, A. E. Mark, and S. J. Marrink, "Electrophoretic mobility does not always reflect the charge on an oil droplet," *Journal of Colloid and Interface Science,* vol. 318, pp. 477-486, Feb 15 2008.
[26] V. Knecht, Z. A. Levine, and P. T. Vernier, "Electrophoresis of neutral oil in water," *Journal of Colloid and Interface Science,* vol. 352, pp. 223-231, Dec 15 2010.
[27] H. Ohshima and K. Furusawa, *Electrical Phenomena at Interfaces, Second Edition,: Fundamentals: Measurements, and Applications*: Taylor & Francis, 1998.
[28] R. J. Hunter, "Foundations in Colloid Science Vol. 2," *Oxford University Press,* 1989.
[29] R. J. Hunter and L. R. White, *Foundations of colloid science Vol. 1*: Clarendon Press, 1987.
[30] P. C. Hiemenz and R. Rajagopalan, *Principles of Colloid and Surface Chemistry, Third Edition, Revised and Expanded*: Taylor & Francis, 1997.
[31] R. F. Probstein, *Physicochemical Hydrodynamics: An Introduction*: Wiley, 2005.
[32] E. Buxbaum, "Cationic electrophoresis and electrotransfer of membrane glycoproteins," *Analytical Biochemistry,* vol. 314, pp. 70-76, 2003.
[33] H. C. Shum, D. Lee, I. Yoon, T. Kodger, and D. A. Weitz, "Double emulsion templated monodisperse phospholipid vesicles," *Langmuir,* vol. 24, pp. 7651-7653, Aug 5 2008.
[34] P. W. Chen, R. M. Erb, and A. R. Studart, "Designer Polymer-Based Microcapsules Made Using Microfluidics," *Langmuir,* vol. 28, pp. 144-152, Jan 10 2012.
[35] A. Abbaspourrad, N. J. Carroll, S. H. Kim, and D. A. Weitz, "Polymer Microcapsules with Programmable Active Release," *Journal of the American Chemical Society,* vol. 135, pp. 7744-7750, May 22 2013.
[36] C. J. Martinez, J. W. Kim, C. W. Ye, I. Ortiz, A. C. Rowat, M. Marquez, and D. Weitz, "A Microfluidic Approach to Encapsulate Living Cells in Uniform

Alginate Hydrogel Microparticles," *Macromolecular Bioscience,* vol. 12, pp. 946-951, Jul 2012.
[37] A. Khayari, A. T. Perez, F. J. Garcia, and A. Castellanos, "Dynamics and deformation of a drop in a DC electric field," *2003 Annual Report Conference on Electrical Insulation and Dielectric Phenomena,* pp. 682-685, 2003.
[38] J. Bibette, F. L. Calderon, and P. Poulin, "Emulsions: basic principles," *Reports on Progress in Physics,* vol. 62, pp. 969-1033, Jun 1999.
[39] G. R.-J. G. Russell-Jones and R. Himes, "Water-in-oil microemulsions for effective transdermal delivery of proteins," *Expert Opinion on Drug Delivery,* vol. 8, pp. 537-546, Apr 2011.
[40] D. J. McClements, *Food Emulsions: Principles, Practice, And Techniques*: CRC PressINC, 2005.
[41] P. W. Voorhees, "The Theory of Ostwald Ripening," *Journal of Statistical Physics,* vol. 38, pp. 231-252, 1985.
[42] J. Jiao, "Ostwald ripening of water-in-hydrocarbon emulsions," *Journal of Colloid and Interface Science,* vol. 264, pp. 509-516, 2003.
[43] K. L. K. Cook and R. W. Hartel, "Mechanisms of Ice Crystallization in Ice Cream Production," *Comprehensive Reviews in Food Science and Food Safety,* vol. 9, pp. 213-222, 2010.
[44] M. Kahlweit and H. Reiss, "On the Stability of Microemulsions," *Langmuir,* vol. 7, pp. 2928-2933, Dec 1991.
[45] G. I. Taylor, "The viscosity of a fluid containing small drops of another fluid," *Proceedings of the Royal Society of London Series a-Containing Papers of a Mathematical and Physical Character,* vol. 138, pp. 41-48, Oct 1932.
[46] G. I. Taylor, "The formation of emulsions in definable fields of flow," *Proceedings of the Royal Society of London Series a-Mathematical and Physical Sciences,* vol. 146, pp. 0501-0523, Oct 1934.
[47] J. C. Lopez-Montilla, P. E. Herrera-Morales, S. Pandey, and D. O. Shah, "Spontaneous emulsification: Mechanisms, physicochemical aspects, modeling, and applications," *Journal of Dispersion Science and Technology,* vol. 23, pp. 219-268, 2002.
[48] W. D. Bancroft, "The theory of emulsification, V," *Journal of Physical Chemistry,* vol. 17, pp. 501-519, Jun 1913.
[49] W. D. Bancroft, "The theory of emulsification VI," *Journal of Physical Chemistry,* vol. 19, pp. 275-309, Apr 1915.
[50] F. Leal-Calderon, V. Schmitt, and J. Bibette, *Emulsion Science: Basic Principles*: Springer, 2007.
[51] G. L. Hasenhuettl and R. W. Hartel, *Food Emulsifiers and Their Applications*: Springer, 2008.
[52] J.-L. Salager. (2002, SURFACTANTS Types and Uses. Available: http://nanoparticles.org/pdf/Salager-E300A.pdf
[53] D. Myers, *Surfactant Science and Technology*: Wiley, 2005.
[54] S. U. Pickering, "Emulsions," *Journal of the Chemical Society,* vol. 91, pp. 2001 - 2021, 1907.
[55] U. El-Jaby, M. Cunningham, and T. F. L. McKenna, "Comparison of Emulsification Devices for the Production of Miniemulsions," *Industrial & Engineering Chemistry Research,* vol. 48, pp. 10147-10151, Nov 18 2009.
[56] I. Kobayashi, Y. Murayama, T. Kuroiwa, K. Uemura, and M. Nakajima, "Production of monodisperse water-in-oil emulsions consisting of highly

uniform droplets using asymmetric straight-through microchannel arrays," *Microfluidics and Nanofluidics,* vol. 7, pp. 107-119, 2008.

[57] D. H. Lee, H. Hwang, and J. K. Park, "Generation and manipulation of droplets in an optoelectrofluidic device integrated with microfluidic channels," *Applied Physics Letters,* vol. 95, Oct 2009.

[58] C. Cheng, L. Chu, and R. Xie, "Preparation of highly monodisperse W/O emulsions with hydrophobically modified SPG membranes," *Journal of Colloid and Interface Science,* vol. 300, pp. 375-382, 2006.

[59] A. D'Innocenzo, F. Paladini, and L. Renna, "Experimental study of dripping dynamics," *Physical review. E, Statistical, nonlinear, and soft matter physics,* vol. 65, p. 056208, 2002 May (Epub 2002 Apr 2002.

[60] D. Funfschilling, H. Debas, H. Z. Li, and T. G. Mason, "Flow-field dynamics during droplet formation by dripping in hydrodynamic-focusing microfluidics," *Physical Review E,* vol. 80, Jul 2009.

[61] T. Fu, Y. Ma, D. Funfschilling, C. Zhu, and H. Z. Li, "Squeezing-to-dripping transition for bubble formation in a microfluidic T-junction," *Chemical Engineering Science,* vol. 65, pp. 3739-3748, 2010.

[62] B. Abismail, J. P. Canselier, A. M. Wilhelm, H. Delmas, and C. Gourdon, "Emulsification by ultrasound: drop size distribution and stability," *Ultrasonics Sonochemistry,* vol. 6, pp. 75-83, Mar 1999.

[63] J. P. Canselier, H. Delmas, A. M. Wilhelm, and B. Abismail, "Ultrasound Emulsification—An Overview," *Journal of Dispersion Science and Technology,* vol. 23, pp. 333-349, 2002.

[64] E. Nazarzadeh and S. Sajjadi, "Viscosity effects in miniemulsification via ultrasound," *AIChE Journal,* vol. 56, pp. 2751-2755, 2010.

[65] K. Kamogawa, G. Okudaira, M. Matsumoto, T. Sakai, H. Sakai, and M. Abe, "Preparation of oleic acid/water emulsions in surfactant-free condition by sequential processing using midsonic-megasonic waves," *Langmuir,* vol. 20, pp. 2043-2047, Mar 16 2004.

[66] M. Sivakumar, A. Towata, K. Yasui, T. Tuziuti, T. Kozuka, Y. Iida, M. M. Maiorov, E. Blums, D. Bhattacharya, N. Sivakumar, and M. Ashok, "Ultrasonic cavitation induced water in vegetable oil emulsion droplets - A simple and easy technique to synthesize manganese zinc ferrite nanocrystals with improved magnetization," *Ultrasonics Sonochemistry,* vol. 19, pp. 652-658, May 2012.

[67] M. C. Ula El-Jaby, and Timothy F. L. McKenna, "Comparison of Emulsification Devices for the Production of Miniemulsions," vol. 48 (22), pp 10147–10151, 2009.

[68] S. Okushima, T. Nisisako, T. Torii, and T. Higuchi, "Controlled production of monodisperse double emulsions by two-step droplet breakup in microfluidic devices," *Langmuir,* vol. 20, pp. 9905-9908, Nov 9 2004.

[69] P. B. Umbanhowar, V. Prasad, and D. A. Weitz, "Monodisperse emulsion generation via drop break off in a coflowing stream," *Langmuir,* vol. 16, pp. 347-351, Jan 25 2000.

[70] R. Seemann, M. Brinkmann, T. Pfohl, and S. Herminghaus, "Droplet based microfluidics," *Reports on Progress in Physics,* vol. 75, Jan 2012.

[71] Y. J. Kang and D. Q. Li, "Electrokinetic motion of particles and cells in microchannels," *Microfluidics and Nanofluidics,* vol. 6, pp. 431-460, Apr 2009.

[72] D. Attwood and A. T. Florence, *Surfactant systems: their chemistry, pharmacy and biology*: Chapman and Hall, 1983.

[73] A. M. Schoeler, D. N. Josephides, S. Sajjadi, C. D. Lorenz, and P. Mesquida, "Charge of water droplets in non-polar oils," *Journal of Applied Physics,* vol. 114, p. 144903, 2013.
[74] P. Atkins, *Elements of Physical Chemistry*, 3rd ed.: Oxford University Press, 2002.
[75] D. Möbius, R. Miller, and V. B. Fainerman, *Surfactants: Chemistry, Interfacial Properties, Applications: Chemistry, Interfacial Properties, Applications*: Elsevier Science, 2001.
[76] N. V. Churaev, B. V. Derjaguin, and V. M. Muller, *Surface Forces*: Springer US, 2013.
[77] Malvern, "Zeta Potential Theory," ed: Zetasizer Nanoseries, 2008.
[78] M. Kaszuba, J. Corbett, F. M. Watson, and A. Jones, "High-concentration zeta potential measurements using light-scattering techniques," *Philosophical Transactions of the Royal Society a-Mathematical Physical and Engineering Sciences,* vol. 368, pp. 4439-4451, Sep 28 2010.
[79] R. J. Hunter, *Zeta Potential in Colloid Science: Principles and Applications*: Academic Press, 1988.
[80] C. Quilliet and B. Berge, "Electrowetting: a recent outbreak," *Current Opinion in Colloid & Interface Science,* vol. 6, pp. 34-39, 2001.
[81] K. Choi, A. H. C. Ng, R. Fobel, and A. R. Wheeler, "Digital Microfluidics," *Annual Review of Analytical Chemistry, Vol 5,* vol. 5, pp. 413-440, 2012.
[82] A. R. Wheeler, "Chemistry - Putting electrowetting to work," *Science,* vol. 322, pp. 539-540, Oct 24 2008.
[83] S. K. Cho and H. Moon, "Electrowetting on dielectric (EWOD): New tool for bio/micro fluids handling," *Biochip Journal,* vol. 2, pp. 79-96, Jun 20 2008.
[84] P. Mesquida, "Charge Writing with an Atomic Force Microscope Tip and Electrostatic Attachment of Colloidal Particles to the Charge Patterns," Doctoral Thesis, Technical Sciences, Swiss Federal Institute of Technology, Zurich, 2002.
[85] D. J. Im, M. M. Ahn, B. S. Yoo, D. Moon, D. W. Lee, and I. S. Kang, "Discrete Electrostatic Charge Transfer by the Electrophoresis of a Charged Droplet in a Dielectric Liquid," *Langmuir,* vol. 28, pp. 11656-11661, Aug 14 2012.
[86] D. S. Reichmuth, S. K. Wang, L. M. Barrett, D. J. Throckmorton, W. Einfeld, and A. K. Singh, "Rapid microchip-based electrophoretic immunoassays for the detection of swine influenza virus," *Lab on a Chip,* vol. 8, pp. 1319-1324, Aug 2008.
[87] D. Kohlheyer, J. C. T. Eijkel, A. van den Berg, and R. B. M. Schasfoort, "Miniaturizing free-flow electrophoresis - a critical review," *Electrophoresis,* vol. 29, pp. 977-993, Mar 2008.
[88] H. Aoki, H. Kurita, K. Takashima, T. Paillat, and A. Mizuno, "Generation of Water Droplet in Fluorocarbon Using Electrostatic Atomization," in *Industry Applications Society Annual Meeting (IAS), 2010 IEEE*, 2010, pp. 1-4.
[89] J. S. Eow, M. Ghadiri, A. O. Sharif, and T. J. Williams, "Electrostatic enhancement of coalescence of water droplets in oil: a review of the current understanding," *Chemical Engineering Journal,* vol. 84, pp. 173-192, Dec 2001.
[90] N. Naujoks, P. Mesquida, and A. Stemmer, "Electrical SPM-Based Nanofabrication Techniques," in *Scanning Probe Microscopy*, S. Kalinin and A. Gruverman, Eds., ed: Springer New York, 2007, pp. 833-857.

[91] E. M. Blanco, S. A. Nesbitt, M. A. Horton, and P. Mesquida, "A Multiprotein Microarray on Silicon Dioxide Fabricated by Using Electric-Droplet Lithography," *Advanced Materials*, vol. 19, pp. 2469-2473, 2007.
[92] P. Mesquida and A. Stemmer, "Attaching silica nanoparticles from suspension onto surface charge patterns generated by a conductive atomic force microscope tip," *Advanced Materials*, vol. 13, pp. 1395-1398, 2001.
[93] P. Mesquida and E. M. Blanco, "Microdroplets as a Tool for 'Soft' Patterning," *Proceedings of the Institution of Mechanical Engineers, Part N: Journal of Nanoengineering and Nanosystems*, vol. 223, pp. 113-119, September 1, 2009 2009.
[94] M. Fluorinert™, "electronic Liquid FC-77, Product Information," ed. St. Paul, Minnesota, USA, (access date 15 February 2011).
[95] P. Mesquida, E. M. Blanco, and R. A. McKendry, "Patterning amyloid peptide fibrils by AFM charge writing," *Langmuir*, vol. 22, pp. 9089-9091, Oct 24 2006.
[96] P. Mesquida and A. Stemmer, "Maskless nanofabrication using the electrostatic attachment of gold particles to electrically patterned surfaces," *Microelectronic Engineering*, vol. 61-2, pp. 671-674, Jul 2002.
[97] Y.-M. Jung, H.-C. Oh, and I. S. Kang, "Electrical charging of a conducting water droplet in a dielectric fluid on the electrode surface," *Journal of Colloid and Interface Science*, vol. 322, pp. 617-623, 2008.
[98] J. Hølto, G. Berg, and L. E. Lundgaard, "Electrocoalescence of Drops in a Water-in Oil Emulsion," in *2009 Annual Report Conference on Electrical Insualtion and Dielectric Phenomena*, 2009 pp. 196 - 199.

Chapter 2 Methodology

2.1 Chapter Abstract

This Methodology chapter describes the way in which the electrophoretic mobility of water droplets was measured by optical microscopy and the droplet charge was determined. Two types of electrophoresis are discussed and reasons for using single droplet electrophoresis are explained. The chapter highlights the effect that liquid-liquid slip at the water-oil interface has on interpreting electrophoretic measurements quantitatively and outlines a process for calibrating any electrophoretic set-up.

2.2 Multiple Droplet Electrophoresis

The literature has focused on two types of microdroplet electrophoresis used to determine the charge of water droplets dispersed in oil [1-14]. In one method, numerous droplets are dispersed in oil [1-4], whilst the other is concerned with the electrophoresis of a single droplet [5-14].

The advantage of analysing multiple droplets at the same time is the ease at which these emulsions can be produced using ultrasound. First used for the creation of emulsions by Wood and Loomis in the 1920s [15], ultrasound has become an effective method for creating emulsions, with ultrasonic wave frequencies ranging from 20 kHz to tens of MHz [16-18]. Ultrasonic waves are generated either electronically (magnetostrictive transducers, reverse piezoelectric effect) or mechanically (siren, whistle) [19, 20].

Although the precise reasons for droplet rupture are not fully established [21], Bondy's suggestion of cavitations (i.e. the formation, growth and impulsive collapse of bubbles in a liquid) being the main source of droplet rupture, is widely accepted in the field [22]. When a digital sonifier is immersed inside a water-and-oil mixture (Figure 2.1), the

ultrasonic waves induced create unstable bubbles (cavitations, Figure 2.1b), which, upon implosion near the phase boundary, become areas of high pressure, which cause the dispersed fluid to rupture into smaller droplets.

(a) (b)

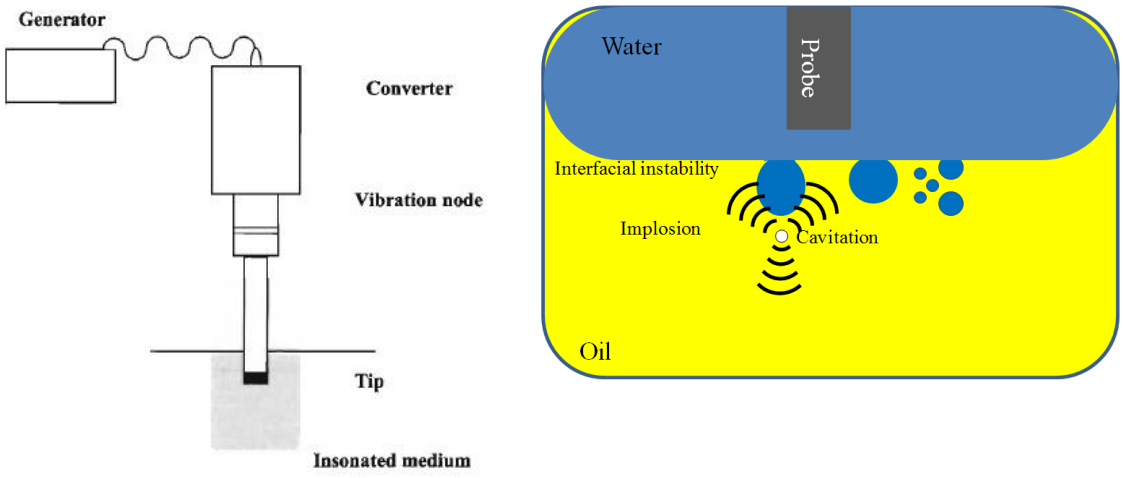

Figure 2.1 Ultrasonic emulsion creation a) type of piezoelectric transducer used in experiments (image taken from [19]). b) Schematic image depicting the creation of a water-in-oil emulsion using ultrasound

Li and Fogler [23, 24] describe the process of drop formation as a two-step process, which begins with primary interfacial instability that leads to the rupture of dispersed phase droplets into the continuous phase. This is followed by transient cavitation, generating micro streaming and high pressure shock waves, creating extremely small droplets (Figure 2.2). Cavitations occur when, during the sonication process, the ultrasound pressure amplitude reaches a critical value, known as cavitational threshold [21, 25, 26].

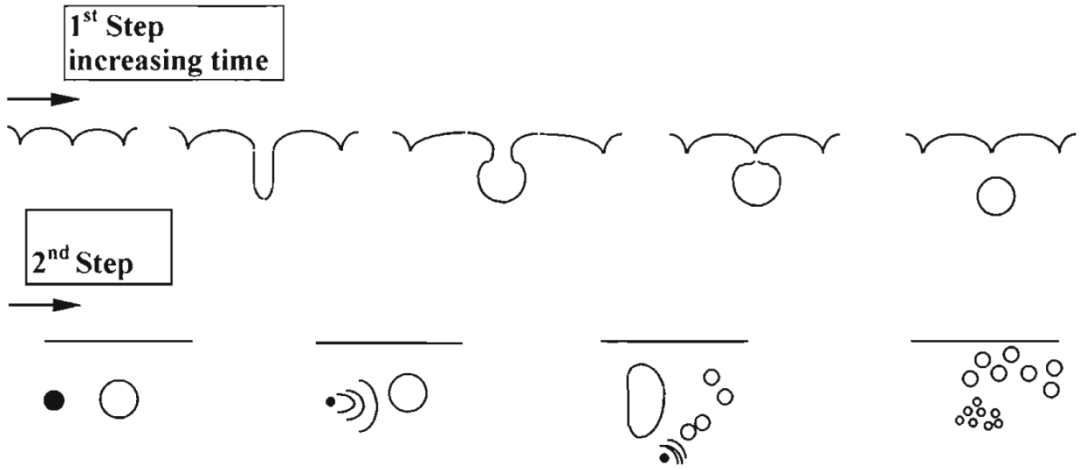

Figure 2.2 Two-step droplet formation as described by Li and Fogler [19]

The viscosity of the continuous phase has a great effect on the cavitational threshold as it is the adhesive force between the liquid molecules; the greater the viscosity, the greater the adhesion force and the greater the cavitational threshold [21]. Nazarzadeh et al. [16] reported that, for oil-in-water emulsions, the viscosity ratio (dispersed/continuous phase) is of importance and found that the smallest droplet sizes can be produced using a viscosity ratio of around 1.0. They argued that this achieves the maximum efficiency for energy transfer. It has also been reported that smaller droplets are formed in the presence of surfactant and at longer sonication times [27, 28].

To conduct and investigate the electrophoretic mobility of water droplets, a vessel (also known as an electrophoretic cell) that contains the continuous oil phase and two electrodes is needed. One such device has been presented by Mesquida [1] (Figure 2.3), which consisted of two electrodes, which were exposed to the continues oil phase and encased in PMMA and glued with silicone sealant to a microscope glass slide. The electrodes were a distance, d = 500 μm, apart and connected to a DC power supply. To investigate the electrophoretic mobility of the water droplets, water-in-oil dispersions without surfactant were created using an ultrasonic bath. The polydisperse emulsion

was then transferred to an electrophoretic cell and a combined voltage of ΔV = +66 V was applied across the two electrodes.

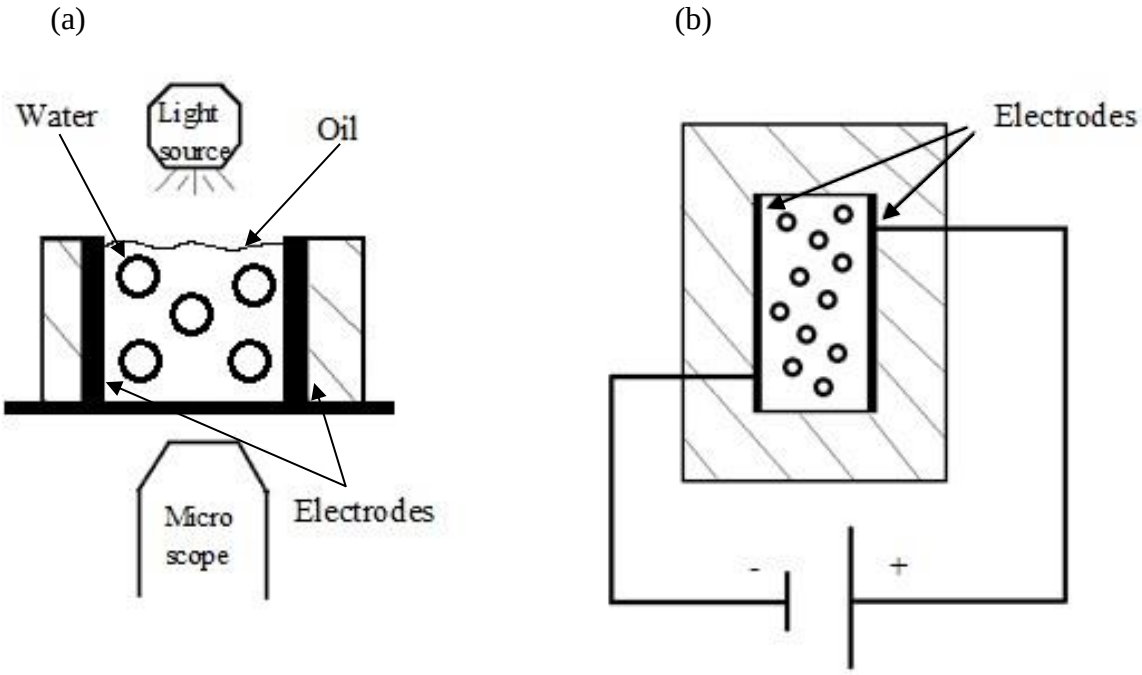

Figure 2.3 Schematic image of the multiple droplet electrophoretic cell design, side view (a) and top view (b).

Stefanidis [4] and others [1-3] observed that the electrophoretic mobility of water droplets in the oil, $\vec{v}_{elec}$, is always superposed by the collective movement of the droplets together with the continuous phase, due to convection flows, $\vec{v}_{conv}$. Therefore, the following expression for the total velocity, $\vec{v}$, was defined as [1]:

$$\vec{v} = \vec{v}_{conv} + \vec{v}_{elec}, \qquad \text{Equation 2-1}$$

To differentiate between $\vec{v}_{conv}$ and $\vec{v}_{elec}$, an alternating voltage between 0V and 66V was applied with a frequency of 1 Hz, so that the field was off for the first 0.5 seconds, followed by a 0.5 s period where the field was present. Therefore to find the electrophoretic mobility, $\vec{v}_{elec}$, of the water droplets, assuming that the conditions

within the cell do not change, velocity $\vec{v}_{conv}$ (E = 0 V/mm) was subtracted from $\vec{v}$ ($E \neq 0$ V/mm).

2.2.1 Multiple Droplet Electrophoresis – Experimental Set-Up

Water-in-oil emulsions were created using a digital sonifier (Branson 450, Ultrasonic Corp., 400W, frequency 19.850–20.050 kHz), at various amplitudes (Figure 2.1a). In total, four non-polar, non-conductive oils were investigated: two fluorocarbons (FC-77 and perfluorodecalin) and two alkanes (hexadecane and n-heptane). For all experiments (unless otherwise specified), a 40 g water-in-oil dispersion was created with 1% water (i.e. 0.4 g) and 99% oil (i.e. 39.6 g). The mixture was placed in a 50 ml beaker and a sonication horn was immersed in the solution. To reduce the effect of temperature increase when using the sonifier, the beaker was placed inside an ice bath. Each sample was continuously sonified for 30 s. An inverted microscope with a 20x objective, mounted with a Moticam 3000 camera, was used to take dispersion snapshots, so that droplet diameters could be investigated. Several droplets were measured and the average droplet size was calculated. Figure 2.4 depicts an example of an analysed snapshot.

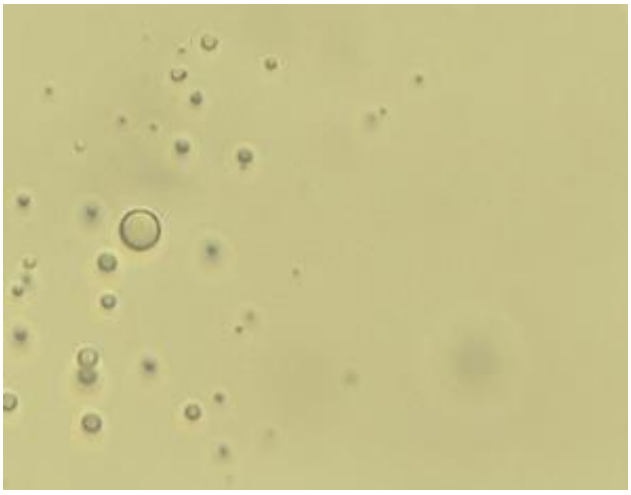

Figure 2.4 Example of 1% water dispersed in FC-77 - after 30s sonication at 360 W.

It has already been shown that water nano-emulsions can be created in n-heptane using surfactant Span 83 and a simple homogeniser [29]. Therefore the possibility of creating surfactant-free water nano-emulsions using ultrasound and the effect of the ultrasonication power on water droplet size in n-heptane was studied. To reduce the effects of coalescence, a small water volume fraction of ø = 0.01 was chosen.

80 µl of the dispersion were transferred to the electrophoretic cell (Figure 2.3), using a micropipette (Finnpipette® Focus single channel pipette – volume 1-100 µl, Sigma-Aldrich, Dorset, UK). The cell was placed on top of an inverted microscope with a 20x objective, which was connected to a camera (Moticam 3000, Motic, Causeway Bay, Hong Kong). The electrodes within the cell were a distance, d = 500 µm, apart and connected to three DC power supplies (two Rapid DC Power Supplies and one Manson EP-603, 0-120V). A combined voltage of ΔV = 100 V (E = 2 kV/cm) was applied across the two electrodes and the electrophoretic cell was cleaned after each experiment.

Motic Image software was used to record short videos of the electrophoretic motion of the water droplets in oil. It was decided to observe the mobility of the water droplets at the midplane of the cell to reduce the effect of convection at the top (due to oil evaporation) and wall effects at the bottom of the cell. Image sequences were then extracted using the VirtualDub software (version 1.9.11, [30]) and droplet movement was analysed in ImageJ (version 1.46r, [31]), using the MtrackJ plug-in.

2.2.2 Effects of Ultrasonic Amplitude on Droplet Size

Figure 2.5 shows that the average droplet size increases with ultrasonication power, which can be accredited to the fact that a higher energy input aids coalescence [27]. An increased energy input results in a significant temperature rise, which means that the viscosity of the dispersed phase and thus the interfacial tension is reduced. This agrees

with what has been discussed by Canselier [19] and observed by Higgins [32], who investigated oil-water emulsions. The standard deviation rises at higher ultrasonic amplitudes as the polydispersity of the emulsion is increased.

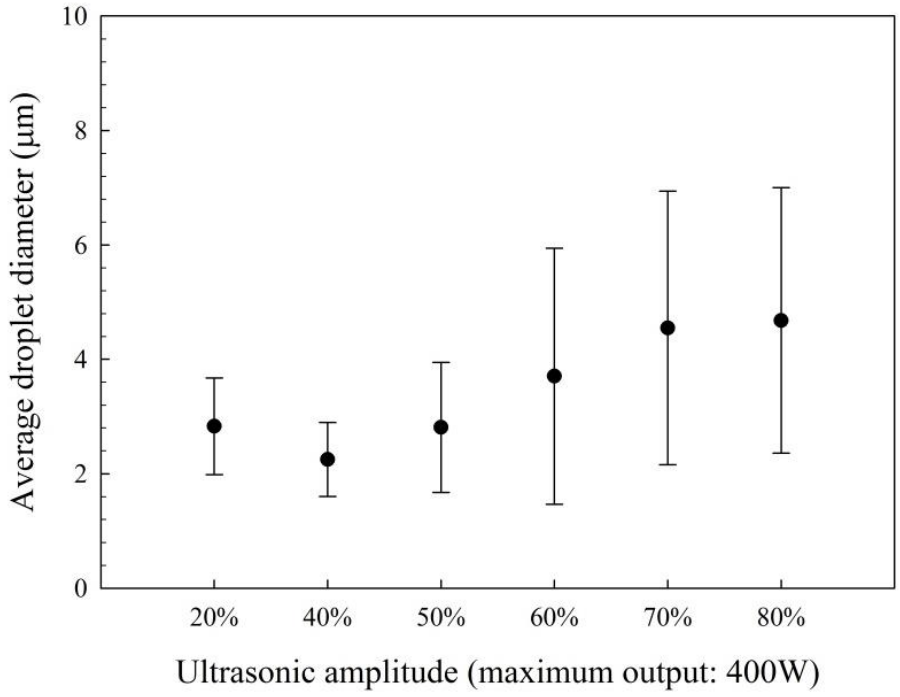

Figure 2.5 1% water in n-heptane without surfactant sonified at various amplitudes. Error bars represent the standard deviation of the average droplet size.

Further experiments were conducted with three other oils, FC-77, perfluorodecalin (PFD) and hexadecane to investigate whether a similar trend would occur. It can be seen from Figure 2.6 that increasing the amplitude has no effect on decreasing the average droplet size in the additional three oils investigated. In fact, average water droplet size increased with higher amplitudes for PFD and the hydrocarbon oils. However, the difference in droplet size decreases with increasing viscosity ratio, and is smallest for ratios close to 1, which agrees with results presented by Nazarzadeh et al. [16]. It

appears that at low ultrasonic amplitude, smaller average droplet sizes were achieved at low viscosity ratios.

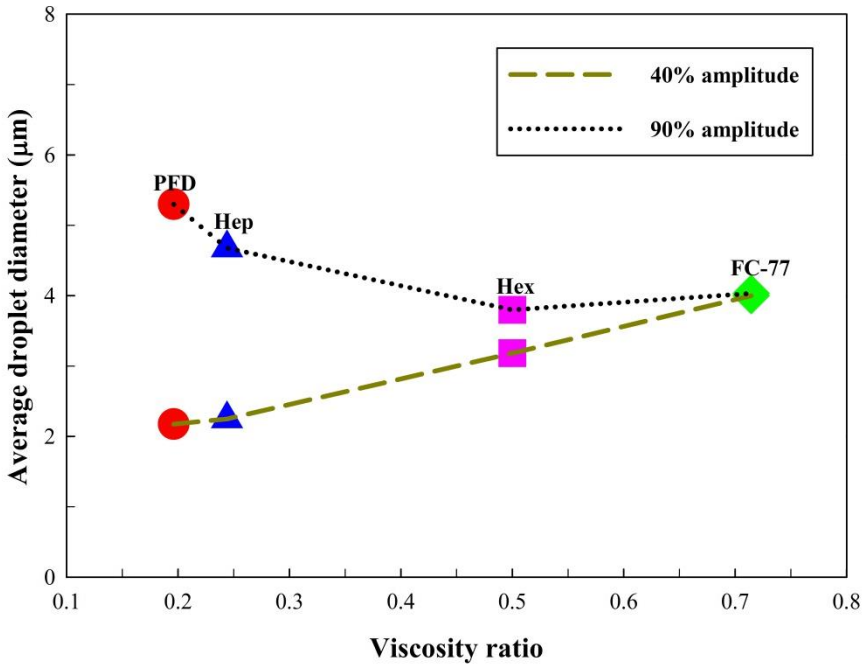

Figure 2.6 Average droplet diameter versus viscosity ratio in Perfluorodecalin (red dot), n-heptane (blue triangle), hexadecane (purple square) and FC-77 (green diamond).

These results show that that water-in-oil emulsions can be created using ultrasound, although in the absence of surfactant it was not possible to create stable, monodisperse emulsions. Increasing ultrasonic amplitude had no profound effect on average droplet size, independent of the viscosity ratio (Figure 2.6) at the given frequency of 20 kHz. This makes it unsuitable for use in electrophoretic experiments and it would be more beneficial to consider other forms of emulsification, such as microfluidisation.

2.2.3 Additional Experimental Complications

Other complications were identified when employing the experimental set-up outlined above. The direction of droplet flow differed depending on their positon within the cell. It was observed that water droplets near the glass/oil interface at the bottom of the cell would flow towards the negative electrode, which would indicate a net, positive droplet charge. However, near the air/oil interface at the top of the cell, water droplets would travel in the opposite direction (i.e. towards the positive electrode). It has been observed by Stefanidis [4] that vortices appear near the oil/air interface, due to the rapid evaporation of fluorocarbon oils at room temperature, which could explain this phenomenon. Alternatively, the high volume fraction of water within oil could cause this difference in droplet migration. Consider a cluster of droplets with a given charge, which becomes attracted to an electrode as a voltage is applied. This mass movement of droplets will, in effect, displace oil, which in turn could displace water droplets of less charge going in the opposite direction, therefore creating a variation in flow within the cell. Another reason for the varying droplet movement could have been the fact that the droplets oscillate at different speeds depending on their size once they have made contact with a biased electrode, as observed by Hase and others [8, 33, 34].

Secondly, one must consider the potential for electrocoalescence in a multi-drop system. Holto et al. [2] showed that, at high water volume fractions, water droplets may gain a charge by contact with another droplet or coalesce when droplets have an opposite charge. To further illustrate this, an experiment, which focused on two monodisperse droplets (droplet A and B, Figure 2.7a) carrying an equal but opposite charge, was conducted, where droplets A and B carried a charge of 2×10^{-11} C and -2.6×10^{-11} C, respectively (details of how the charge was calculated is discussed in section 2.3.2). Figure 2.7 shows how the droplets move towards each other (Figure 2.7a and Figure

2.7b), before coalescing (Figure 2.7c) and forming a larger droplet, C (Figure 2.7d). Droplet C then continues to travel towards the positive electrode with a combined, measured charge of -0.6×10^{-11} C.

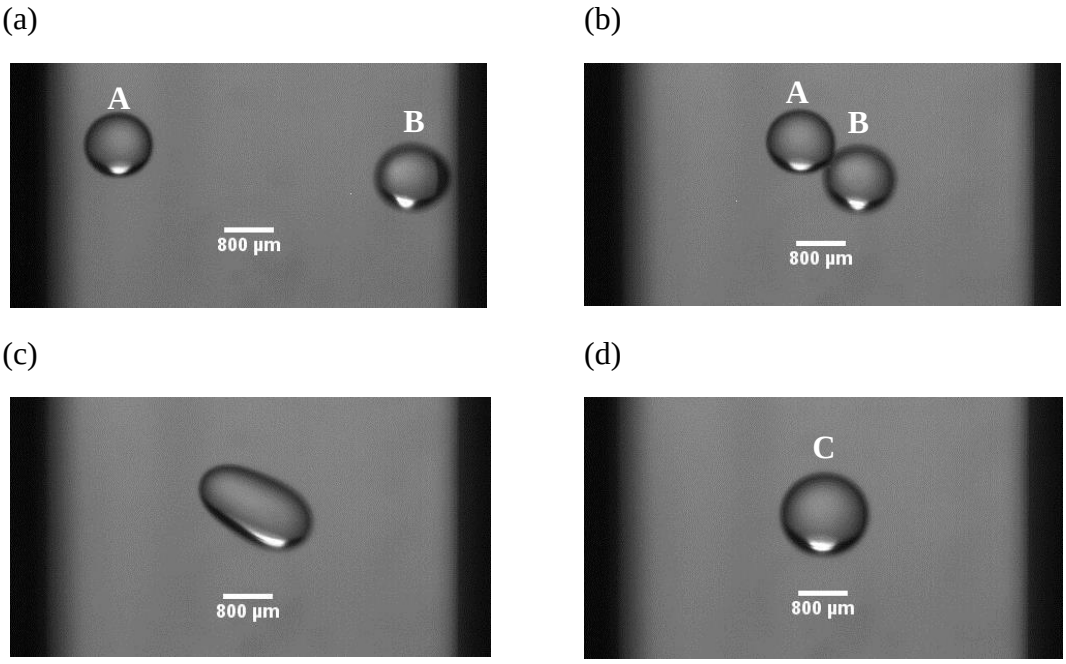

Figure 2.7 Two droplets of opposite charge coalescing a) after touching negative (left) and positive electrode (right) at time, t = 7.83s b) before contact, t = 8.04s c) moment of coalescence, t = 8.05s d) larger coalesced droplet, t = 8.10s. Letters A, B and C are droplet markers.

2.2.4 Multiple Droplet Electrophoresis – Conclusion

As will be discussed in chapters 3, 4 and 5, water droplets clearly undergo discharging and re-charging with opposite polarity when making contact with a biased electrode [8, 12, 34-39]. Using a multiple droplet electrophoretic, microscopic set-up, only droplets in the middle of the electrophoretic cell could be investigated, which made it impossible to differentiate between the initial electrophoretic motion of droplets (i.e. before contact with an electrode) and the electrophoretic motion of droplets after they had made contact with an electrode. This, combined with the difficulties of producing stable, monodisperse water-in-oil emulsions using ultrasound, led to the conclusion that the

analysis of initial electrophoretic mobility of water under high electric field strength should not be performed with multiple droplets.

2.3 Single Droplet Electrophoresis

A different approach to analysing the electrophoretic motion of water is single droplet electrophoresis (SDE) – the study of a single water droplet dispersed in a continuous oil phase. It is important for SDE that one is able to control the droplet's size, which can best be achieved using microfluidic devices. Microfluidics enables the user to process and manipulate fluids within microchannels, where at least one dimension such as diameter or width, is less than 1mm [40]. It is an emerging science, which offers a variety of applications [41] ranging from the precise production of drug delivery systems [42] to droplet manipulation schemes [43].

Different styles of SDE apparatus have been described in the literature [5-14]. However, they all follow a basic structural design. A set of electrodes is attached to a transparent container (cuvette), also known as a cell, and filled with the continuous oil phase. The cell is then placed in between a light source and a high speed camera. Using a micropipette, a single droplet is injected into the oil, the electric field is applied and the motion of the droplet is tracked by the camera (Figure 2.8).

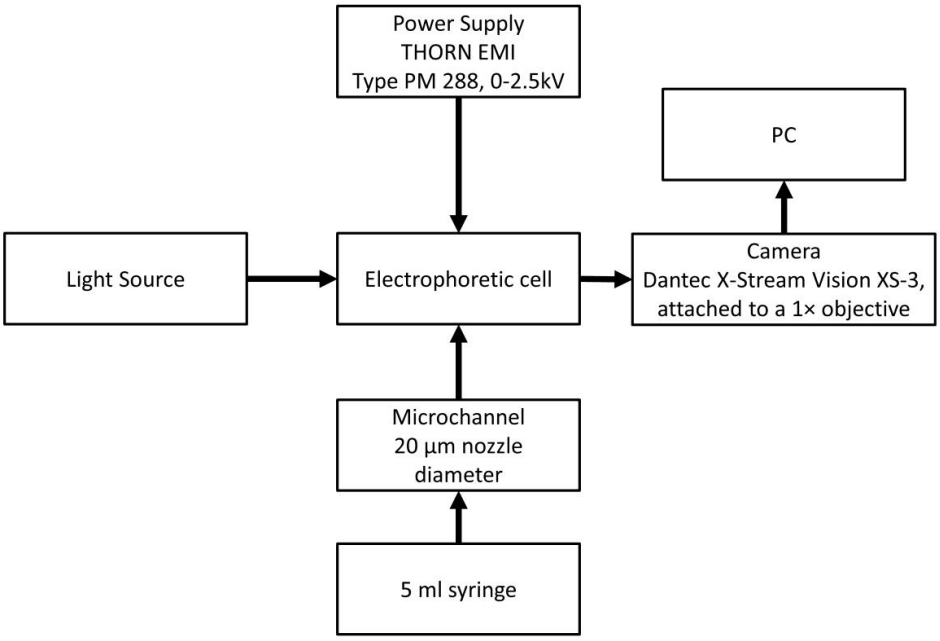

Figure 2.8 Block Diagram of a typical SDE experimental set up, used for experiments within this thesis

2.3.1 Experimental Apparatus

In order to investigate single droplet electrophoresis, a new cell was built. Two flat, bare copper plate electrodes were attached to the inside of a transparent, rectangular polystyrene cuvette (4.5 cm high and 1 cm × 1 cm base area) with a 6.5 mm gap (Figure 2.9a) and connected to a DC voltage power supply (0 – 2 kV). The cuvette was filled with either silicone or paraffin oil and positioned between a light source and a high-speed camera (Dantec X-Stream Vision XS-3, attached to a 1× objective). One water droplet was injected individually into the oil using a 20 µm sized (inner diameter) hydrophobic glass micropipette. Each pipette was fabricated by pulling glass capillaries (Inner Diameter 0.7 mm, Outer Diameter 1 mm) to fine, tapered ends (nozzle diameter < 1 µm), using a pipette puller (P-1000, Sutter Instrument, Novato, USA). The ends of the capillaries were then cut by diamond-scoring to a 20 µm nozzle diameter,

before being cleaned using low-pressure air plasma (Plasma cleaner Femto timer (version 1), Diener Electronic, Ebhausen, Germany). The clean glass micropipettes were then placed inside a sealed glass container and heated in an oven at 120ºC for one hour in the presence of 0.2 ml octadecylmethoxsilane (FluroChem, Hadfield, UK), which evaporated and thereby coated the inside and outside of the glass channels with a hydrophobic layer. The dish was then allowed to cool and the hydrophobicity was tested by comparing contact angles of water between a coated and a non-coated micropipette. The oils prevented any current flow due to their extremely high resistivity and, as the water microdroplets used in all experiments were much smaller than 6.5 mm, they could not bridge the gap and accidentally cause a short-circuit.

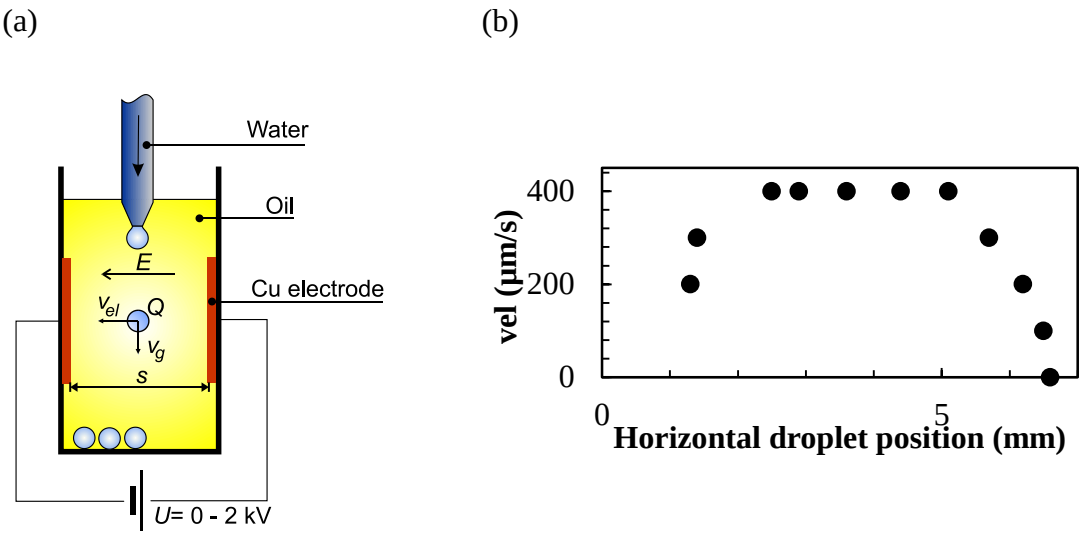

Figure 2.9 a) Vertical set-up for electrophoretic measurements. Individual water droplets are injected into the oil and sink to the bottom of the cuvette with a gravitational terminal velocity, v_g. Once the droplet reaches the middle between the Cu electrodes separated by a distance, s, the voltage, U, is applied, creating a homogenous electric field, E, that causes the droplet carrying a net charge, Q, to be displaced with a horizontal velocity component, v_{el}, due to Coulomb force. b) Velocity, v_{el}, in silicone oil as function of horizontal position between electrodes in (a), where 0 represents the contact made between droplet and electrode on the left, and 6.5 mm represents the droplet making contact with the electrode on the right; droplet radius = 830 µm; E = 1.1 kV/cm.

2.3.2 General Measurement Principle

The general principle of determining droplet charge, Q, by micro-electrophoresis is to subject an individual droplet to a homogenous, electric field, E, which leads to the Coulomb-force, $F_C = QE$, acting on the droplet. If E is orientated as in Figure 2.9a, then gravity and buoyancy do not need to be taken into account. When the field is applied, the droplet is accelerated and, due to the viscosity of oil, quickly reaches a constant, terminal velocity, v_{el}, determined by the balance of F_C and the hydrodynamic drag force, F_D. For small Reynolds numbers, the drag force is usually described by Stokes' drag, F_s, which is derived from the Navier-Stokes equation and is a frictional force, which acts on a sphere moving in a viscous fluid [44, 45]:

$$F_S = 6\eta\pi Rv \qquad \text{Equation 2-2}$$

where η = dynamic viscosity of the oil, R = droplet radius and v = droplet velocity.

In order to measure the droplet velocity, v_{el}, high-speed images (100 fps, 20 µm/pixel) of individual, moving droplets were recorded. Each water droplet was injected individually into the oil using a 20 µm sized (inner diameter) hydrophobic glass micropipette, which was filled with water. The droplet size was controlled by adjusting the pressure within the pipette. Once the droplet reached the desired size within the oil, it was detached by lowering the cuvette and, thus, shearing and detaching the droplet from the micropipette. As water has a higher density than oil, the droplet fell slowly in vertical direction due to gravity. To reduce possible residual charging of the electrodes, their polarity was alternated after each individual droplet experiment. The velocity of the droplets was measured in the middle of the cuvette, where the side-wall effects could be assumed to be minimal and where the terminal velocity had been reached (Figure 2.9b). At terminal velocity $F_C = F_S$, and the charge, Q, can be calculated from

$$Q = \left(\frac{6\eta\pi Rs}{U}\right)v_{el}$$ Equation 2-3

where $E = U/s$, s = the gap between the electrodes, U = the voltage applied between the electrodes and v_{el} = the horizontal velocity component of the droplet motion, which is parallel to the electric field lines (Figure 2.9a).

All experiments were conducted at 21ºC.

2.3.3 Wall Effect and Slip Correction

Stokes' drag, F_S, is derived from the Navier-Stokes equation. If the particle is falling under gravity, it will reach terminal velocity when the buoyancy, drag and gravitational forces are balanced, which under Stokes is defined as:

$$v_{Stokes} = \frac{2}{9}\frac{(\rho_w - \rho_{oil})}{\eta}R^2,$$ Equation 2-4

where ρ_w and ρ_{oil} are the density of water and oil, respectively.

However, Stokes' drag, or Stokes' law, applies to rigid, spherical particles with smooth surfaces, where a no-slip condition is assumed at the particle/medium interface. Also, the medium must be infinitely extended, *i.e.*, the particle must be unaffected by any wall-effects or interaction with other particles.

For a liquid particle, such as a water droplet, it must be taken into account that shear force at the droplet/oil interface can lead to liquid flows at the surface of and within the droplet. In this case, an analytical expression for the drag force cannot be derived from first principles anymore and empirical models must be used. Depending on the model, results can differ by as much as 33% [38] (Figure 2.11).

Previous works have established a variety of models for terminal velocity prediction of a spherical droplet moving in a quiescent fluid under gravity/buoyancy [44-49], including alterations of Stokes' drag, such as Hadamard-Rybczynski drag [47], Ladenburg drag [48] and Happel-and-Bart drag [49]. Often, multiplication factors are experimentally determined and applied to the generic expression for the velocity of a falling/buoyant droplet subject to pure Stokes' drag in a quiescent fluid.

Hadamard and Rybczynski [47] were the first to independently derive an analytical expression for the fluid motion around a spherical bubble with no surfactants present and altered Stokes' drag by multiplying the drag expression by a coefficient, λ, which accounts for the effects of the different viscosities inside (η_w) and outside of the sphere (η_{oil}), where the terminal velocity of the bubble is defined as [47]:

$$v_{HR} = \frac{2}{3}\frac{R^2 g(\rho_w - \rho_{oil})}{\eta_{oil}}\lambda, where\ \lambda = \frac{\eta_{oil}+\eta_w}{2\eta_{oil}+3\eta_w} \quad \text{Equation 2-5}$$

Fulmer et al. [50] pointed out that the extent of the liquid and the height of the cylindrical column of liquid (or, in this particular case, the height of the electrophoretic cell) affect the rate at which the droplet falls.

By solving two hydrodynamic equations, Ladenburg [48] was able to account for variations in the volume of the liquid and the height of the liquid column and, thus, analytically and experimentally arrived at an equation for the terminal velocity of a rigid sphere falling in a cylinder:

$$v_{Ladenburg} = \left\{\frac{2}{9}\frac{(\rho_w - \rho_{oil})}{\eta_{oil}}R^2 g\right\} / \left\{(1 + \frac{2.4R}{r_{cylinder}})(1 + \frac{3.3R}{h_{cylinder}})\right\} \quad \text{Equation 2-6}$$

Where $r_{cylinder}$ is the inside radius of the cylinder and $h_{cylinder}$ the height of the cylinder.

Happel and Bart [49] analysed Ladenburg's drag approximation to determine an expression for drag on a droplet inside a square duct. They developed a new, general solution in Cartesian coordinates for a sphere settling under creeping-motion conditions along an axis of a square duct and a first correction of Stokes' drag was obtained:

$$v_{HBterminal} = \left\{\frac{2}{9}\frac{(\rho_w - \rho_{oil})}{\eta_{oil}} R^2 g\right\} / \left\{(1 + 1.903266\frac{R}{l})\right\} \quad \text{Equation 2-7}$$

However, all these correction factors are specific to a particular experimental set-up and contain various parameters, such as viscosities, as well as geometric parameters of the set-up [47-50]. It was therefore decided to calibrate a drag correction factor specific to the experimental set-up used in all experiments.

2.3.4 Determination of Drag Correction Function C(R)

Figure 2.10 shows an experiment to determine the correction factor to account for the specific parameters of the system, such as viscosity, internal flows, slip etc. As the droplet charge and, thus, F_C is not known, gravity was used to apply the known force:

$$F_g = mg = BR^3, \quad \text{Equation 2-8}$$

with B=(4/3)$\pi\rho g$=const and $\rho = \rho_w - \rho_{oil}$, the difference between the density of water, ρ_w, and oil, ρ_{oil}, respectively. The terminal velocity, v_g, and the radius, R, are determined by video-imaging droplets of different sizes.

The cuvette was rotated by 90° compared to Figure 2.9a (Figure 2.10), so that the droplets fell in the same direction and under the similar geometric parameters (the electrodes were removed in order to allow for space to detach a droplet) as in the later electrophoretic experiments under the electric field.

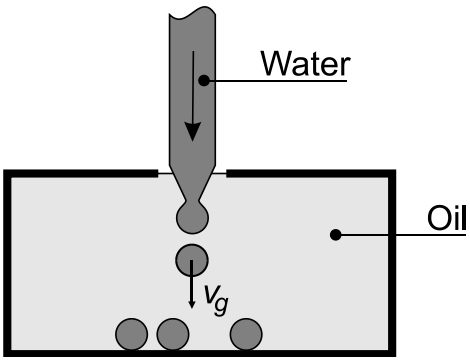

Figure 2.10 Horizontal set-up for drag force calibration. The cuvette is rotated by 90° and the electrodes are removed; the droplets sink with gravitational terminal velocity, v_g.

In analogy to earlier works [8, 9, 34, 36, 51], it was assumed that the drag force, F_D, is best described by Stokes' drag, F_S, with a correction function, *C(R)*,

$$F_D = F_S C(R) = A v_g R C(R) \qquad \text{Equation 2-9}$$

with $A=6\eta\pi$.

v_g was measured against *R* to determine *C(R)* from the force balance $F_D = F_G$ and, thus,

$$A v_g R C(R) = B R^3$$

$$\therefore v_g = \frac{BR^2}{AC(R)}, \qquad \text{Equation 2-10}$$

with $A=6\eta\pi$, $B=(4/3)\pi\rho g$ and $\rho=\rho_w - \rho_{oil}$, the difference between the density of water, ρ_w, and oil, ρ_{oil}, respectively.

It must be stressed that *C(R)* includes the hydrodynamic properties of the particular liquids used and the geometric parameters of the cuvette, which means that a change of the viscosities, the cuvette or the direction of the motion would require recalibration. In the electrophoretic measurements, Q can then be determined from the force balance $F_D = F_C$:

$$\boldsymbol{Q = \frac{AC(R)v_{el}R}{E} = \frac{AC(R)sv_{el}R}{U}} \qquad \text{Equation 2-11}$$

(a) silicone oil (b) paraffin oil

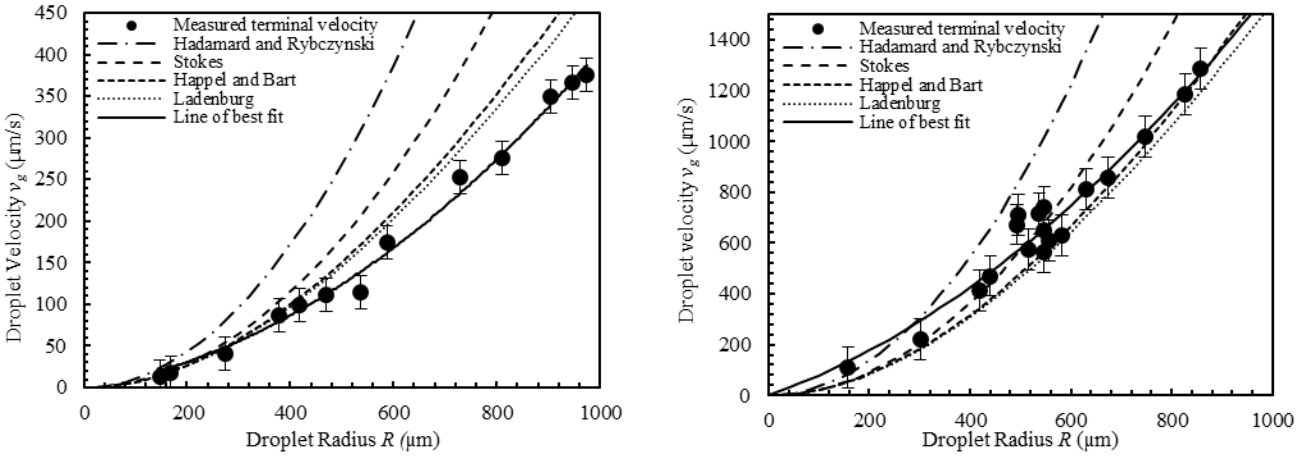

Figure 2.11 Dependence of terminal velocity, v_g, on droplet radius in with horizontal set-up from Figure 2.10, fitted to the experimental data using the least-squares method; Hadamard-and-Rybczynski drag calculated with $C(R)= (2\eta_{oil} + 3\eta_w)/(\eta_{oil} + \eta_w)$ in Equation 2-10; Stokes' drag with $C(R) = 1$ in Equation 2-10; Happel-and-Bart drag with $C(R) = (1 + 380.7\ m^{-1}\ R)$ in Equation 2-10; Ladenburg drag with $C(R) = (1 + 106.7\ m^{-1}\ R)\ (1 + 330\ m^{-1}\ R)$ in Equation 2-10. (a) for silicone oil: Continuous line: $v_g(R) = aR^2+bR$, with $a = 315\ s^{-1}m^{-1}$ and $b = 0.1\ s^{-1}$, standard deviation of replication experiments = 10µms^{-1}, measurement accuracy of v_g approx. 20 µms^{-1} (error bars) (b) for paraffin oil: Continuous line: $v_g(R) = aR^2 + bR$, with $a = 905\ s^{-1}m^{-1}$ and $b = 0.7\ s^{-1}$, standard deviation of replication experiments = 80µms^{-1} (error bars).

Figure 2.11 shows the data from the droplet fall experiments. The terminal velocities of deionised water droplets, v_g, were determined against their radii, R, which ranged from 150 µm to 1 mm, in silicone (Figure 2.11a) and paraffin oil (Figure 2.11b). With the constraint that $v_g(R = 0) = 0$, the best fit function to the data was found to be the 2nd-order polynomial $v_g = aR^2 + bR$ (with $a_{silicone} = 315.3\ s^{-1}m^{-1}$, $b_{silicone} = 0.0906\ s^{-1}$, $a_{paraffin} = 905\ s^{-1}m^{-1}$ and $b_{paraffin} = 0.7008\ s^{-1}$) Thus equating:

$$v_g = \frac{BR^2}{AC(R)} = aR^2 + bR, \qquad \text{Equation 2-12}$$

yields

$$AC(R) = \frac{BR}{aR+b}, \qquad \text{Equation 2-13}$$

which can be used to calculate Q in Equation 2-11. This function now takes into account the geometry of the cuvette and possible slip at the droplet oil interface. It is used in all subsequent electrophoretic measurements.

By determining Q, the surface charge density, σ, is calculated as follows:

$$\sigma = \frac{Q}{A} = \left\{ \frac{s v_{el} R^2}{U} \frac{(4/3)\pi\rho g}{aR+b} \right\} / A, \qquad \text{Equation 2-14}$$

where Q = droplet charge, A = surface area of a spherical droplet, s = distance between the electrodes, v_{el} = velocity of the droplet, R = radius of the droplet, U = applied voltage, ρ = density difference between dispersed and continuous phase, g = gravitational acceleration. The quantities a and b are the oil-specific, hydrodynamic drag coefficients determined above using Equation 2-13.

The main measurement uncertainties are those of the radius, R (± 20 µm), and of the droplet velocity, v_{el}, (± 30 µms^{-1}). The uncertainty of s and U can be neglected, and the independent calibration of a and b introduces a possible, systematic error in the magnitude of σ of about 35%. From the error propagation in Equation 2-14 [52], the measurement uncertainty of σ can be estimated to approximately ±3.4 ×10^{-7} Cm^{-2} in silicone and ±2.8 ×10^{-7} Cm^{-2} in paraffin oil.

2.4 Estimation of Droplet Deformation

The interfacial tension, γ, between silicone oil and water was measured as 38.2 mN/m and as 41.0 mN/m between paraffin oil and water, using the pendant drop method (FTÅ200, First Ten Angstroms, Inc., Virginia, USA). These were used to calculate the electrical Weber number, the ratio of the restoring interfacial tension force and the

deforming electrical field force. In the work described in this thesis, the electrical Weber number, $We_{electric} = \varepsilon_{oil} E^2 R \gamma^{-1}$, ranged from 0.006 to 0.116 in silicone and from 0.006 to 0.041 in paraffin oil. Both were much smaller than 1, indicating very small and therefore negligible droplet deformation. This was confirmed by visual observation of the videos; pure water droplets did not deform significantly from their spherical shape within the measurement accuracy.

2.5 Droplet Tracking (Matlab)

As already discussed, high-speed images (100 fps, 20 µm/pixel) of individual, moving droplets were recorded, in order to measure the droplet velocity, v_{el},. This droplet tracking mechanism was automated by adapting the Circular Hough Transform Function in Matlab [53], where droplets were tracked over time. A graphical user interface (GUI) was designed using Matlab's GUI development environment (GUIDE), which is called by running the function *untitled.m* (Appendix A). The user selects the image folder (Figure 2.12A) and loads the images into the GUI (Figure 2.12B). The images will be previewed in the adjacent panel (Figure 2.12H) and the user can manipulate the sliders next to the panel to zoom in/out ((Figure 2.12I) or to review all images (Figure 2.12J). Once the images have been uploaded, the user can define the radius of the droplet using slider on the left (Figure 2.12D) or by typing the radius size into the box below. The preview button (Figure 2.12C) allows the user to check the droplet size within the image. Should the droplet size be two small or too large, the slider needs to be adjusted accordingly. A sampling frequency can be defined by using the slider or text box provided (Figure 2.12E). Once droplet size and sampling frequency have been set, the "Track droplet" button is pushed (Figure 2.12F), which calls the function *andreasgui2* (Appendix B) and the droplet size and position is recorded for each image (based on the frequency set). All data points are saved into a

tracked.mat matrix file in the image folder and displayed in the table inside the GUI (Figure 2.12K). The table allows the user to define the image scale (in pixels/μm) and the voltage applied (in V). The compute button calls the *andreascompute2.m* function (Appendix C), which analyses the image sequence recorded to determine the velocities of the droplet before and after contact with the electrodes. Using these sequences, the initial charge of the droplet before contact, *Q*, the charge after first contact, *Q2*, and the charge after second contact, *Q3*, are calculated using Equation 2.11. As an additional control measure, all velocities were also recorded in an Excel spreadsheet.

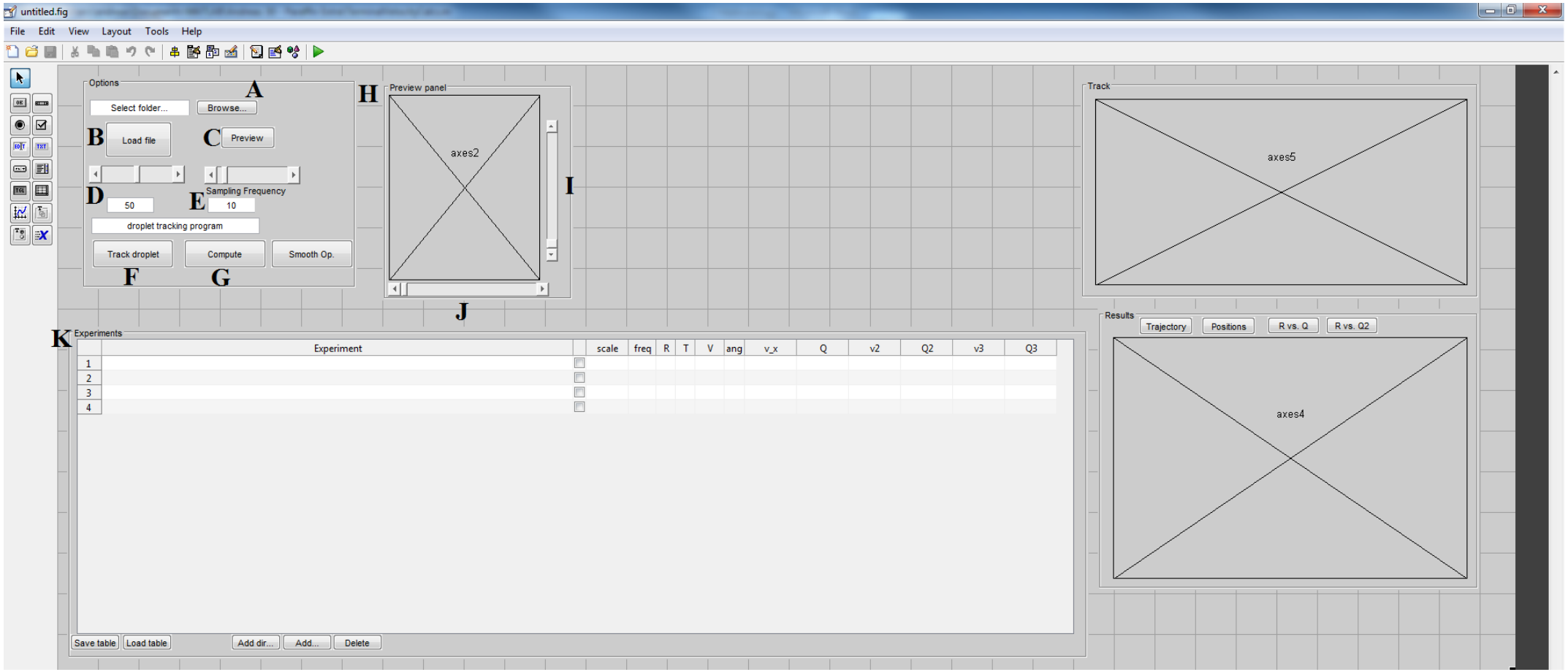

Figure 2.12 Matlab graphical user interface

2.6 Charge v. Applied voltage

Jung et al. reported that electrical charging of water droplets, in contact with a biased electrode increases with an increase in electric field strength [37]. To investigate whether this would also apply to the initial droplet charge (i.e. the charge of a droplet before contact with an electrode), the velocities of a single deionised water droplet injected into silicone oil, at increasing field strength were recorded. The droplet was injected into the oil and a voltage of 1.1 kV was applied. Due to the Coulomb force, the droplet travelled towards the negatively charged electrode but, before the droplets made contact with the electrode, the direction of the field was reversed, the voltage increased to 1.5 kV and the droplet started moving in the opposite direction. For a second time, and before the droplet could make contact with an electrode, the direction of the field was reversed and the voltage increased to 1.7 kV. The three different droplet velocities were recorded. Figure 2.13 shows that, within the measurement accuracy, the initial droplet charge of droplets moving in the vertical set-up (Figure 2.9a) does not depend on the voltage applied.

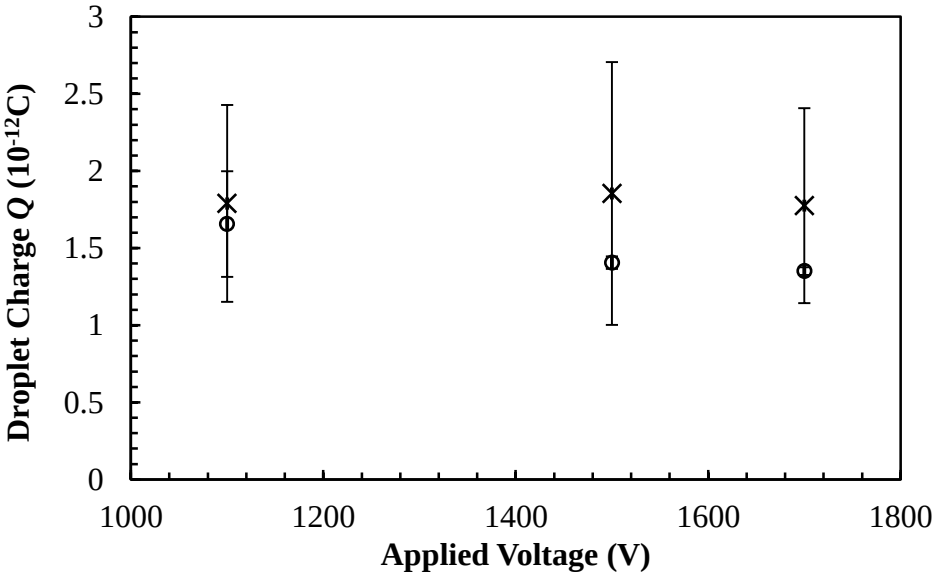

Figure 2.13 Dependence of initial water droplet charge on applied voltage in silicone oil, for a droplet radius of 430 µm (○) and 530 µm (×). Error bars represent the standard deviation of 3 droplets.

2.6.1 Impact of electric field on oil viscosity

Studies have shown that the application of an electric or magnetic field can have an effect on oil viscosity [54-57]. Goncalves et al. [55], for example, observed a 39% reduction in viscosity in a sample of crude oil after a 1 minute exposure to a magnetic field of 1.3 T. The change in viscosity in the presence of an electrical field might also be significant in the experimental set-up outlined above (Figure 2.9). If true, then the increase in droplet velocity, for example, could be explained by a reduction in viscosity, rather than greater droplet charge. A simple control experiment was therefore conducted, to check if the settling velocity of a simple water droplet (i.e. the terminal velocity of a droplet falling due to gravity) changes before and after application of an electric field. The electrophoretic cell (Figure 2.9) was filled with oil, injected with a deionised water droplet and the settling velocities of five droplets were recorded. For the next set of experiments, an electric field E = 3.8 kV/cm was applied for 1 minute, before the water droplet was injected into the oil and its settling velocity recorded.

	Fresh oil		**After application of 3.8 kV/cm**	
	Radius [μm]	Settling velocity [μm/s]	Radius [μm]	Settling velocity [μm/s]
Exp 1	530	137	528	155
Exp 2	545	143	528	137
Exp 3	560	159	557	158
Exp 4	560	159	560	164
Exp 5	595	171	561	166
Mean		154		156
Standard Deviation		13.5		11.5

Table 2.1 Settling velocities of water droplets in silicone oil before and after an electric field was applied.

	Fresh oil		After application of 3.8 kV/cm	
	Radius [μm]	Settling velocity [μm/s]	Radius [μm]	Settling velocity [μm/s]
Exp 1	560	700	560	624
Exp 2	560	669	560	642
Exp 3	560	684	560	623
Exp 4	560	696	560	640
Exp 5	560	662	560	644
Mean		682		635
Standard Deviation		16.5		10.0

Table 2.2 Settling velocities of water droplets in paraffin oil before and after an electric field was applied.

Table 2.1 shows that application of an electric field has no impact on the settling velocity of a water droplet dispersed in silicone oil. As shown in Table 2.2, the settling velocity of a water droplet in paraffin oil after the application of an electric field is reduced by about 8%. Although this is a slight reduction in velocity, it is still within the measurement accuracy and is therefore not expected to influence results.

2.6.2 Solder Flux Complications

During preliminary experiments conducted with paraffin oil, water droplets initially travelled towards the positive electrode, implying that water droplets in paraffin oil have an initial, negative electrophoretic mobility. However, once the electrophoretic cell was cleaned, subsequent experiments showed that the water droplets travelled towards the negative electrode. Further investigations showed that the flux within the solder, used to attach the wiring to the copper electrodes, would dissolve in the paraffin oil (Figure 2.14a) and thus impact the electrophoretic behaviour of the water droplets dispersed in the oil. A vigorous

cleaning regime was developed to avoid any such problems in subsequent experiments (Figure 2.14b).

(a) (b)

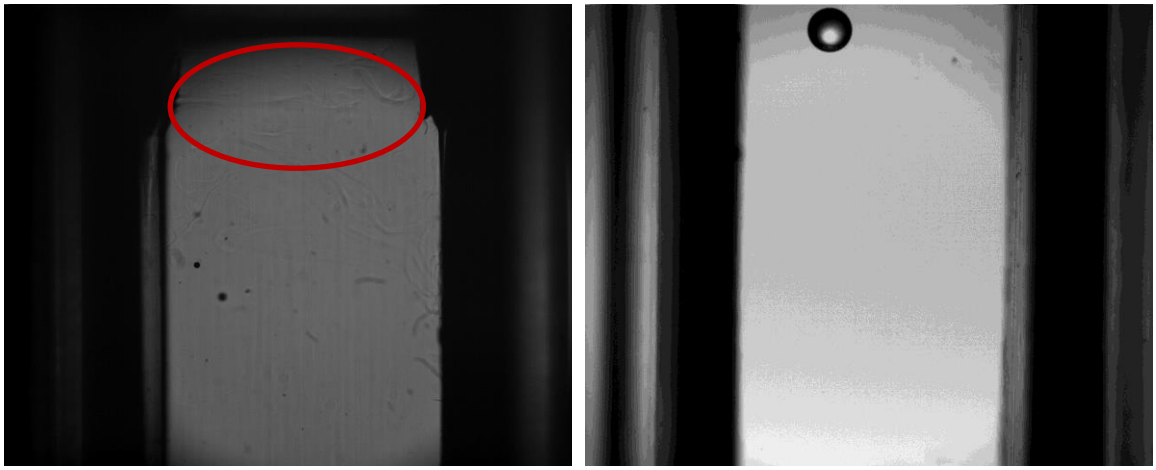

Figure 2.14 a) Solder (dark grey schlieren, highlighted lines) dissolving in Paraffin b) There is no visible solder after the cell has been cleaned.

2.7 References

[1] P. Mesquida, "Charge Writing with an Atomic Force Microscope Tip and Electrostatic Attachment of Colloidal Particles to the Charge Patterns," Doctoral Thesis, Technical Sciences, Swiss Federal Institute of Technology, Zurich, 2002.

[2] J. Holto, G. Berg, and L. E. Lundgaard, "Electrocoalescence of Drops in a Water-in-Oil Emulsion," *Ceidp: 2009 Annual Report Conference on Electrical Insulation and Dielectric Phenomena*, pp. 208-211, 2009.

[3] F. Asi, "Optical Path Tracking of Microdroplets," MSc, Mechanical Engineering, King's College London, London, 2010.

[4] S. Stefanidis, "Final Year Project," BEng, Mechanical Engineering, King's College London, London, 2010.

[5] J. C. Baygents and D. A. Saville, "Electrophoresis of Drops and Bubbles," *Journal of the Chemical Society-Faraday Transactions*, vol. 87, pp. 1883-1898, Jun 21 1991.

[6] J. S. Eow, M. Ghadiri, A. O. Sharif, and T. J. Williams, "Electrostatic enhancement of coalescence of water droplets in oil: a review of the current understanding," *Chemical Engineering Journal*, vol. 84, pp. 173-192, Dec 2001.

[7] J. Hølto, G. Berg, and L. E. Lundgaard, "Electrocoalescence of Drops in a Water-in Oil Emulsion," in *2009 Annual Report Conference on Electrical Insualtion and Dielectric Phenomena*, 2009 pp. 196 - 199.

[8] D. J. Im, J. Noh, D. Moon, and I. S. Kang, "Electrophoresis of a Charged Droplet in a Dielectric Liquid for Droplet Actuation," *Analytical Chemistry*, vol. 83, pp. 5168-5174, Jul 1 2011.

[9] D. J. Im, J. Noh, N. W. Yi, J. Park, and I. S. Kang, "Influences of electric field on living cells in a charged water-in-oil droplet under electrophoretic actuation," *Biomicrofluidics*, vol. 5, Dec 2011.

[10] V. Knecht, H. J. Risselada, A. E. Mark, and S. J. Marrink, "Electrophoretic mobility does not always reflect the charge on an oil droplet," *Journal of Colloid and Interface Science*, vol. 318, pp. 477-486, Feb 15 2008.

[11] C. P. Lee, H. C. Chang, and Z. H. Wei, "Charged droplet transportation under direct current electric fields as a cell carrier," *Applied Physics Letters*, vol. 101, p. 014103, Jul 2 2012.

[12] D. W. Lee, D. J. Im, and I. S. Kang, "Electrophoretic motion of a charged water droplet near an oil-air interface," *Applied Physics Letters*, vol. 100, p. 221602, May 28 2012.

[13] J. Prischmann, "Basics and Theory of Electrophoresis," ed: North Dakota State Seed Department, 2010.

[14] A. M. Schoeler, D. N. Josephides, S. Sajjadi, C. D. Lorenz, and P. Mesquida, "Charge of water droplets in non-polar oils," *Journal of Applied Physics*, vol. 114, p. 144903, 2013.

[15] R. W. Wood and A. L. Loomis, "The physical and biological effects of high-frequency sound-waves of great intensity.," *Philosophical Magazine*, vol. 4, pp. 417-436, Sep 1927.

[16] E. Nazarzadeh and S. Sajjadi, "Viscosity effects in miniemulsification via ultrasound," *AIChE Journal*, vol. 56, pp. 2751-2755, 2010.

[17] K. Kamogawa, G. Okudaira, M. Matsumoto, T. Sakai, H. Sakai, and M. Abe, "Preparation of oleic acid/water emulsions in surfactant-free condition by sequential processing using midsonic-megasonic waves," *Langmuir*, vol. 20, pp. 2043-2047, Mar 16 2004.

[18] M. Sivakumar, A. Towata, K. Yasui, T. Tuziuti, T. Kozuka, Y. Iida, M. M. Maiorov, E. Blums, D. Bhattacharya, N. Sivakumar, and M. Ashok, "Ultrasonic cavitation induced water in vegetable oil emulsion droplets - A simple and easy technique to synthesize manganese zinc ferrite nanocrystals with improved magnetization," *Ultrasonics Sonochemistry,* vol. 19, pp. 652-658, May 2012.
[19] J. P. Canselier, H. Delmas, A. M. Wilhelm, and B. Abismail, "Ultrasound Emulsification—An Overview," *Journal of Dispersion Science and Technology,* vol. 23, pp. 333-349, 2002.
[20] F. Leal-Calderon, V. Schmitt, and J. Bibette, *Emulsion Science: Basic Principles*: Springer, 2007.
[21] O. Behrend, K. Ax, and H. Schubert, "Influence of continuous phase viscosity on emulsification by ultrasound," *Ultrasonics Sonochemistry,* vol. 7, pp. 77-85, 2000.
[22] C. Bondy and K. Sollner, "On the mechanism of emulsification by ultrasonic waves," *Transactions of the Faraday Society,* vol. 31, pp. 0835-0842, 1935.
[23] M. K. Li and H. S. Fogler, "Acoustic Emulsification. Part 1. Instability of Oil-Water Interface to Form Initial Droplets," *Journal of Fluid Mechanics,* vol. 88, pp. 499-&, 1978.
[24] M. K. Li and H. S. Fogler, "Acoustic Emulsification. Part 2. Breakup of Large Primary Oil Droplets in a Water Medium," *Journal of Fluid Mechanics,* vol. 88, pp. 513-&, 1978.
[25] S. G. Gaikwad and A. B. Pandit, "Ultrasound emulsification: Effect of ultrasonic and physicochemical properties on dispersed phase volume and droplet size," *Ultrasonics Sonochemistry,* vol. 15, pp. 554-563, Apr 2008.
[26] J. P. Lorimer and T. J. Mason, "Sonochemistry. Part 1 - The physical aspects," *Chemical Society Reviews,* vol. 16, pp. 239-274, Jun 1987.
[27] S. Kentish, T. J. Wooster, M. Ashokkumar, S. Balachandran, R. Mawson, and L. Simons, "The use of ultrasonics for nanoemulsion preparation," *Innovative Food Science and Emerging Technologies,* vol. 9, pp. 170-175, 2008.
[28] S. Mujumdar, P. S. Kumar, and A. B. Pandit, "Emulsification by ultrasound: relation between intensity and emulsion quality," *Indian Journal of Chemical Technology,* vol. 4, pp. 277-284, 1997.
[29] J. Jiao, "Ostwald ripening of water-in-hydrocarbon emulsions," *Journal of Colloid and Interface Science,* vol. 264, pp. 509-516, 2003.
[30] Virtualdub. Available: http://www.virtualdub.org/
[31] National-Institutes-of-Health. (2004). *ImageJ* Available: http://imagej.nih.gov/ij/
[32] D. M. Higgins and D. M. Skauen, "Influence of power on quality of emulsions prepared by ultrasound," *Journal of Pharmaceutical Sciences,* vol. 61, pp. 1567-70, Oct 1972.
[33] D. J. Im and I. S. Kang, "Electrohydrodynamics of a drop under nonaxisymmetric electric fields," *Journal of Colloid and Interface Science,* vol. 266, pp. 127-140, Oct 1 2003.
[34] M. Hase, S. N. Watanabe, and K. Yoshikawa, "Rhythmic motion of a droplet under a DC electric field," *Physical Review E,* vol. 74, p. 046301, Oct 2006.
[35] M. Takinoue, Y. Atsumi, and K. Yoshikawa, "Rotary motion driven by a direct current electric field," *Applied Physics Letters,* vol. 96, p. 104105, Mar 2010.
[36] M. Jalaal, B. Khorshidi, and E. Esmaeilzadeh, "An experimental study on the motion, deformation and electrical charging of water drops falling in oil in the presence of high voltage DC electric field," *Experimental Thermal and Fluid Science,* vol. 34, pp. 1498-1506, Nov 2010.

[37] Y.-M. Jung, H.-C. Oh, and I. S. Kang, "Electrical charging of a conducting water droplet in a dielectric fluid on the electrode surface," *Journal of Colloid and Interface Science,* vol. 322, pp. 617-623, 2008.
[38] D. J. Im, M. M. Ahn, B. S. Yoo, D. Moon, D. W. Lee, and I. S. Kang, "Discrete Electrostatic Charge Transfer by the Electrophoresis of a Charged Droplet in a Dielectric Liquid," *Langmuir,* vol. 28, pp. 11656-11661, Aug 14 2012.
[39] B. Vajdi Hokmabad, B. Sadri, M. R. Charan, and E. Esmaeilzadeh, "An experimental investigation on hydrodynamics of charged water droplets in dielectric liquid medium in the presence of electric field," *Colloids and Surfaces A: Physicochemical and Engineering Aspects,* vol. 401, pp. 17-28, 2012.
[40] G. T. Vladisavljevic, N. Khalid, M. A. Neves, T. Kuroiwa, M. Nakajima, K. Uemura, S. Ichikawa, and I. Kobayashi, "Industrial lab-on-a-chip: Design, applications and scale-up for drug discovery and delivery," *Advanced Drug Delivery Reviews,* vol. 65, pp. 1626-1663, Nov 15 2013.
[41] A. Huebner, S. Sharma, M. Srisa-Art, F. Hollfelder, J. B. Edel, and A. J. deMello, "Microdroplets: A sea of applications?," *Lab on a Chip,* vol. 8, pp. 1244-1254, 2008.
[42] J. W. Chung, K. Lee, C. Neikirk, C. M. Nelson, and R. D. Priestley, "Photoresponsive Coumarin-Stabilized Polymeric Nanoparticles as a Detectable Drug Carrier," *Small,* vol. 8, pp. 1693-1700, Jun 11 2012.
[43] S. Y. Teh, R. Lin, L. H. Hung, and A. P. Lee, "Droplet microfluidics," *Lab on a Chip,* vol. 8, pp. 198-220, 2008.
[44] R. Clift, J. R. Grace, and E. Weber, *Bubbles, Drops, and Particles*: Dover Publications, 2005.
[45] H. Lamb and R. Caflisch, *Hydrodynamics*: Cambridge University Press, 1993.
[46] L. G. Leal, *Advanced Transport Phenomena: Fluid Mechanics and Convective Transport Processes*: Cambridge University Press, 2007.
[47] W. Rybczynski, "Über die fortschreitende Bewegung einer flüssigen Kugel in einem zähen Medium (German)," *Bulletin International de l'Academie des Sciences de Cracovie,* pp. 40–46, 1911.
[48] R. Ladenburg, "Über den Einfluß von Wänden auf die Bewegung einer Kugel in einer reibenden Flüssigkeit," *Annalen Der Physik,* vol. 328, pp. 447-458, 1907.
[49] J. Happel and E. Bart, "Settling of a Sphere Along Axis of a Long Square Duct at Low Reynolds-Number," *Applied Scientific Research,* vol. 29, pp. 241-258, 1974.
[50] E. I. Fulmer and J. C. Williams, "A method for the determination of the wall correction for the falling sphere viscometer," *Journal of Physical Chemistry,* vol. 40, pp. 143-149, Jan 1936.
[51] B. S. Hamlin and W. D. Ristenpart, "Transient reduction of the drag coefficient of charged droplets via the convective reversal of stagnant caps," *Physics of Fluids,* vol. 24, Jan 2012.
[52] L. Kirkup, *Experimental Methods: An Introduction to the Analysis and Presentation of Data*: John Wiley & Sons Australia, Limited, 1994.
[53] T. Peng. (2005). *Detect circles with various radii in grayscale image via Hough Transform*. Available: http://www.mathworks.co.uk/matlabcentral/fileexchange/9168-detect-circles-with-various-radii-in-grayscale-image-via-hough-transform
[54] F. Homayuni, A. A. Hamidi, A. Vatani, A. A. Shaygani, and R. F. Dana, "The Viscosity Reduction of Heavy and Extra Heavy Crude Oils by a Pulsed Magnetic Field," *Petroleum Science and Technology,* vol. 29, pp. 2407-2415, 2011.
[55] J. L. Goncalves, A. J. F. Bombard, D. A. W. Soares, R. D. M. Carvalho, A. Nascimento, M. R. Silva, G. B. Alcantara, F. Pelegrini, E. D. Vieira, K. R. Pirota, M. I. M. S. Bueno, G. M. S. Lucas, and N. O. Rocha, "Study of the Factors Responsible

for the Rheology Change of a Brazilian Crude Oil under Magnetic Fields," *Energy & Fuels,* vol. 25, pp. 3537-3543, Aug 2011.

[56] Y. V. Loskutova, N. V. Yudina, and S. I. Pisareva, "Effect of magnetic field on the paramagnetic, antioxidant, and viscosity characteristics of some crude oils," *Petroleum Chemistry,* vol. 48, pp. 51-55, Jan 2008.

[57] R. Tao and X. Xu, "Reducing the viscosity of crude oil by pulsed electric or magnetic field," *Energy & Fuels,* vol. 20, pp. 2046-2051, Sep 20 2006.

Chapter 3 Charge of Water Droplets in Non-Polar Oils

3.1 Chapter Abstract

This chapter describes the electrophoretic motion of water droplets dispersed in two non-polar oils, silicone and paraffin oil, to determine droplet charge. Individual micrometre sized water droplets were injected into the oils using a concentric microchannel arrangement and the electrophoretic motion was recorded and analysed by optical microscopy. It was found that the initial surface charge density of surfactant-free droplets, directly after injection from a micropipette, was positive and of the order of 10^{-6} C/m^2, regardless of pH and ion concentration in the range from pH4 to pH10 and from 0.01 mmol/l to 1.5 mol/l, respectively. The nature and polarity of the charge is explained by anisotropic orientation of water molecules at the interface rather than selective adsorption of ions.

3.2 Introduction

Charges at the water–hydrophobic medium (oil or air) interface have been the subject of considerable scientific interest and debate, due to their significance for emulsion stability and in various applications in the field of microfluidics [1-5] and colloid science [6-16]. Especially with the advent of digital microfluidics [17-19] (that is, the use of water droplets as tiny compartments inside microfluidic, lab-on-a-chip devices [1-4]), it has become more important to have information about the electrophoretic behaviour and charge of water droplets. This is because repulsion or attraction between droplets can affect the performance of microfluidic devices and because electrostatic fields can be used to manipulate droplets [17-20]. An important question here is the dependence of the interface charge on the type and concentration of ions in the aqueous phase, not only because these are parameters that are often prescribed by the emulsion

formulation, but also because pH and ion concentration can give scientists some clues about the actual nature of the interface charge [13]. Investigations into interface charge are often based on electrophoretic techniques, either by direct observation of the motion of microscopic oil droplets in electric fields [21] or by related light-scattering and electro-acoustic techniques [12, 13]. In most cases, oil-in-water emulsions are investigated [12, 13, 21]. There are surprisingly little data regarding the electrophoretic mobility of water droplets dispersed in a non-polar oil. Apart from carrying a native charge, water-in-oil droplets can also be deliberately charged through direct contact with a voltage-biased electrode [22]. The great advantage is obviously the degree of control with respect to sign and magnitude of the charge. From a practical point-of-view, it would be necessary to know if and to what extent this "artificial" surface charge is influenced by the chemical droplet properties (pH, ion concentration, etc). Various research groups performed such controlled charging of water droplets [17, 18, 23-31]. Im et al. have investigated the charge transfer between electrodes and droplets in more detail [23] and have, for example, recently presented a droplet manipulation scheme, whereby a water droplet is given a charge from an electrode and is then driven by electric fields [17]. However, the influence of fundamental parameters on droplet charge has not been investigated.

This chapter helps to elucidate some of the properties of droplet charge from measurements of the electrophoretic mobility of individual water droplets in two different, non-polar oils of similar, physical fluid properties: silicone and paraffin oil. These two oils were chosen because they have a similar, molecular structure, with the difference that silicone oil contains siloxane (...-Si-O-...) groups as repetitive units in the molecular backbone, whereas paraffin oil contains only carbon atoms (...-C-C-...) and consists of a mixture of alkanes, C_nH_{2n+2}, with n=16...24. They are suitable and often

used in microfluidics [32, 33], due to their inertness, stability, non-hazardous and inexpensiveness.

3.3 Experimental Set-Up

All micro-electrophoretic experiments were conducted in the same electrophoretic cell as outlined in the Methodology Chapter. The cell was filled with either silicone or paraffin oil (Figure 3.1) and each water droplet was injected individually into the oil using the 20 µm sized (inner diameter) hydrophobic glass micropipette (Figure 3.1), which was centred in the middle of the cell (aligned concentrically). The velocity was measured by recording high-speed images (100 fps, 20 µm/pixel) of individual, moving droplets and analysed using the adapted Circular Hough Transform. Overall, 200 droplets were investigated and all experiments were conducted at 21ºC.

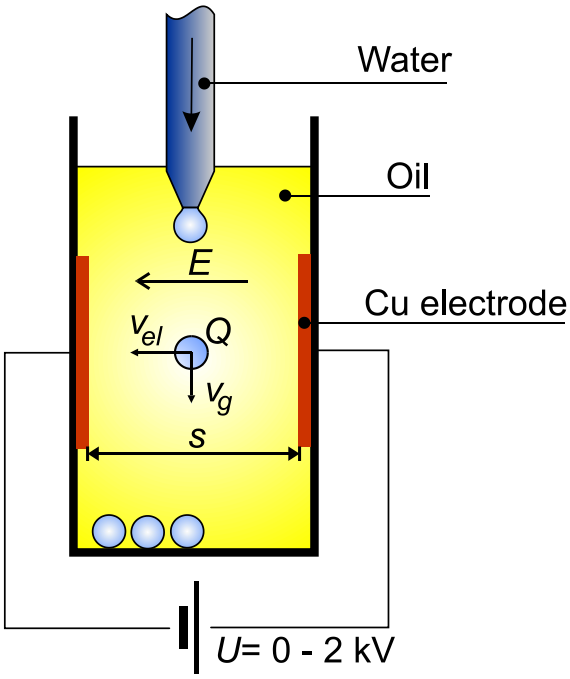

Figure 3.1 Experimental set-up for electrophoretic experiments, where the droplet radius is varied, distance between electrodes, s = 6.5 mm, and electric field, E = 2.31 kV/cm.

3.4 Results

3.4.1 Electrophoretic experiments: General droplet behaviour

It was observed that, as soon as the electric field was applied after release of the droplets from the micropipette, all droplets travelled towards the negative electrode in silicone oil and in paraffin oil. This showed that droplets have a positive, initial, native net charge before making contact with an electrode.

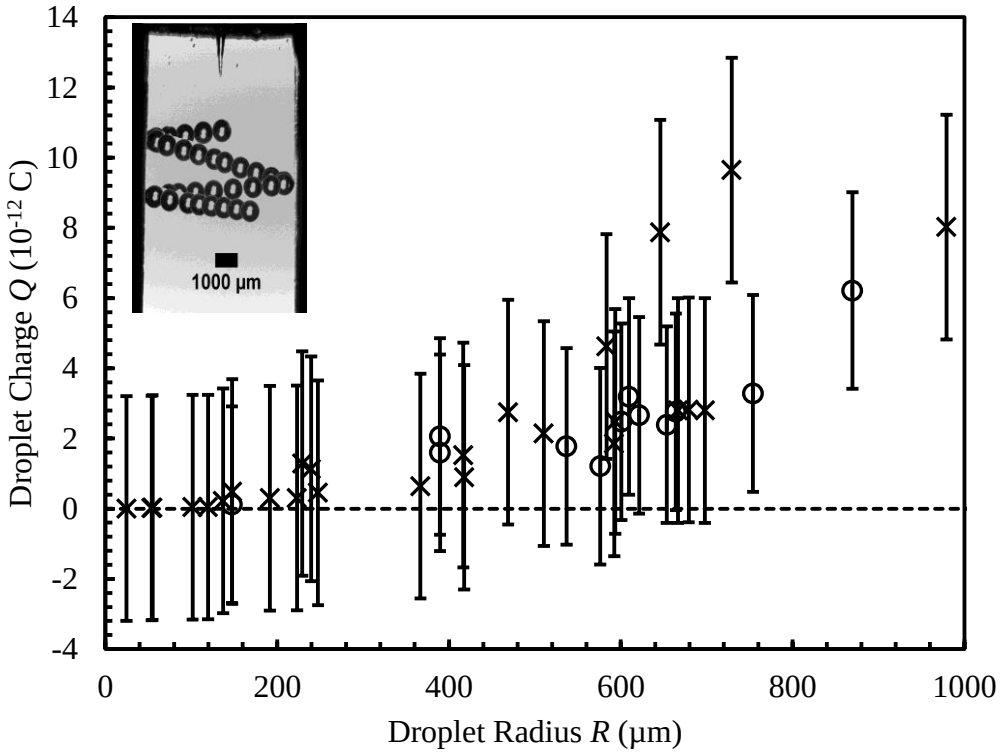

Figure 3.2 Dependence of native droplet charge on oil type, silicone oil (×) and paraffin oil (○), before first contact with a biased electrode. Values for Q calculated with Equation 2-11, where: E = 2.31 kV/cm, with $a_{silicone}$ = 315 $s^{-1}m^{-1}$, $a_{paraffin}$ = 905 $s^{-1}m^{-1}$, $b_{silicone}$ = 0.1 s^{-1}, $b_{paraffin}$ = 0.7 s^{-1}, $B_{silicone}$ =1440 $kgm^{-2}s^{-2}$, $B_{paraffin}$ = 5750 $kgm^{-2}s^{-2}$; measurement accuracy of R approx. 20 µm; the accumulative error of Q Equation 2-11, due to measurement inaccuracy, is 3.2 × 10^{-12} C for silicone oil and 2.8 × 10^{-12} C for paraffin oil (error bars). Inset: General droplet behaviour

Figure 3.2 shows the results of the electrophoretic measurements with deionised water droplets. The droplet charge was determined from the measured, horizontal velocity

component, v_{el}, and the droplet radius, R, using Equation 2-11 ($a_{silicone} = 315\ s^{-1}m^{-1}$, $a_{paraffin} = 905\ s^{-1}m^{-1}$, $b_{silicone} = 0.1\ s^{-1}$, $b_{paraffin} = 0.7\ s^{-1}$, $B_{silicone} = 1440\ kgm^{-2}s^{-2}$, $B_{paraffin} = 5753\ kgm^{-2}s^{-2}$, $s = 6.5$ mm, $U = 1.5$ kV). The droplet charge increases non-linearly with increasing R. From the charge-*vs*.-radius relation, one can deduce some information about the distribution of the charge in a droplet, namely whether the charge is located predominantly on the droplet surface or evenly distributed across the entire volume of the droplet. If the charge was located mainly on the surface, the overall amount would scale with the surface area, $\sim R^2$, under the assumption that the surface charge density, σ, is constant. However, if the charge was evenly distributed in the volume then the overall amount would scale with the volume, $\sim R^3$, assuming that the volume (space) charge density, ξ, is constant. From the spread of data presented in Figure 3.2, it is not immediately obvious which charge distribution is more appropriate. However, in some instances, the water droplet charge may depend on the continuous phase. Although these two oils have a similar, molecular structure, the difference is that silicone oil contains siloxane (...-Si-O-...) groups as repetitive units in the molecular backbone, whereas paraffin oil contains only carbon atoms (...-C-C-...), which suggests that there could be a difference in interfacial affinity of water molecules to the oil interface due to the presence or absence of oxygen atoms in the oil. Near the electrode, the droplets elongated slightly towards the electrode, forming a small tip, which eventually made contact with the electrode. After contacting the electrode for a fraction of a second, the droplets were repelled and travelled towards the other electrode, where the process repeated itself in the opposite direction leading to a back-and-forth motion between the two electrodes while continuing to slowly fall due to gravity (inset Figure 3.2). This general behaviour of an apparent, native charge followed by active charging has also been observed by other groups [23-25, 27, 28, 34, 35], although only one

attempt has been made so far to specify the exact nature of the droplet charge [35]. Recently Choi et al. [35] suggested that the native droplet charge originates from ionisation of surface chemical groups at the water droplet and the pipette tip interface. However, in most papers, it is simply accepted that water droplets in a non-polar oil are subject to electrophoretic motion without discussing the origin of the charge any further. The interpretation is that droplets are discharged and recharged with opposite polarity each time they are in contact with a metal electrode.

3.4.2 Influence of Ions on Droplet Charge

One of the main arguments in the debate about water/oil interface charge is that ions, either from added salts or OH^- and H_3O^+ ions, are responsible for the charge and the observed, electrophoretic mobility [13, 36]. In order to investigate the nature of the effective droplet charge further, ions were added to the water at various concentrations. The ionic concentration (Figure 3.3) and the pH (Figure 3.4) were varied over a wide range. Electrolyte ions are normally the charged species, which determine the electrical properties of water such as conductivity, electrostatic screening, surface and interface charges, etc. Without any added ions, i.e., in deionised water, the only charged species are H_3O^+ and OH^- in equal concentrations ($\approx 10^{-7}$ mol/l) from the autoprotolysis of water. If ions were responsible for the charge of a droplet, then one would expect a significant change in behaviour upon large variation of ion concentration.

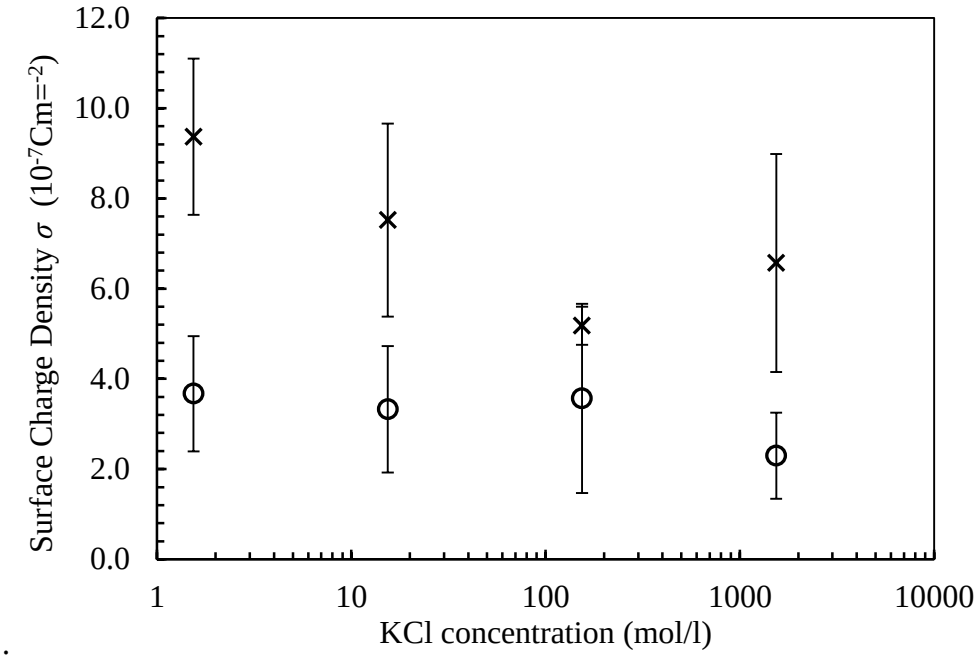

Figure 3.3 Influence of KCl concentration on droplet surface charge density in silicone oil (×) and paraffin oil (O), before contact with an electrode. Droplet radius = 630 µm; *E* = 2.31 kV/cm. Error bars represent the standard deviation of 10 monodisperse droplets.

Figure 3.3 shows the ionic strength dependence of the surface charge density of water droplets, both in silicone and in paraffin oil. The ionic strength was varied by adjusting the concentration of potassium chloride (KCl) between 1.5×10^{-4} mol/l and 1.5 mol/l. All experiments were performed with a similar droplet size in order to minimise its effect on the charge measurement. No significant dependence of the droplet charge on the ionic strength could be found in either of the two oils.

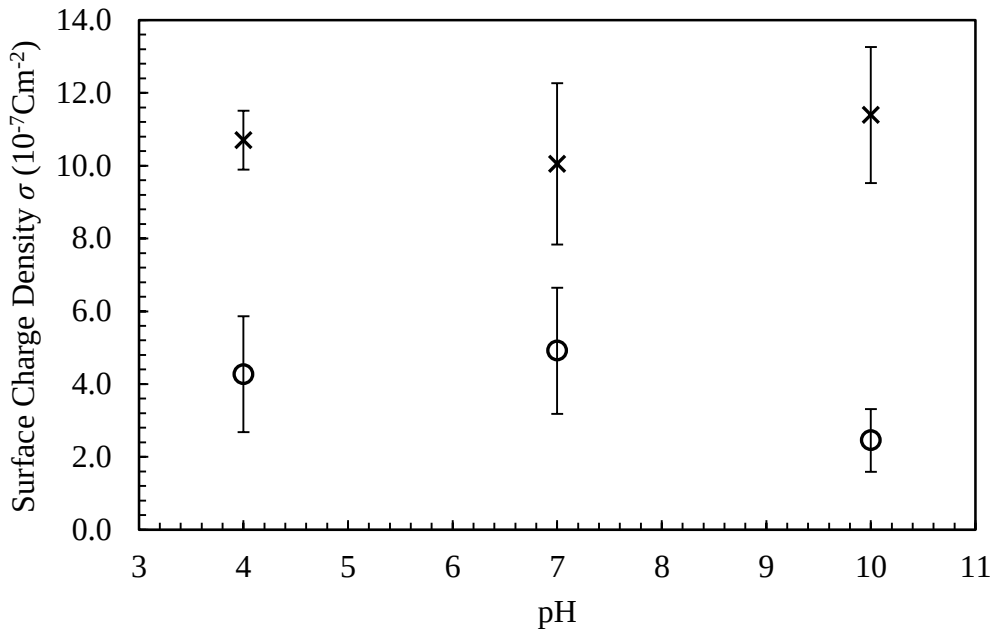

Figure 3.4 Influence of pH on droplet surface charge density in silicone oil (×) and paraffin oil (○) before contact with an electrode. Droplet radius = 630 μm; E = 2.31 kV/cm. Error bars represent the standard deviation of 10 monodisperse droplets.

A similar result was observed for different pH between 4 and 10 (Figure 3.4). Bearing in mind that pH is a logarithmic quantity, it can be seen that even six orders of magnitude in difference of H_3O^+ and OH^- concentration has no significant effect on the effective droplet charge observed in the electrophoretic measurements. As in the case of deionised water (Figure 3.2), the droplet charge is always greater in silicone oil than in paraffin oil, independently of any ion concentration.

3.4.3 Influence of Chaotropic Agent

It has been shown in Figure 3.4 that the surface charge of water droplets is greater in silicone than in paraffin oil. A possible explanation could be the anisotropic orientation of water molecules at the interface. To test this theory, varying concentrations of Urea were added to the water phase. Urea is a chaotropic agent that can disrupt the bonding

network of hydrogen inside the water molecule and can thus reduce the amount of ordering.

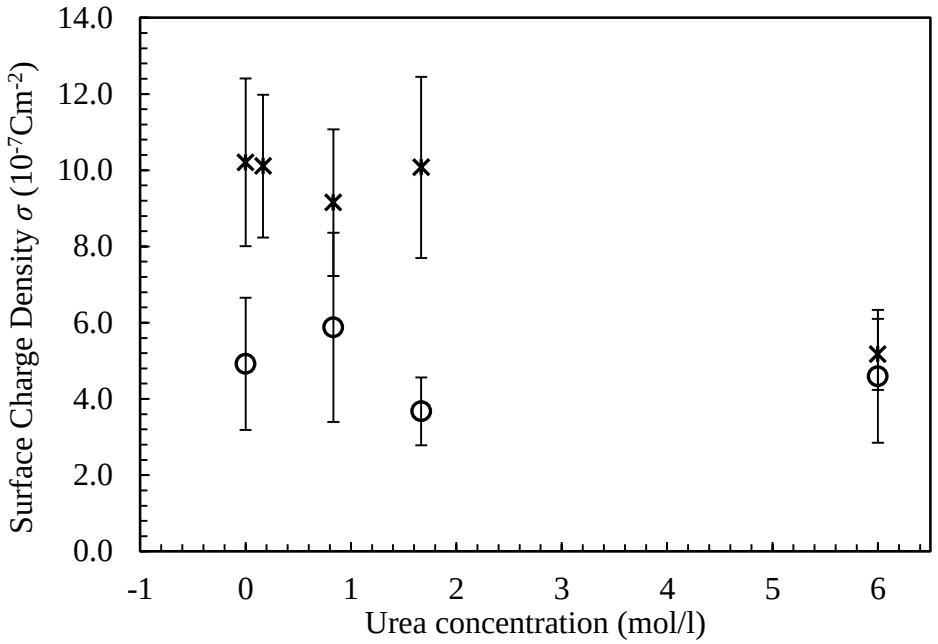

Figure 3.5 Influence of Urea concentration on droplet surface charge density in silicone (×) and paraffin oil (○), before contact with an electrode. Droplet radius = 630 µm; E = 2.31 kV/cm. Error bars represent the standard deviation of 10 monodisperse droplets.

Figure 3.5 shows that the initial surface charge density of water droplets in silicone oil decreases with an increasing urea concentration. The surface charge density of water droplets in paraffin oil however seems unaffected. This observation agrees with the theory discussed above. By adding a chaotropic agent and thus disrupting the bonding network of hydrogen inside the water droplet, could explain the reduction in surface charge density of the water droplet in silicone oil.

3.4.4 Molecular dynamics simulations

In order to obtain an atomistic description of the water/oil interface that is present in this experimental systems, classical molecular dynamic simulations were conducted. The

simulations described in this section were conducted by Dr. Chris Lorenz as part of collaborative work undertaken [37]. This is the only section within this thesis where others have contributed data.

Two systems were simulated: one containing 50 chains of polydimethylsiloxane (silicone oil) and 10320 water molecules; the other containing 250 chains of paraffin and 5200 water molecules. Both simulations were carried out using the LAMMPS molecular dynamics package [38]. All interactions in the system were modelled using the COMPASS forcefield [39], and all hydrogen containing bonds were constrained using the SHAKE algorithm [40]. A 1 fs timestep was used during all simulations, and the final adsorption simulations were run for more than 10 ns. A more detailed description of the atomistic molecular dynamic simulation undertaken, can be found in [37].

The trajectories from the molecular dynamics simulations were used to determine the distribution of charge near the silicone/water and paraffin/water interfaces [37]. Each atom within the system was assigned a partial charge. These were used to determine a time average distribution of the cumulative surface charge throughout the simulated systems, which is illustrated in Figure 3.6.

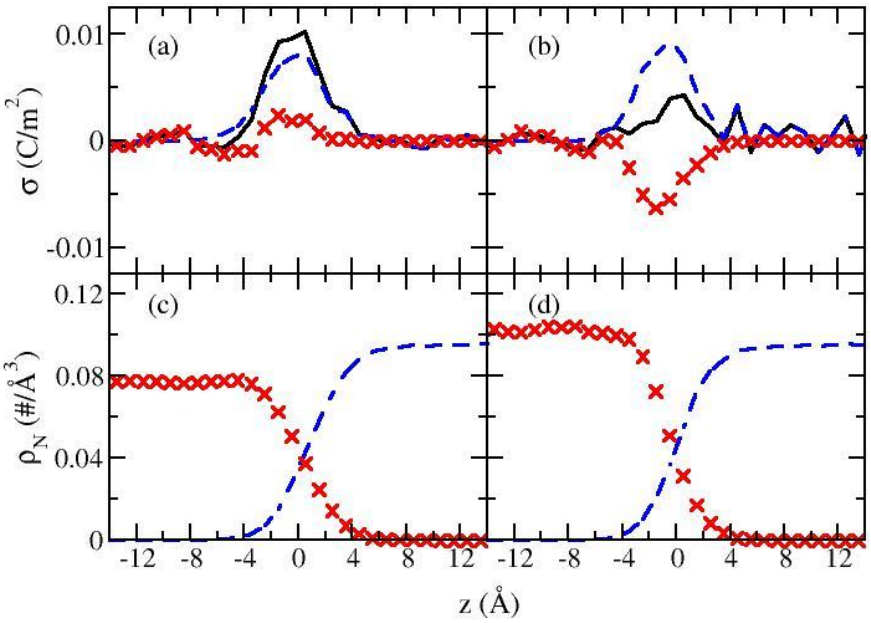

Figure 3.6 Cumulative surface charge density [(a) & (b)] and number density [(c) & (d)] calculated from the trajectories generated from the molecular dynamics simulations of the silicone/water [(a) & (c)] and the paraffin/water [(b) & (d)] systems. The black line is representative of the total charge of the system (–), while the red X's (×) and blue dashed lines (---) represent the oil and water contributions to the measured quantity, respectively. Taken, with permission, from [37].

Figure 3.6 shows that the total surface charge at both interfaces (silicone/water and paraffin/water) is positive and follows the same general trend. The cumulative surface charge density is equal to zero throughout the system except within the 8Å thick interfacial region of each system, where both water and oil are present in the systems. The cumulative surface charge density of the water atoms is similar in both cases and ranges from a minimum of -0.0001 Cm^{-2} at z = -4Å, to a maximum of approximately 0.009 Cm^{-2} at z=0Å (which is the point where there is an equal number of oil and water atoms). The cumulative surface charge density decreases again to near zero at z~4Å.

However, the cumulative surface charge density of the silicone system in the interfacial region is about twice as high compared to the paraffin system. The cumulative surface charge density distribution of the oil phase in the two systems is also significantly different. In the silicone/water system, the cumulative surface charge density distribution of the oil phase is nearly zero throughout the oil phase with a slightly negative region [at approximately 4Å (-2Å < z < -2Å) from the silicone/water interface] followed by a slightly positive region (-2Å < z < 2Å). Whereas in the paraffin/water system, the cumulative surface charge density distribution within the paraffin becomes significantly negative (~0.008 Cm^{-2}) at the water/paraffin interface. This negatively charged region can be attributed to the re-orientation of the methyl groups at the terminal end of the paraffin molecules [37], because there is a carbon rich region (-4Å < z < -2Å) which corresponds to the negative trend in the cumulative surface charge density of paraffin, followed by a hydrogen rich region (-2Å < z < 2Å) which causes the surface cumulative surface charge density of the paraffin to increase back to zero.

To obtain a better understanding of the nature of this apparent positive, cumulative surface charge, the orientation of the water molecules at both the silicone and paraffin interface was investigated. In order to characterise the orientation, the angle between each O-H bond of the water molecule and the z-axis, which in the simulations is perpendicular to the oil/water interface, is calculated. The angle is defined such that it has a value greater than 90° if the hydrogen is nearer to the oil interface ("pointed down") than the oxygen. The value of the angle is less than 90° if the hydrogen is further from the oil interface than the oxygen ("pointed up"). If the angle is equal to 90°, then the oxygen and hydrogen are the same distance from the oil interface as the bond is parallel to the interface [37].

The probability distribution that a water molecule will be oriented in such a fashion (i.e. two O-H bonds make the angles OH1 and OH2 with the z-axis) is shown in Figure 3.7. One can see from the histograms that, in both cases, a significant ordering of water molecules at the interface does not occur, as evidenced by the broad distribution of orientations measured. However, in the silicone/water system, water molecules are more likely to be orientated in such a way that one hydrogen is pointed down and one hydrogen is pointed up ($\theta_{OHi} < 90°$ and $\theta_{OHj} > 90°$) compared to the paraffin/water system. This preference can be explained by the fact that the hydrogen atoms of the water molecules and the oxygen atoms in the silicone chains can interact with each other. Paraffin oil molecules do not contain any hydrogen bond donors or acceptors. Additionally, in the paraffin system, there are more water molecules oriented with both hydrogens in the same z-plane as the oxygen ($\theta_{OHi} \sim 90°$ and $\theta_{OHj} \sim 90°$) near the interface than in the silicone/water system.

When comparing the distribution of the water orientations near the interface (Figure 3.7 (a) – (d)) to those in the bulk region of the water (Figure 3.7 (e) & (f)), it was clear that, near the interface, the water molecules do not orient such that they have both hydrogens pointing down ($\theta_{OHi} < 90°$ and $\theta_{OHj} < 90°$) or up ($\theta_{OHi} > 90°$ and $\theta_{OHj} > 90°$) with the same frequency that they do in the bulk. In the bulk, the orientations with both hydrogens pointing in a given direction are just as common as the orientation where one hydrogen is pointed up and one hydrogen is pointed down. This change is due to the reduced number of hydrogen bonding partners in the oil molecules.

PDMS/water

Paraffin/water

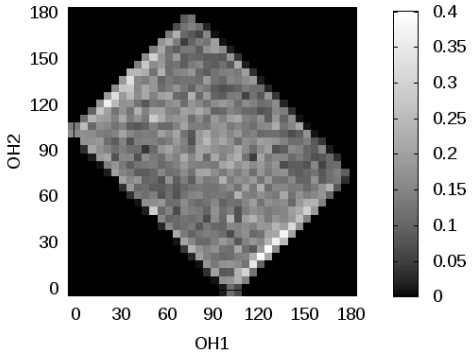

(a) -2Å < z < 0Å

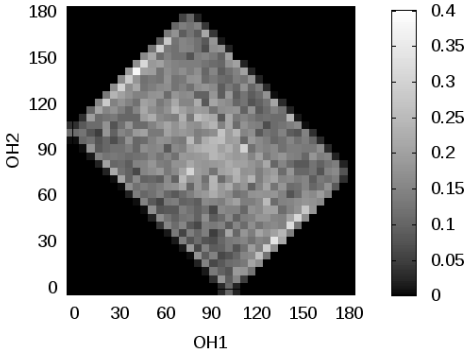

(b) -2Å < z < 0Å

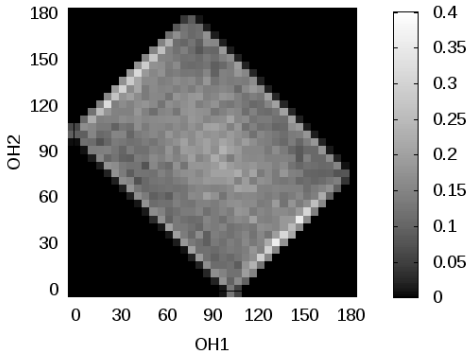

(c) 0Å < z < 2Å

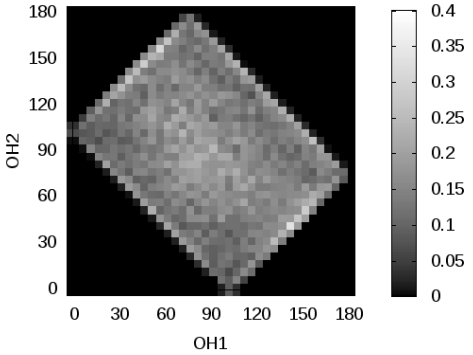

(d) 0Å < z < 2Å

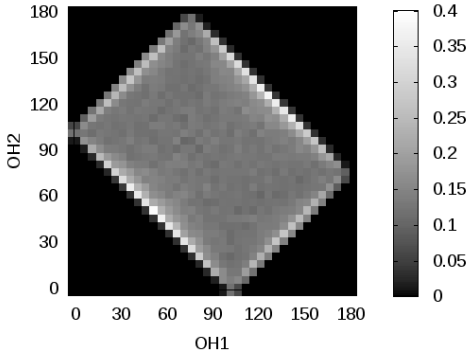

(e) 18Å < z < 20Å

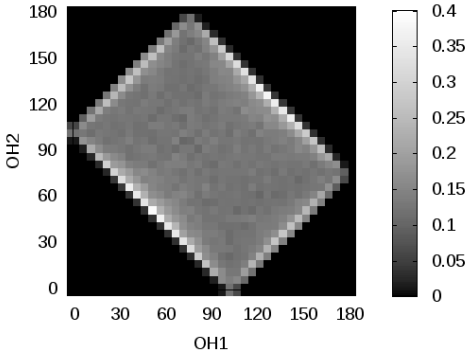

(f) 18Å < z < 20Å

Figure 3.7 Probability that a water molecule is oriented such that the angles between its two O-H bonds and the z-axis are OH1 and OH2, respectively. These plots represent the probability distribution for waters within -2Å - 0Å ((a) & (b)) and 0 Å – 2 Å ((c) & (d)) from the oil interface, as well as in the bulk ((e) & (f)). Figures (a), (c) & (e) represent the water molecules in the PDMS/water system, and figures (b), (d) & (f) represent the water molecules in the paraffin/water system. Taken, with permission, from [37].

3.5 Discussion

3.5.1 The native charge

Interface charges are usually formed by a preferential affinity of specific ions to the interface and the charge, zeta-potential and ion (and counter-ion) distribution in the adjacent liquid phase(s) are described by the Poisson-Boltzmann equation and double-layer theory (Chapter 1) [41]. In the classical case of solid, colloidal particles dispersed in water, this means that there is preferential adsorption of ions of one polarity onto the particles, whereas counter-ions of opposite polarity form a more mobile, diffuse layer extending into the water phase. The net result in an external electric field is electrophoretic motion of the particles in one direction and motion of the diffuse cloud into the opposite direction. However, in the case of the continuous phase being a non-polar oil with no significant solubility for ions and the dispersed particles being liquid water droplets, the whole concept of preferential adsorption and double-layer formation is not applicable.

There is scarce literature regarding the native charge of water droplets dispersed in oil and observations are conflicting. Similarly to this work, Im et al. observed positive electrophoretic mobility in silicone oil, that is, motion of the droplets in direction of the electric field vector towards the negative electrode [23, 42]. They also showed that addition of electrolyte salts did not have any effect [23]. However, Lee et al. [31] observed water droplets initially moving towards the positive electrode in silicone oil, thus implying the presence of negative charges at the water/oil interface. With a dodecane oil, water droplets were reported to show positive electrophoretic mobility [34].

In one comprehensive study on oil droplets dispersed in water without any surfactants, Marinova et al. [13] found a negative zeta-potential and, hence, surface charge, which was clearly dependent on the pH of water. It was, therefore, attributed to the preferred adsorption of OH^- ions at the water-oil interface. However, a direct comparison with this work is difficult because dispersed and continuous phase are inverted and oils other than silicone or paraffin oil were studied.

This chapter and results from various other works in the literature, clearly demonstrate non-zero electrophoretic mobility of oil droplets in deionised water or deionised water droplets in oil. There are two lines of thought regarding the dominating cause for this droplet mobility: preferential adsorption of ions in the water phase (*i.e.* OH^- or H_3O^+ ions from the autoprotolysis of water) [13] or anisotropic orientation of water molecules at the interface [43]. Results presented in this chapter point towards the latter interpretation. Large changes in pH or ionic strength have no significant influence on the effective charge (Figure 3.3 and Figure 3.4) and the fact that one can see a slight, anisotropic distribution of water molecule orientation at the PDMS interface (Figure 3.7) and a reduction in surface charge through the addition of urea (Figure 3.5), indicates this as an actual cause of the electrophoretic mobility. Other molecular dynamics simulations of the behaviour of water molecules at the water/heptane interface strongly support this interpretation [10].

Several other research groups have observed that water droplets clearly undergo discharging and re-charging with opposite polarity when making contact with a biased electrode [23-30]. Considering that the charge is much greater after contact and that charge of either polarity can be transferred to the droplets, it can be concluded that the contact-charging mechanism is probably different from that of the native water/oil interface charging.

Literature comparison is difficult because studies have used different oils and different experimental methods, which are sensitive to different length scales. For the same reasons, Knecht et al. pointed out that electrophoretic mobility does not always reflect interface charge directly [10].

For this reason, and in view of droplet microfluidic applications, the charge that is calculated in all experiments is the effective droplet charge, that is, the charge defined by Equation 2-11, which links the observed electrophoretic mobility, $\mu_e = v_{el}/E$, and the charge, Q, by a simple proportionality. In other words, non-zero Q does not necessarily mean that ions of one polarity are preferentially adsorbed at the water/oil interface.

3.6 Conclusion

To summarise, it was observed that the native charge and electrophoretic mobility of pure water droplets in silicone and paraffin oil is positive, is independent of ion concentration, and can be reduced in silicone oil through the addition of urea. From these observations and computer simulations, it can be concluded that the native charge is probably due to anisotropic orientation of water molecules at the interface rather than selective adsorption of ions. It could be that the water dipoles have a slight preference to be oriented with their "positive ends", i.e., the H-atoms, towards the silicone oil. In another work, this was determined experimentally by Sum Frequency Scattering (SFS), which is extremely sensitive to the first layer of water molecules at an interface [43]. The droplets, therefore, exhibit a positively charged surface and consequential, positive electrophoretic mobility as no counter ions are present in the silicone oil. A tentative explanation for this preferential orientation of water molecules could be the fact that silicone molecules contain a high number of oxygen atoms, i.e., electronegative atoms, with two lone electron pairs. The electropositive H-atoms of the water molecules may have an affinity towards these O-atoms of the silicone and could possibly even form

hydrogen bonds. The reduction of the surface charge through the addition of urea would also support this assumption. However, one has to be careful not to over-interpret the results, as the general hydrophobicity of siloxanes and silicones speaks against an overall high affinity of water to silicone. Furthermore, paraffin molecules do not contain any hydrogen bond donors or acceptors.

3.7 References

[1] A. D. Griffiths and D. S. Tawfik, "Miniaturising the laboratory in emulsion droplets," *Trends in Biotechnology*, vol. 24, pp. 395-402, 2006.

[2] A. Huebner, S. Sharma, M. Srisa-Art, F. Hollfelder, J. B. Edel, and A. J. deMello, "Microdroplets: A sea of applications?," *Lab on a Chip*, vol. 8, pp. 1244-1254, 2008.

[3] G. S. Fiorini and D. T. Chiu, "Disposable microfluidic devices: fabrication, function, and application," *Biotechniques*, vol. 38, pp. 429-446, Mar 2005.

[4] S. Y. Teh, R. Lin, L. H. Hung, and A. P. Lee, "Droplet microfluidics," *Lab on a Chip*, vol. 8, pp. 198-220, 2008.

[5] J. S. Eow, M. Ghadiri, A. O. Sharif, and T. J. Williams, "Electrostatic enhancement of coalescence of water droplets in oil: a review of the current understanding," *Chemical Engineering Journal*, vol. 84, pp. 173-192, Dec 2001.

[6] S. Pal and S. Bandyopadhyay, "Effects of protein conformational motions in the native form and non-uniform distribution of electrostatic interaction sites on interfacial water," *Chemical Physics*, vol. 420, pp. 35-43, Jul 2013.

[7] V. Knecht, Z. A. Levine, and P. T. Vernier, "Electrophoresis of neutral oil in water," *Journal of Colloid and Interface Science*, vol. 352, pp. 223-231, Dec 15 2010.

[8] M. Vazdar, E. Pluharova, P. E. Mason, R. Vacha, and P. Jungwirth, "Ions at Hydrophobic Aqueous Interfaces: Molecular Dynamics with Effective Polarization," *Journal of Physical Chemistry Letters*, vol. 3, pp. 2087-2091, Aug 2012.

[9] J. K. Beattie, A. N. Djerdjev, and G. G. Warr, "The surface of neat water is basic," *Faraday Discussions*, vol. 141, pp. 31-39, 2009.

[10] V. Knecht, H. J. Risselada, A. E. Mark, and S. J. Marrink, "Electrophoretic mobility does not always reflect the charge on an oil droplet," *Journal of Colloid and Interface Science*, vol. 318, pp. 477-486, Feb 15 2008.

[11] G. V. Franks, A. M. Djerdjev, and J. K. Beattie, "Absence of specific cation or anion effects at low salt concentrations on the charge at the oil/water interface," *Langmuir*, vol. 21, pp. 8670-8674, Sep 13 2005.

[12] J. K. Beattie and A. M. Djerdjev, "The pristine oil/water interface: Surfactant-free hydroxide-charged emulsions," *Angewandte Chemie-International Edition*, vol. 43, pp. 3568-3571, 2004.

[13] K. G. Marinova, R. G. Alargova, N. D. Denkov, O. D. Velev, D. N. Petsev, I. B. Ivanov, and R. P. Borwankar, "Charging of oil-water interfaces due to spontaneous adsorption of hydroxyl ions," *Langmuir*, vol. 12, pp. 2045-2051, Apr 17 1996.

[14] J. C. Carruthers, "The electrophoresis of certain hydrocarbons and their simple derivatives as a function of ph," *Transactions of the Faraday Society*, vol. 34, pp. 300-307, 1938.

[15] A. J. Taylor and F. W. Wood, "The Electrophoresis of Hydrocarbon Droplets in Dilute Solutions of Electrolytes," *Transactions of the Faraday Society*, vol. 53, pp. 523-529, 1957.

[16] B. W. DICKINSON, "The effect of PH upon the electrophoretic mobility of emulsions of certain hydrocarbons and aliphatic halides," *Transactions of the Faraday Society*, vol. 37, pp. 140-148, 1941.

[17] D. J. Im, B. S. Yoo, M. M. Ahn, D. Moon, and I. S. Kang, "Digital Electrophoresis of Charged Droplets," *Analytical Chemistry,* vol. 85, pp. 4038-4044, Apr 16 2013.
[18] K. Choi, M. Im, J. M. Choi, and Y. K. Choi, "Droplet transportation using a pre-charging method for digital microfluidics," *Microfluidics and Nanofluidics,* vol. 12, pp. 821-827, Mar 2012.
[19] M. J. Jebrail, M. S. Bartsch, and K. D. Patel, "Digital microfluidics: a versatile tool for applications in chemistry, biology and medicine," *Lab on a Chip,* vol. 12, pp. 2452-2463, 2012.
[20] J. R. Millman, K. H. Bhatt, B. G. Prevo, and O. D. Velev, "Anisotropic particle synthesis in dielectrophoretically controlled microdroplet reactors," *Nature Materials,* vol. 4, pp. 98-102, Jan 2005.
[21] Y. G. Gu and D. Q. Li, "Electric charge on small silicone oil droplets dispersed in ionic surfactant solutions," *Colloids and Surfaces a-Physicochemical and Engineering Aspects,* vol. 139, pp. 213-225, Aug 10 1998.
[22] A. Khayari, A. T. Perez, F. J. Garcia, and A. Castellanos, "Dynamics and deformation of a drop in a DC electric field," *2003 Annual Report Conference on Electrical Insulation and Dielectric Phenomena,* pp. 682-685, 2003.
[23] D. J. Im, J. Noh, D. Moon, and I. S. Kang, "Electrophoresis of a Charged Droplet in a Dielectric Liquid for Droplet Actuation," *Analytical Chemistry,* vol. 83, pp. 5168-5174, Jul 1 2011.
[24] M. Hase, S. N. Watanabe, and K. Yoshikawa, "Rhythmic motion of a droplet under a DC electric field," *Physical Review E,* vol. 74, p. 046301, Oct 2006.
[25] Y.-M. Jung, H.-C. Oh, and I. S. Kang, "Electrical charging of a conducting water droplet in a dielectric fluid on the electrode surface," *Journal of Colloid and Interface Science,* vol. 322, pp. 617-623, 2008.
[26] M. Takinoue, Y. Atsumi, and K. Yoshikawa, "Rotary motion driven by a direct current electric field," *Applied Physics Letters,* vol. 96, p. 104105, Mar 2010.
[27] M. Jalaal, B. Khorshidi, and E. Esmaeilzadeh, "An experimental study on the motion, deformation and electrical charging of water drops falling in oil in the presence of high voltage DC electric field," *Experimental Thermal and Fluid Science,* vol. 34, pp. 1498-1506, Nov 2010.
[28] D. J. Im, M. M. Ahn, B. S. Yoo, D. Moon, D. W. Lee, and I. S. Kang, "Discrete Electrostatic Charge Transfer by the Electrophoresis of a Charged Droplet in a Dielectric Liquid," *Langmuir,* vol. 28, pp. 11656-11661, Aug 14 2012.
[29] B. Vajdi Hokmabad, B. Sadri, M. R. Charan, and E. Esmaeilzadeh, "An experimental investigation on hydrodynamics of charged water droplets in dielectric liquid medium in the presence of electric field," *Colloids and Surfaces A: Physicochemical and Engineering Aspects,* vol. 401, pp. 17-28, 2012.
[30] D. W. Lee, D. J. Im, and I. S. Kang, "Electrophoretic motion of a charged water droplet near an oil-air interface," *Applied Physics Letters,* vol. 100, p. 221602, May 28 2012.
[31] C. P. Lee, H. C. Chang, and Z. H. Wei, "Charged droplet transportation under direct current electric fields as a cell carrier," *Applied Physics Letters,* vol. 101, p. 014103, Jul 2 2012.
[32] J. T. Cabral and S. D. Hudson, "Microfluidic approach for rapid multicomponent interfacial tensiometry," *Lab on a Chip,* vol. 6, pp. 427-436, Mar 2006.
[33] T. Ohashi, H. Kuyama, N. Hanafusa, and Y. Togawa, "A simple device using magnetic transportation for droplet-based PCR," *Biomedical Microdevices,* vol. 9, pp. 695-702, Oct 2007.

[34] P. J. Bailes, J. G. M. Lee, and A. R. Parsons, "An experimental investigation into the motion of a single drop in a pulsed DC electric field," *Chemical Engineering Research & Design,* vol. 78, pp. 499-505, Apr 2000.
[35] D. Choi, H. Lee, D. J. Im, I. S. Kang, G. Lim, D. S. Kim, and K. H. Kang, "Spontaneous electrical charging of droplets by conventional pipetting," *Scientific Reports,* vol. 3, p. 2037, 2013.
[36] R. Zimmermann, U. Freudenberg, R. Schweiss, D. Kuttner, and C. Werner, "Hydroxide and hydronium ion adsorption - A survey," *Current Opinion in Colloid & Interface Science,* vol. 15, pp. 196-202, Jun 2010.
[37] A. M. Schoeler, D. N. Josephides, S. Sajjadi, C. D. Lorenz, and P. Mesquida, "Charge of water droplets in non-polar oils," *Journal of Applied Physics,* vol. 114, p. 144903, 2013.
[38] S. Plimpton, "Fast Parallel Algorithms for Short-Range Molecular-Dynamics," *Journal of Computational Physics,* vol. 117, pp. 1-19, Mar 1 1995.
[39] H. Sun, "COMPASS: An ab initio force-field optimized for condensed-phase applications - Overview with details on alkane and benzene compounds," *Journal of Physical Chemistry B,* vol. 102, pp. 7338-7364, Sep 17 1998.
[40] J. P. Ryckaert, G. Ciccotti, and H. J. C. Berendsen, "Numerical-Integration of Cartesian Equations of Motion of a System with Constraints - Molecular-Dynamics of N-Alkanes," *Journal of Computational Physics,* vol. 23, pp. 327-341, 1977.
[41] J. Lyklema, H. P. van Leeuwen, M. Vliet, and A. M. Cazabat, *Fundamentals of interface and colloid science* vol. 5: Academic Pr, 2005.
[42] D. J. Im, J. Noh, N. W. Yi, J. Park, and I. S. Kang, "Influences of electric field on living cells in a charged water-in-oil droplet under electrophoretic actuation," *Biomicrofluidics,* vol. 5, Dec 2011.
[43] R. Vacha, S. W. Rick, P. Jungwirth, A. G. F. de Beer, H. B. de Aguiar, J. S. Samson, and S. Roke, "The Orientation and Charge of Water at the Hydrophobic Oil Droplet-Water Interface," *Journal of the American Chemical Society,* vol. 133, pp. 10204-10210, Jul 6 2011.

Chapter 4 Controlling the surface charge of water droplets in non-polar oils

4.1 Chapter Abstract

The chapter shows that the surface charge and, hence, the electrophoretic mobility of water droplets dispersed in non-polar oils can be adjusted in magnitude and sign through the addition of ionic surfactants. The positive, native charge of water-in-oil droplets is reduced by increasing the concentration of the anionic surfactant SDS in the water. At high enough SDS concentration, the droplet charge becomes negative. This mechanism works with both silicone and paraffin oil and is limited by the critical micelle concentration of SDS in water at which the interface is saturated by the surfactant. Direct, physical contact-charging of water droplets at biased electrodes, however, overrides any charge due to chemical species at the water-oil interface and confers an overall charge of the same sign as the electrode potential to the droplets.

4.2 Introduction

Water-in-oil microdroplets are an attractive "tool" in lab-on-a-chip devices, as they offer simple compartmentalisation [1], constitute tiny reaction chambers [2] and can be used to perform "digital" operations [2-4]. One of the many benefits they offer is the ability of micrometre sized droplets (typically ranging from 1μm to 500μm) to act as encapsulating templates (micro-reaction chambers) in a high-throughput environment [5, 6]. However, microscopic droplet manipulation is not always easy to achieve efficiently by traditional, hydraulic methods based on pumps, channels and valves, which, ideally, require miniaturised, on-chip fluid-handling components. A possible alternative is manipulation by electric fields and signals, which is simple to implement on-chip using electrode arrays and suitable wiring.

Here, water droplets dispersed in non-polar oil are manipulated by exploiting the fundamental phenomenon of electrophoretic motion, i.e. motion in response to an external, electric field. An advantage of this method is that localised electric fields are much easier to generate and to control compared to the often more complex pressure or flow fields [7]. To this end, it is necessary to know the net charge of water microdroplets dispersed in oil and, ideally, to have simple means to adjust this charge.

A physical method to actively charge droplets is through direct contact with a voltage-biased electrode [8-18]. This type of direct, physical charge transfer between electrodes and droplets has been investigated in more detail in the literature [9]. An alternative, chemical method could be the introduction of additives. It is known that surfactants can alter the surface charge of oil droplets dispersed in water (O/W emulsions) by being adsorbed at the droplet interface [19, 20]. However, the influence of ionic surfactants on the charge of water droplets in oil (W/O emulsions) has, so far, received little attention. From a practical point-of-view, it would also be necessary to know if and to what extent the addition of a surfactant influences the surface charge of a droplet before and after contact with a biased electrode.

The results presented in this chapter help to determine the effects of surfactants on droplet surface charge, by conducting electrophoretic measurements of water droplets in the same oils as before – silicone and paraffin oil.

4.3 Experimental Set-Up

All micro-electrophoretic experiments were performed in the same transparent, rectangular electrophoretic cell as described in the Methodology chapter (Figure 4.1). The cell was filled with either silicone or paraffin oil and positioned between a light source and a high-speed camera. Each water droplet was injected individually into the oil using a hand held micropipette (Finnpipette® Focus single channel pipette - volume 0.3-3 µl, Sigma-Aldrich,

Dorset, UK), instead a pulled glass microcapillary, described in the Methodology chapter. The reason for this slight change in experimental procedure is that the use of surfactant in the dispersed water phase would often cause blockages inside the capillary. Using this handheld device the droplet radius was kept constant at $R = 500\ \mu m \pm 20\ \mu m$. An electric field of 2.3 kV/cm was used for all surfactant-free experiments, whereas an electric field of 1.2 kV/cm was used in the experiments with surfactants to avoid excessive droplet deformation due to reduced interfacial tension. All experiments were conducted at room temperature (21ºC) and, overall, 230 droplets were investigated.

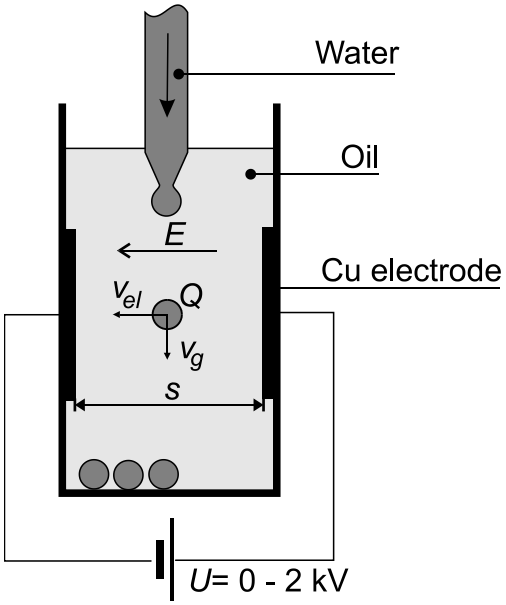

Figure 4.1 Experimental set-up for electrophoretic measurements, as described in the Methodology chapter.

4.4 Results and discussion

In the absence of a surfactant, all water droplets (injected into the cell using the hand held pipette) travelled towards the negative electrode as soon as the electric field was applied (as discussed in Chapter 3), thereby showing that the droplets had an initial, native, positive net surface charge before making contact with an electrode (surface charge density $10 \times 10^{-7}\ Cm^{-2} \pm 3.4 \times 10^{-7}\ Cm^{-2}$ for silicone and $5 \times 10^{-7}\ Cm^{-2} \pm 2.8 \times 10^{-7}\ Cm^{-2}$ for paraffin

oil). The surfactant-free droplets then made contact with the negative electrode, where they were discharged and recharged with opposite polarity and repelled towards the positive electrode. A general back-and-forth motion was observed, which has been previously described and has been observed by others [9-11, 13, 14, 21] in more detail. Essentially, the droplets behave like conducting spheres in a dielectric medium [22]. The charge acquired by a conducting sphere in contact with a biased electrode is described by the perfect conductor theory [9, 22-24]. This equation is based on derivation of by Felici [24], who analytically arrived at this expression:

$$Q_{sphere} = \frac{\pi^2}{6}(4\pi R^2 \varepsilon_{medium} E) \qquad \text{Equation 4-15}$$

where R is the radius of the sphere, ε_{medium} the permittivity of the surrounding medium.

To check its validity and applicability for this experimental set-up, an additional control experiment was conducted. Using the experimental set-up described in Figure 4.1, the electrophoretic cell was re-calibrated using metallic spheres of density 8.64 g/cm^3 (R = 580 µm) in silicone oil. The same spheres were then injected into silicone oil and their electrophoretic mobility was recorded. As the sphere had a much greater density than the silicone oil, a very high electric field (E = 3.8 kV/cm) had to be applied in order to record any electrophoretic motion of the sphere. It was found that the actual droplet charge and surface charge density acquired by the metallic sphere were 8×10^{-11} C and 1.9×10^{-5} Cm^{-2}, respectively, compared to theoretical values of 6.2×10^{-11} C and 1.5×10^{-5} Cm^{-2}. Although there was a 25% difference between the actual and theoretical value, it was still within the experimental error (35%). In comparison, the surface charge density acquired by a water droplet of similar radius after contact with an electrode was found to be 1.3×10^{-5} Cm^{-2} (Figure 4.2). This suggests that the perfect conductor theory for metal spheres can feasibly be applied to water droplets as well.

Figure 4.2 illustrates the magnitudes of the surface charge density of pure water droplets after they made contact with a biased electrode in silicone and paraffin oil. For a given *R*, the surface charge magnitude of a water droplet in both non-polar oils after first and second contact with an electrode is 10 times greater than before contact (see Chapter 3) and remains constant regardless of whether the droplet has acquired a positive or a negative surface charge. As shown in Figure 4.2, the magnitude of surface charge of water droplets in silicone oil was twice as high compared to the surface charge of water droplets in paraffin oil.

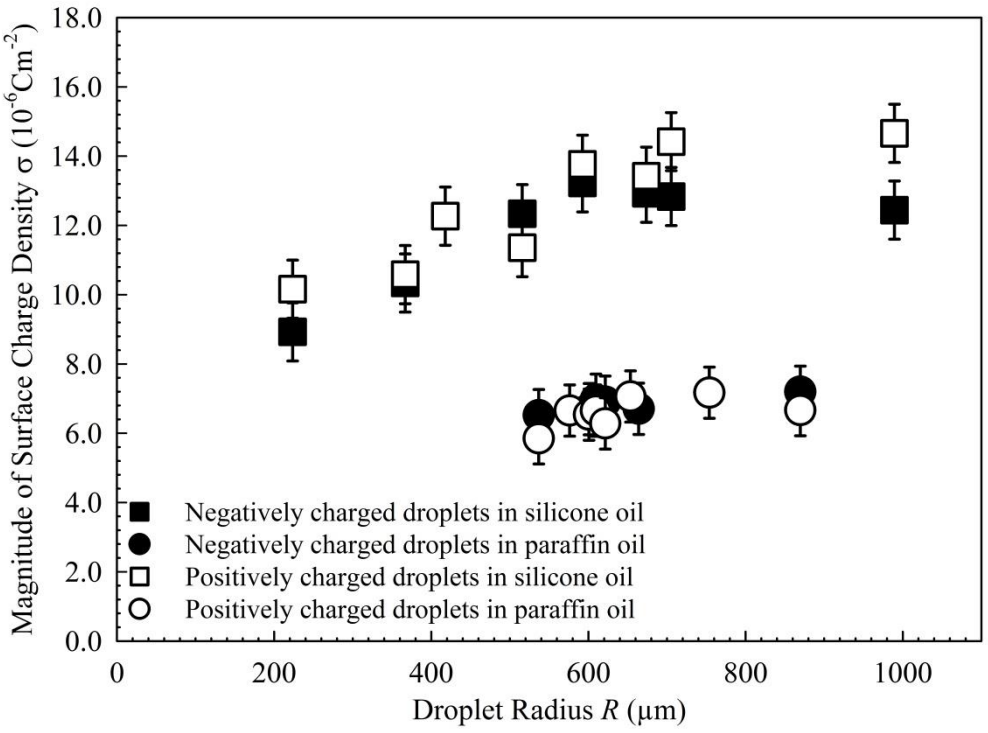

Figure 4.2 Magnitudes of surface charge density after a droplet is charged on a biased electrode. Negatively charged droplets in paraffin (●) and silicone (■) oil after first contact with negatively charged electrode and positively charged droplets in paraffin (○) and silicone (□) oil after second contact with positively charged electrode under electric field E = 2.3 kV/cm. Error bars represent the standard deviation of 10 droplets.

The calculated surface charge density of water droplets in silicone oil was significantly greater than similar data presented by Im et al. [9]. However, Im et al. used the Hadamard-

Rybczynski (HR) drag force coefficient, whilst the system used here has been calibrated (see Methodology chapter). When applying the HR coefficient in silicone and paraffin oil for a droplet radius of 500 μm, for example, the calculated surface charge density is reduced to 5.6×10^{-6} Cm^{-2} and 3.9×10^{-6} Cm^{-2}, respectively; the former mirrors the results presented by Im et al. This underlines the importance of calibrating the system.

A standard deviation of the surface charge magnitudes in both oils after contact with a charged electrode was determined, using the data presented in Figure 4.2. The measurement accuracy was found to be 1.5×10^{-6} Cm^{-2} (after negative contact) and 2.1×10^{-6} Cm^{-2} (after positive contact) in silicone oil and 1.3×10^{-6} Cm^{-2} (after negative contact) and 1.4×10^{-6} Cm^{-2} (after positive contact) in paraffin oil.

4.4.1 Influence of surfactants on the initial charge of droplets

To investigate the effect of ionic surfactants on the droplet charge, various concentrations of the anionic surfactant Sodium Dodecyl Sulfate (SDS) and cationic surfactant Hexadecyltrimethylammonium bromide (CTAB) were added to the water phase. Figure 4.3a and Figure 4.3b show the effects on the initial surface charge density before first contact with a biased electrode.

When the anionic surfactant SDS is added to the water droplets (Figure 4.3a), the surface charge density of the water droplets is altered. It was observed that, below a concentration of 1 g/l SDS, the surface charge density is reduced but still positive in both paraffin and silicone oil. At a concentration greater than 1.5 g/l SDS, droplets travelled towards the positive electrode, which means that their net surface charge is negative. The magnitude of the negative surface charge increases further with increasing SDS concentration up to a value of about 2.5 g/l, at which point the critical micelle concentration (CMC) of SDS is reached. At concentrations higher than the CMC, the surface charge density of water in both oils becomes

independent of SDS concentration, with -6×10^{-7} Cm^{-2} $\pm$ 3.4×10^{-7} Cm^{-2} for silicone and -5×10^{-7} Cm^{-2} $\pm$ 2.8×10^{-7} Cm^{-2} for paraffin oil. The interpretation is that the hydrophobic tails of the SDS molecules "pin" their negatively-charged sulphate groups at the water-oil interface, whereas the positive sodium counter-ions disperse in solution throughout the volume of the droplets. As the sulphate groups are, thus, located predominantly at the interface, they dominate the overall net charge of the droplets and their electrophoretic mobility. The same trend has been observed by Gu et al. for silicone oil droplets dispersed in a water and ionic surfactant (either SDS or CTAB) solution [19].

The point of zero charge, that is the SDS concentration at which the net surface charge is zero (dashed, horizontal lines in Figure 4.3a and Figure 4.3b), cannot be determined directly by an electrophoretic measurement as, in this case, the droplets do not move anymore. However, one can determine an approximate value for the point of zero charge by fitting a straight line through the data shown in Figure 4.3a. Using the least-squares method, a best-fit function to the data points (omitting the highest data point at 25 g/l) was found to be the 1st-order polynomial $\sigma = a\varphi + b$ (with φ = SDS mass concentration (g/l), $a_{silicone}$ = -5.5×10^{-9} Cm/g, $b_{silicone}$= 7.8×10^{-6} Cm^{-2}, $a_{paraffin}$ = -3.4×10^{-9} Cm/g and $b_{paraffin}$ = 5.5×10^{-6} Cm^{-2}). Thus, the point of zero charge is in the region of 1.4 g/l and 1.6 g/l for silicone and paraffin oil, respectively.

The addition of the cationic surfactant CTAB had a much smaller, if any, effect on the surface charge density (Figure 4.3b), even at concentrations 10 times greater than its CMC. The sign of the charge was not changed upon increased CTAB concentration. This is in agreement with the previous interpretation, which is analogous to the SDS case, namely that the positive trimethylammonium groups of CTAB are "pinned" at the water-oil interface.

It can also be seen from the data in Figure 4.3a and Figure 4.3b that the difference in droplet surface charge density between the two oils is reduced upon addition of both SDS and CTAB.

Without surfactant, the charge of droplets in silicone oil is marginally higher than that of droplets in paraffin oil (Figure 4.3a and Figure 4.3b). At the CMC, however, the droplet charge difference between silicone and paraffin oil becomes insignificant within the measurement error for both SDS and CTAB. The idea that surfactant charges "override" native charges due to molecular orientation could be used to interpret this phenomenon.

(a) (b)

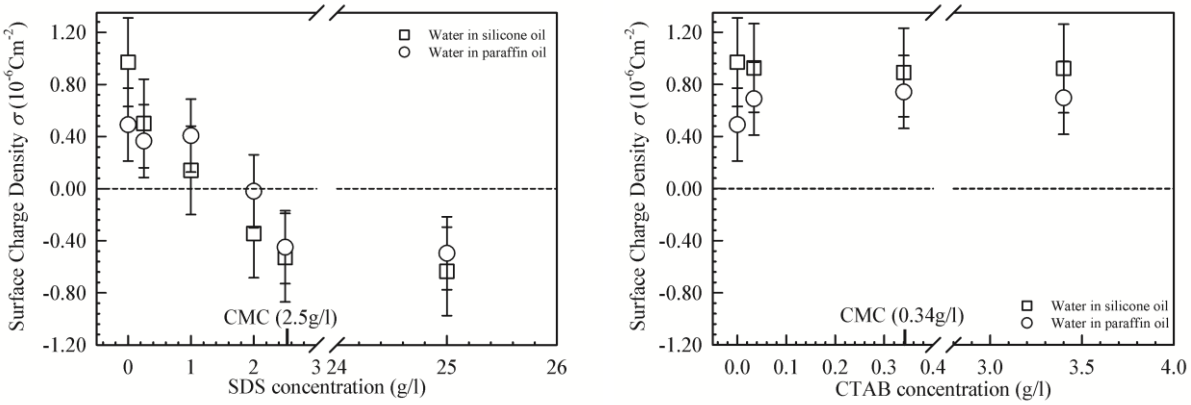

(c)

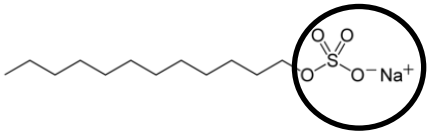

(d)

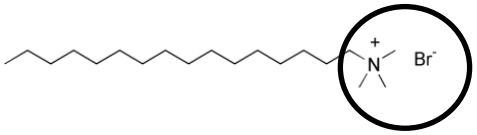

Figure 4.3 Influence of ionic surfactant on initial droplet surface charge in paraffin (○) and silicone (□) oil, where R = 500 μm and E = 1.2 kV/cm, error bars represent the measurement uncertainty of 3.4 ×10^{-7} Cm^{-2} in silicone and 2.8 ×10^{-7} Cm^{-2} in paraffin oil. (a) With increasing anionic surfactant concentration – Sodium Dodecyl Sulfate (SDS), (b) with increasing cationic surfactant concentration – Hexadecyltrimethylammonium Bromide (CTAB), (c) SDS molecule and schematic of SDS affiliation to water droplet, (d) CTAB molecule and schematic of CTAB affiliation to water droplet.

4.4.2 Effect of direct, physical contact-charging of droplets

(a) (b)

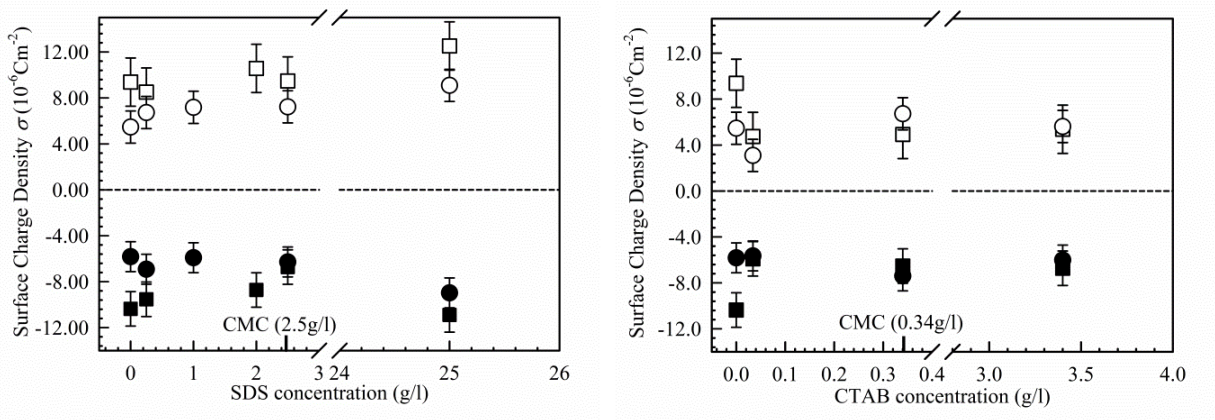

Figure 4.4 Surface charge density of droplets with surfactant after droplets made contact with a positively charged electrode in paraffin (○) and silicone (□) oil, and after contact with a negatively charged electrode in paraffin (●) and silicone (■) oil, where R = 500 μm and E = 1.2 kV/m. (a) anionic surfactant Sodium Dodecyl Sulfate (SDS), (b) cationic surfactant Hexadecyltrimethylammonium Bromide (CTAB). Error bars represent the standard deviation of surface charge densities of pure water droplets of varying size dispersed in silicone (standard deviation = 1.5 $\times 10^{-6}$ Cm^{-2} after contact with a negative electrode, standard deviation = 2.1 $\times 10^{-6}$ Cm^{-2} after contact with a positive electrode) and paraffin oil (standard deviation = 1.3 $\times 10^{-6}$ Cm^{-2} after contact with a negative electrode, standard deviation = 1.4 $\times 10^{-6}$ Cm^{-2} after contact with a positive electrode). It was not possible to obtain electrophoretic data for water droplets with 1 g/l SDS in silicone oil and 2 g/l SDS in paraffin oil, because the surface charge was so small that droplets did not move enough initially to make contact with an electrode.

Figure 4.4 shows the surface charge density of water droplets after they have been charged by direct, physical contact with a biased electrode. Contact with the positive electrode leads to positively charged droplets (Figure 4.4a and b, open symbols) whereas contact with the negative electrode leads to negatively charged droplets (Figure 4.4a and b, solid symbols), regardless of oil type or surfactant present. The surface charge densities obtained by contact-charging are at least 5 times greater than the initial surface charge densities before any electrode contact (Figure 4.3), which points to a molecular charging mechanism different from the one discussed in the previous chapter. Furthermore, within the measurement

accuracy, the surface charge densities of contact-charged droplets are independent of the surfactant concentration, except for the case of droplets which contain CTAB and which are dispersed in silicone oil (Figure 4.4b, square symbols). Here, addition of CTAB reduces the surface charge density by a factor of ~2 compared to that of deionized water but is then largely independent of the actual surfactant concentration. Overall, after electrode contact, droplets with surfactant behave essentially in the same way as those without surfactant [9-11, 13, 14, 21, 25]. Figure 4.4 demonstrates that charging droplets physically at a biased electrode "overrides" any charge due to chemical additives such as surfactants.

4.5 Conclusion

It is already well established that the addition of the anionic surfactant SDS causes the surface charge of oil droplets dispersed in water to become negative [19]. This chapter has shown that this is also true for an inverse emulsion, that is, water droplets dispersed in non-polar oils. The fact that the surface charge density of the water droplets can be adjusted (Figure 4.3a) by addition of SDS, suggests that this very simple method can be used in a variety of applications. For example, as will be shown in the next chapter, core-shell droplets can be manipulated using electrophoresis and ultrathin core-shells can be created using 2.3 g/l SDS. The experimental data presented in this chapter indicates that the initial surface charge of the core-shell droplets can be controlled and clears the way for the use of core-shell droplets in digital microfluidic systems based on a direct electric charging, like the one demonstrated by Im et al. [18].

There has been significant interest in water droplet electrophoresis in the literature in recent years [8-17], especially regarding the use of water droplets as tiny compartments inside microfluidic, lab-on-a-chip devices [1-4, 26]. Efficient droplet manipulation in microfluidics requires droplets to be responsive to an electrical field in a predictable way. Previous results have shown that pure droplets are slow to react to an electric field, move slowly and need a

long time to travel before contact with an electrode. It is also known that a limiting factor that often determines the overall size of the particular droplet delivery system is the droplet's size. One option is to reduce the droplet size through the addition of surfactant, which also stabilises the emulsion and aids the creation of more complex emulsion systems. The knowledge that any charge properties of the surfactant can be overridden through contact with a biased electrode (Figure 4.4) can therefore lead to smaller droplet sizes and more complex emulsion systems.

This chapter has shown that the initial droplet surface charge of water droplets in non-polar oils can be controlled and changed from positive to negative using the anionic surfactant SDS; using the cationic surfactant CTAB has no effect on initial surface charge. The droplet surface charge is increased by a factor of 10 when the droplet touches a biased electrode and any surfactant charge effects are overridden.

4.6 References

[1] A. D. Griffiths and D. S. Tawfik, "Miniaturising the laboratory in emulsion droplets," *Trends in Biotechnology,* vol. 24, pp. 395-402, 2006.

[2] A. Huebner, S. Sharma, M. Srisa-Art, F. Hollfelder, J. B. Edel, and A. J. deMello, "Microdroplets: A sea of applications?," *Lab on a Chip,* vol. 8, pp. 1244-1254, 2008.

[3] S. Y. Teh, R. Lin, L. H. Hung, and A. P. Lee, "Droplet microfluidics," *Lab on a Chip,* vol. 8, pp. 198-220, 2008.

[4] G. S. Fiorini and D. T. Chiu, "Disposable microfluidic devices: fabrication, function, and application," *Biotechniques,* vol. 38, pp. 429-446, Mar 2005.

[5] H. C. Shum, A. Bandyopadhyay, S. Bose, and D. A. Weitz, "Double Emulsion Droplets as Microreactors for Synthesis of Mesoporous Hydroxyapatite," *Chemistry of Materials,* vol. 21, pp. 5548-5555, Nov 24 2009.

[6] P. W. Chen, R. M. Erb, and A. R. Studart, "Designer Polymer-Based Microcapsules Made Using Microfluidics," *Langmuir,* vol. 28, pp. 144-152, Jan 10 2012.

[7] E. Amstad, S. S. Datta, and D. A. Weitz, "The microfluidic post-array device: high throughput production of single emulsion drops," *Lab on a Chip,* vol. 14, pp. 705-709, 2014.

[8] K. Choi, M. Im, J. M. Choi, and Y. K. Choi, "Droplet transportation using a pre-charging method for digital microfluidics," *Microfluidics and Nanofluidics,* vol. 12, pp. 821-827, Mar 2012.

[9] D. J. Im, J. Noh, D. Moon, and I. S. Kang, "Electrophoresis of a Charged Droplet in a Dielectric Liquid for Droplet Actuation," *Analytical Chemistry,* vol. 83, pp. 5168-5174, Jul 1 2011.

[10] M. Hase, S. N. Watanabe, and K. Yoshikawa, "Rhythmic motion of a droplet under a DC electric field," *Physical Review E,* vol. 74, p. 046301, Oct 2006.

[11] Y.-M. Jung, H.-C. Oh, and I. S. Kang, "Electrical charging of a conducting water droplet in a dielectric fluid on the electrode surface," *Journal of Colloid and Interface Science,* vol. 322, pp. 617-623, 2008.

[12] M. Takinoue, Y. Atsumi, and K. Yoshikawa, "Rotary motion driven by a direct current electric field," *Applied Physics Letters,* vol. 96, p. 104105, Mar 2010.

[13] M. Jalaal, B. Khorshidi, and E. Esmaeilzadeh, "An experimental study on the motion, deformation and electrical charging of water drops falling in oil in the presence of high voltage DC electric field," *Experimental Thermal and Fluid Science,* vol. 34, pp. 1498-1506, Nov 2010.

[14] D. J. Im, M. M. Ahn, B. S. Yoo, D. Moon, D. W. Lee, and I. S. Kang, "Discrete Electrostatic Charge Transfer by the Electrophoresis of a Charged Droplet in a Dielectric Liquid," *Langmuir,* vol. 28, pp. 11656-11661, Aug 14 2012.

[15] B. Vajdi Hokmabad, B. Sadri, M. R. Charan, and E. Esmaeilzadeh, "An experimental investigation on hydrodynamics of charged water droplets in dielectric liquid medium in the presence of electric field," *Colloids and Surfaces A: Physicochemical and Engineering Aspects,* vol. 401, pp. 17-28, 2012.

[16] D. W. Lee, D. J. Im, and I. S. Kang, "Electrophoretic motion of a charged water droplet near an oil-air interface," *Applied Physics Letters,* vol. 100, p. 221602, May 28 2012.

[17] C. P. Lee, H. C. Chang, and Z. H. Wei, "Charged droplet transportation under direct current electric fields as a cell carrier," *Applied Physics Letters,* vol. 101, p. 014103, Jul 2 2012.

[18] D. J. Im, B. S. Yoo, M. M. Ahn, D. Moon, and I. S. Kang, "Digital Electrophoresis of Charged Droplets," *Analytical Chemistry,* vol. 85, pp. 4038-4044, Apr 16 2013.

[19] Y. G. Gu and D. Q. Li, "Electric charge on small silicone oil droplets dispersed in ionic surfactant solutions," *Colloids and Surfaces a-Physicochemical and Engineering Aspects,* vol. 139, pp. 213-225, Aug 10 1998.
[20] E. Buxbaum, "Cationic electrophoresis and electrotransfer of membrane glycoproteins," *Analytical Biochemistry,* vol. 314, pp. 70-76, 2003.
[21] P. J. Bailes, J. G. M. Lee, and A. R. Parsons, "An experimental investigation into the motion of a single drop in a pulsed DC electric field," *Chemical Engineering Research & Design,* vol. 78, pp. 499-505, Apr 2000.
[22] A. Khayari and A. T. Perez, "Charge acquired by a spherical ball bouncing on an electrode: comparison between theory and experiment," *Dielectrics and Electrical Insulation, IEEE Transactions on,* vol. 9, pp. 589-595, 2002.
[23] A. Khayari, A. T. Perez, and A. Castellanos, "The charge acquired by a spherical ball bouncing on an electrode: comparison between theory and experiment," *2000 Annual Report Conference on Electrical Insulation and Dielectric Phenomena, Vols. I & Ii,* pp. 470-473, 2000.
[24] N. J. Felici, "Forces et Charges de Petits Objets en Contact avec une Électrode Affectée d'un Champ Électrique," *Revue Générale de l'Électricité* vol. 75, pp. 1145-60, 1966.
[25] A. M. Schoeler, D. N. Josephides, S. Sajjadi, C. D. Lorenz, and P. Mesquida, "Charge of water droplets in non-polar oils," *Journal of Applied Physics,* vol. 114, p. 144903, 2013.
[26] E. M. Blanco, S. A. Nesbitt, M. A. Horton, and P. Mesquida, "A Multiprotein Microarray on Silicon Dioxide Fabricated by Using Electric-Droplet Lithography," *Advanced Materials,* vol. 19, pp. 2469-2473, 2007.

Chapter 5 Electrophoretic Manipulation of multiple emulsion droplets

5.1 Chapter Abstract

This chapter presents the electrophoretic manipulation of multiple-emulsion oil-in-water-in-oil (O/W)/O and water-in-oil-in-water-in-oil (W/O/W)/O core-shell droplets. It was found that the electrophoretic mobility of the droplets is determined solely by the outer water shell, regardless of size or composition of the inner droplets. Similar to simple W/O droplets, it was observed that the surface charge of the outer water shell can be changed and the polarity can be reversed through contact with a biased electrode or through the addition of sodium dodecyl sulfate (SDS). The results have practical implications for the manipulation of oil droplets in a continuous oil phase.

5.2 Introduction

Water-in-oil (W/O) microdroplets are the subject of intense research in the field of digital microfluidics and lab-on-a-chip devices [1-4]. W/O droplets can be used to facilitate and influence bio-chemical reactions [5], can act as tiny compartments inside lab-on-a-chip devices [1-4, 6] or offer droplet manipulation functions [7]. While many reagents, especially biomolecules, such as proteins and sugars, are water-soluble and can, thus, be encapsulated by W/O droplets in principle, this is not the case for hydrophobic peptides or, in general, lipophilic substances. In order to encapsulate lipophilic, non-polar substances within a non-polar continuous phase, one requires so-called double or multiple-emulsions, that is, “emulsions within emulsions” of nested oil-in-water-in-oil, (O/W)/O, droplets, which have already been found to show considerable benefits in both cosmetic [8-10] and pharmaceutical applications [11].

As the continuous oil phase is usually non-conductive, water droplets dispersed in oil can easily be manipulated by electrical fields, as demonstrated in Chapters 3 and 4 and in other studies elsewhere [12-21]. However, the electrostatic manipulation of double or multiple-emulsion droplets has not yet been shown. It needs to be assessed whether the addition of oil droplets within water droplets would change the electrophoretic mobility of the latter, which, in turn, would have implications on the design of (O/W)/O droplet manipulation procedures.

5.3 Experimental Set-Up

All microelectrophoretic experiments were performed using the same transparent, electrophoretic cell and experimental method as described in the Methodology chapter (Figure 5.1). Individual oil-in-water droplets were injected into the continuous 100cst silicone oil phase using a concentric, glass microcapillary channel system (outer channel diameter = 320 μm, inner channel diameter = 70 μm, which were coaxially aligned). Once injected, the core-shell droplets also sink to the bottom of the cuvette, akin to the simple O/W droplets, discussed previously. As soon as the core shell droplet reaches the centre of the electrodes, the voltage is applied. The water shell radius was kept constant (R_{shell} = 800 μm), whilst the radius of the oil core droplet was variable (R_{core} = 0-750 μm). It was decided to use silicone oil in these experiments, due to its higher viscosity. All experiments were conducted at 21ºC.

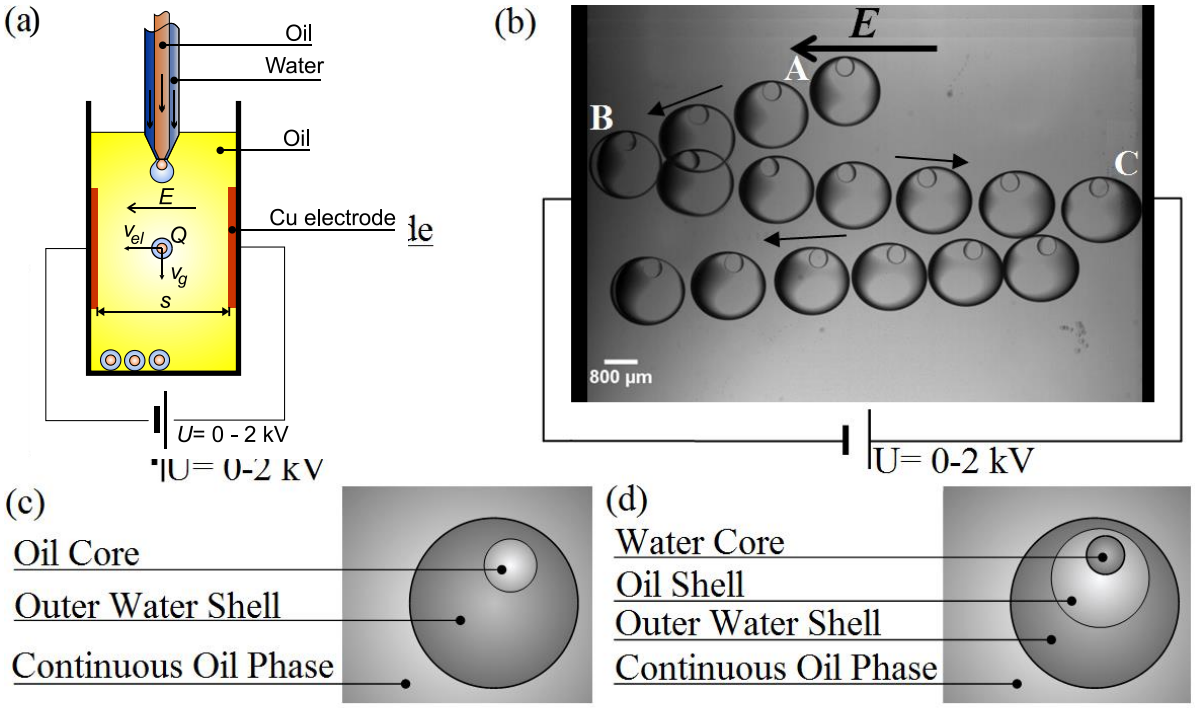

Figure 5.1 (a) Amended experimental set-up through the addition of another microchannel, where outer water shell radius, R_{shell} = 800 µm, distance between electrodes, s = 1.4 cm, and electric field, E = 1.5 kV/cm. (b) Overlaid snapshots of the electrophoretic back-and-forth motion of (O/W)/O droplet between the two electrodes (right, positive, and left, negative, at the edge of the picture) while continuing to slowly fall due to gravity. Arrows represent the direction of motion, where letters A, B and C are positional markers. (c) Definition of terms for an O/W/O droplet and (d) for a W/O/W/O droplet.

5.4 Results

5.4.1 General Behaviour of (O/W)/O Droplets

Without surfactant, it was not possible to create stable (O/W)/O droplets at R_{core} > 500 µm, as the oil core left the water shell by merging with the continuous oil phase. For (O/W)/O droplets with smaller oil core sizes, it was observed that, as soon as the electric field was applied, all droplets initially travelled towards the negative electrode (Figure 5.1 (b), position A), thereby showing that the core-shell droplets have an initial, positive electrophoretic mobility before making contact with an electrode.

Near the electrode, the droplets elongated slightly towards the electrode, forming a small tip, which eventually touched the electrode (Figure 5.1 (b), position B). After contacting the electrode for a fraction of a second, the droplets were repelled and travelled towards the opposite, positive electrode (Figure 5.1 (b), position C), where the process repeated itself in the opposite direction, leading to a back-and-forth motion between the two electrodes while the droplets continued to slowly fall due to gravity. In summary, complex core shell droplets behave in the same fashion as simple W/O droplets, when using the same experimental set-up as outlined previously in Chapters 2, 3 and 4.

The magnitudes of the droplet velocities after the first contact with an electrode were approximately 10× greater than the initial velocity (Figure 5.2). This general behaviour of an initial charge followed by active charging has been discussed previously and has been observed by other researchers [13-15, 17, 18, 22], although no other group seems to have attempted electrophoretic experiments with complex, multiple-droplets so far.

As silicone oil has a lower density than water, the oil cores moved upwards to the top of the water shell (Figure 5.1 (b), position A). As soon as the electric field was applied, the oil core was deflected in the opposite direction relative to the motion of the outer water shell (Figure 5.1 (b), (c) and (d)).

When 2.3 g/l of the anionic surfactant sodium dodecyl sulfate (SDS) was added to the water phase, it was observed that all droplets initially travelled towards the positive electrode, thereby showing that SDS-modified core-shell droplets have an initial, negative, electrophoretic mobility before making contact with an electrode (as outlined in Chapter 4). The SDS-modified core-shell droplets then followed the same type of

motion as the droplets without SDS, i.e. a back-and-forth motion between the two electrodes while continuing to slowly fall due to gravity.

Greater deformation of the SDS-containing droplets compared to the surfactant-free water droplets was observed, which was due to lowered interfacial tension. The addition of surfactant also made the core-shell droplets more stable (i.e. the oil core would no longer merge with the continuous oil phase), allowing greater core-shell size control (Figure 5.2(e)) and larger core-shell ratios to be investigated (Figure 5.2(c) and (d)). Unlike the outer water shell, no deformation of the oil core could be observed.

5.4.2 Influence of the Oil Core Size of (O/W)/O Droplets on the Electrophoretic Mobility

Figure 5.2 shows the influence of the oil core size on the electrophoretic mobility of complex (O/W)/O droplets. Experiments were performed without (Figure 5.2(a) and (b)) and with surfactant (Figure 5.2(c) and 2(d)). Without surfactant, the biggest oil cores that could be produced had a diameter of 0.6× the diameter of the outer water shell (Figure 5.2(a) and (b)), whereas with surfactant, a much wider range of oil core sizes could be produced (Figure 5.2(c), (d) and (e)). The radius of the outer water shell was kept constant at 800 µm. The hypothesis was that the addition of an oil core could change the initial electrophoretic mobility, as oil droplets in water are usually negatively charged [23]. However, analysis of the data in Figure 5.2 indicates only a very weak, if at all existent, effect and dependence on oil core size, regardless of the amount or polarity of charge of the outer water shell in the continuous oil phase. That is, double-emulsion (O/W)/O droplets have essentially the same, or not significantly different, electrophoretic mobility as simple W/O droplets under otherwise identical conditions (oil type, surfactant, contact with biased electrode, etc.) (Chapters 3 and 4).

From this observation, one can conclude that any charge of the oil core is probably screened by the outer water shell. The implications for practical applications are, thus, that complex droplets can be manipulated, and will react in very much the same way as simple droplets. Furthermore, small, charged oil cores can be seen as electrostatically equivalent to globular proteins or cells encapsulated in the water droplets. It is thus unlikely that the addition of charged particles or cells into water microdroplets would greatly affect any electrostatic manipulation procedures in microfluidic devices. This is compatible with previous findings, where no significant influence of electrolyte ions on the electrophoretic mobility of W/O droplets was found (Chapter 3).

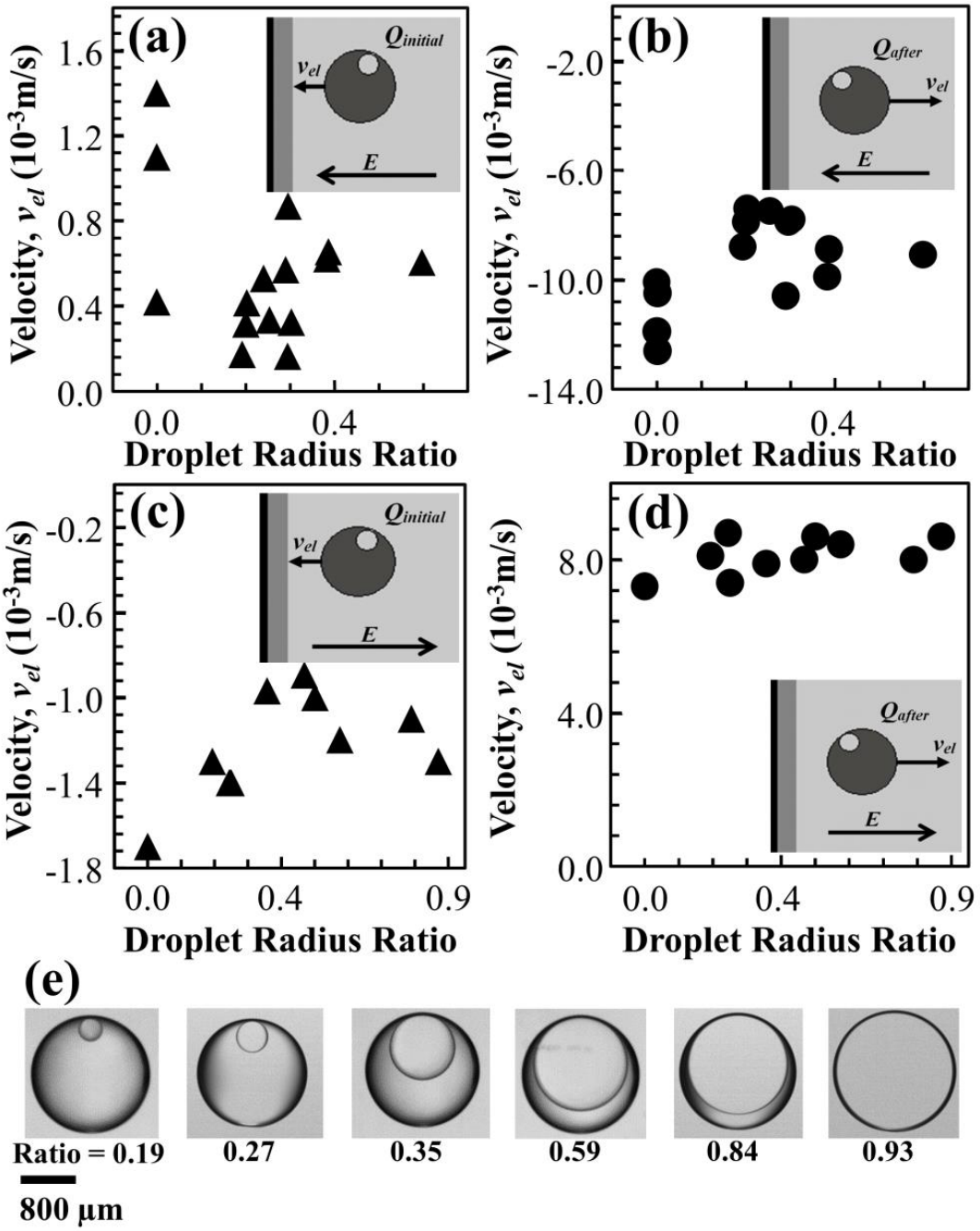

Figure 5.2 (a) and (b) Electrophoretic droplet velocity, v_{el}, of an (O/W)/O droplet versus oil core size, where R_{shell} = constant = 800 µm and R_{core} = 0-500 µm, (a) before contact with an electrode (b) after contact with an electrode. (c) and (d) Electrophoretic droplet velocity, v_{el}, of an (O/W)/O droplet (with 2.30 g/l SDS) in dependence of oil core size, where R_{shell} = constant = 800 µm and R_{core} = 0-750 µm, (c) before contact with an electrode, (d) after contact with an electrode. Each data point represents one individual core-shell drop and the measurement accuracy of v_{el} is approximately 30 µms^{-1} (error bars not shown as they are smaller than the data symbols). (e) Images of droplets with different radius ratios using 2.30 g/l SDS.

5.4.3 Deflection of the Oil Core against the Direction of Motion in Electrostatic Fields

As mentioned above, a deflection of the oil core in opposite direction to the electrophoretic mobility of the water shell was observed, regardless of the actual direction of motion (Figure 5.1b). The question is whether this deflection is due to electrostatic or mechanical forces on the oil core. The latter could be produced by a particular, hydrodynamic flow pattern of the water inside the water shell during the movement.

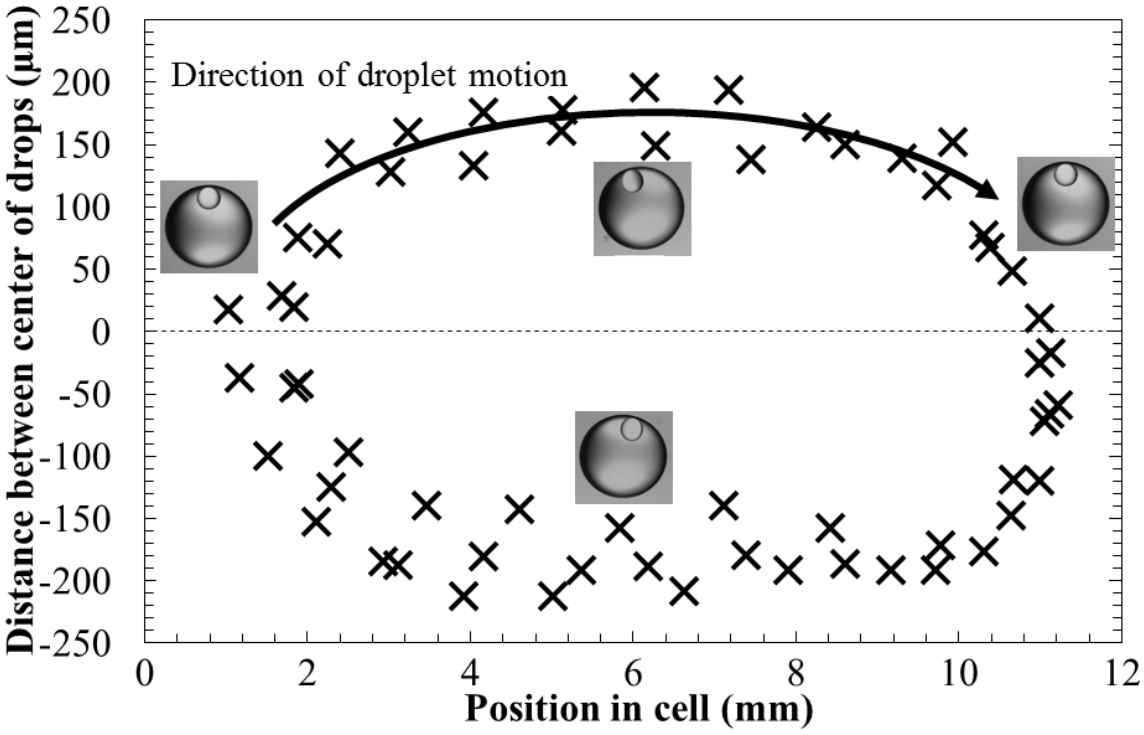

Figure 5.3 Difference in horizontal position of the core relative to the shell during several back-and-forth motions of the (O/W)/O droplet, where R_{shell} = 800 µm, R_{core} = 200 µm and R_{core}/R_{shell} = 0.25. The x-coordinate of the core is subtracted from the shell's x-coordinate, meaning a positive value represents a deflection of the oil core to the left, and a negative value represents a deflection of the oil core to the right. The deflection of the oil core is always opposite to the direction of travel of the (O/W)/O droplet.

If electrostatic forces were responsible for the core deflection, then such a deflection would be observed independently of whether the complex droplet moves or not. This was tested by allowing a complex (O/W)/O droplet to travel towards an electrode but preventing discharge and recharge by electrically insulating the electrode with a thin film of Parafilm M (Sigma-Aldrich, Dorset, UK). Parafilm is a dielectric, which, due to its low thickness and dielectric constant comparable to silicone oil [24], does not significantly change the electric field inside the cuvette. As the droplet could not switch charge at the electrode, it stopped moving and was pinned to the Parafilm-covered electrode (Fig. 4(a) and 4(b)). It was then observed that the oil core did not deflect, regardless of field direction applied (E = 1.5 kV/cm). Only actually moving droplets showed a measureable core deflection (Fig. 4(c) and 4(d)).

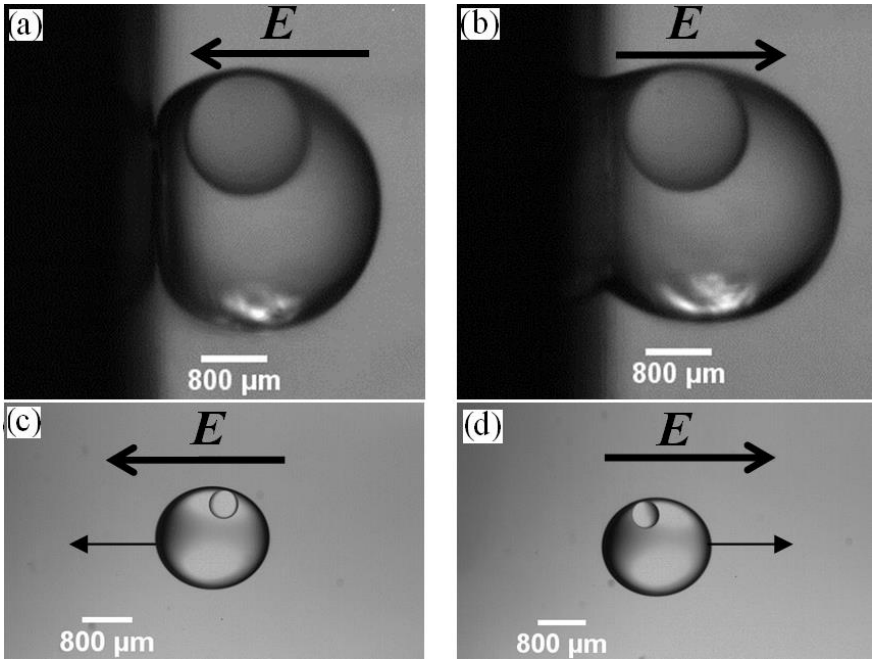

Figure 5.4 Difference in oil core position within the outer water shell between a stationary core-shell and a moving core-shell droplet. (a) and (b) (O/W)/O droplet (with 2.30 g/l SDS) attached to an insulated electrode (left). (a) Negative electrode, (b) positive electrode. (c) and (d) Electrophoretic motion of an (O/W)/O droplet (with 2.30 g/l SDS) away from an electrode, where the arrows indicate the direction of travel. (c) Oil core deflected to the right with respect to the centre of the outer water shell, against the direction of motion, (d) oil core deflected to the left with respect to the centre of the outer water shell, against the direction of motion.

From this, it must be concluded that core deflection is most likely due to mechanical forces acting on the core. As the deflection is always opposite to the direction of travel of the shell, these mechanical forces are most likely due to internal flow inside the water shell. Considering that water droplets are not rigid particles, there is likely to be a substantial amount of internal flow, due to viscous stresses at the oil-water interface when an external force drags the droplets through the oil [25-27].

5.4.4 Droplet deformation

Jung et al. [15] reported that a single deionised water droplet, of radius R_{min}, deforms into a slightly elongated shape (to a radius R_{max}) as it approaches an electrode. The authors argued that the electric field becomes stronger in the gap between the droplet's surface and the electrode and the droplet surface charges become concentrated, causing the droplet to deform into an elongated shape with a sharper tip. Further reducing the interfacial tension between the droplet and the continuous phase by adding surfactant increases the droplet deformability and causes the droplet to elongate more as the electric field is applied. As velocities of v_g and v_{el} before first contact with an electrode are of comparable magnitudes and having observed no droplet deformation in free fall, it is certain that droplet deformation is due the electrical field applied rather than shear. It was observed that the droplet further elongates shortly before, at contact, and shortly after contact with an electrode. The core oil droplet, on the other hand, does not deform at all – neither before nor after contact with an electrode (Figure 5.5).

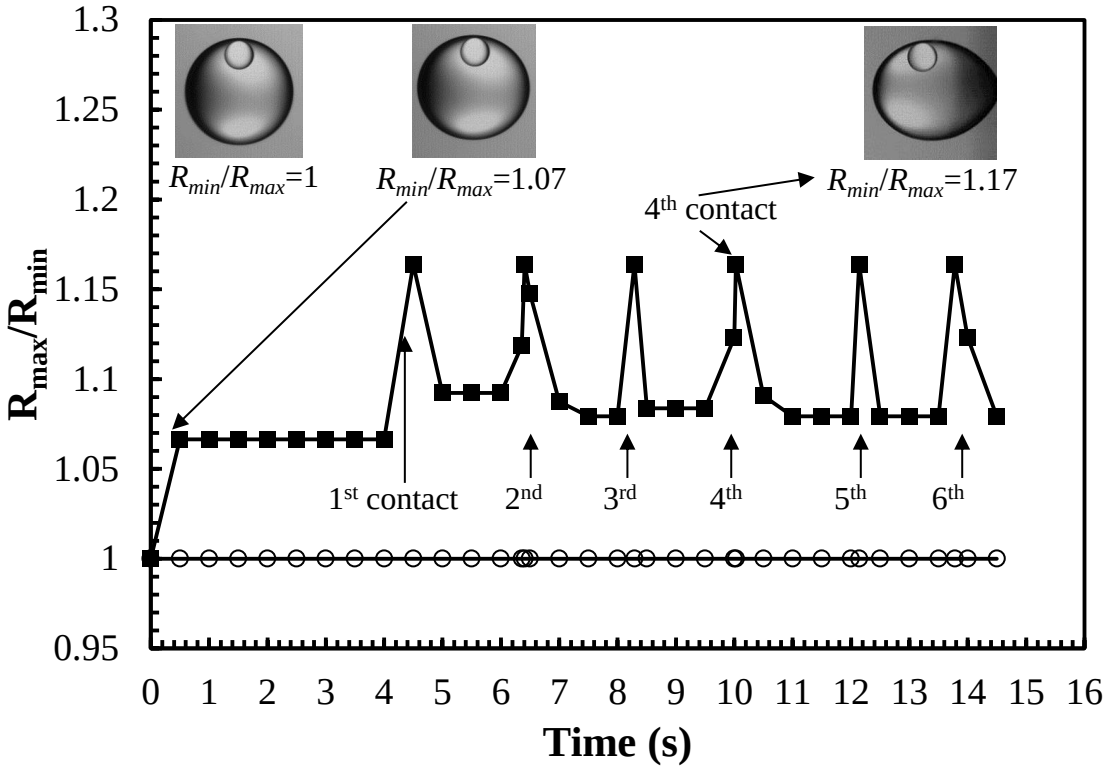

Figure 5.5 Droplet deformation of the outer water droplet with of 2.30 g/l SDS, shell drop deformation (solid squares) and core drop deformation (circles). First contact is with a biased positive electrode. The straight lines between data points are only guidelines to indicate the sequence of measurements.

5.4.5 More complex (W/O/W)/O droplets

Additionally, the electrophoretic mobility of a (W/O/W)/O droplet with 2.30 g/l SDS in both water phases was studied. A water core was injected into an oil shell, which together were injected into an outer water shell, which were then injected into the continuous oil phase (Figure 5.6 (d)) using the same concentric capillary system. The more complex (W/O/W)/O droplet behaved in the same fashion as the (O/W)/O droplets and sank towards the bottom of the cuvette, where, as the droplet reached the centre of the electrodes, an electric field was applied. Figure 5.6 illustrates that the water core was deflected in the same direction as the outer water shell (before and after contact with an electrode), whilst the oil shell was deflected in the opposite direction. However,

the electrophoretic mobility of the (W/O/W)/O droplet remained the same as that of a (O/W)/O droplet.

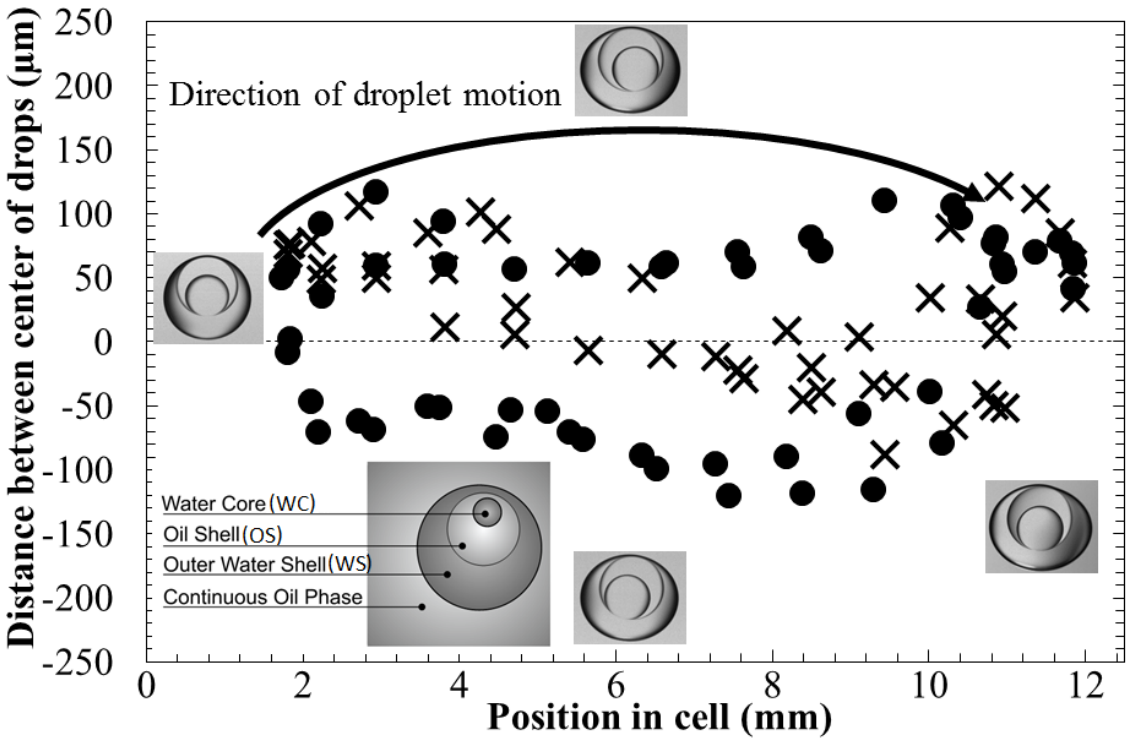

Figure 5.6 Difference in horizontal droplet position within an (W/O/W)/O droplet between the centres of the outer water shell and the oil shell (crosses) and the outer water shell and the water core (solid circles), where $R_{watershell}$ = 960 µm, $R_{oilshell}$ = 650 µm and $R_{watercore}$ = 480 µm. The x-coordinates of the core and the oil shell are subtracted from the water shell's x-coordinate, meaning a positive value represents a slight shift of the water core and oil shell to the left and a negative value represents a slight shift of the water core and oil shell to the right.

5.5 Discussion

As previously discussed, Marinova et al. [23] measured negative electrophoretic mobility of oil droplets, independent of the specific type of non-polar oil, and concluded that non-polar oil droplets dispersed in water carry a negative effective surface charge. In addition, previous chapters have presented positive electrophoretic mobility of simple deionised water droplets in oil and concluded that there was anisotropic orientation of

water molecules at the interface, causing water droplets dispersed in non-polar oil to carry an initial positive effective surface charge.

When simple W/O droplets are brought into contact with a biased electrode, they acquire charge with the same polarity as the electrode (Chapter 4). However, in the case of (W/O/W)/O droplets (Figure 5.6), only the outer water shell, WS, came into contact with the electrode and could, therefore, acquire an additional charge. The inner water core, WC, (Figure 5.6 inset) was physically separated from the electrode by the insulating oil shell, OS. Therefore, no charge transfer between the WC and the electrode could take place and the WC only had its own initial charge. It has already been shown that the initial charge of water droplets is at least a factor of 10 smaller by magnitude than any charge acquired at an electrode, as demonstrated in Figure 5.2a,b. This, again, leads to the conclusion that internal flow of liquids within the droplets rather than electrostatic force is responsible for deflection of the inner cores/shells (Figure 5.6). In terms of future work, it would be interesting to investigate this internal flow by methods such as particle image velocimetry or similar [28].

5.6 Conclusion

To summarise, this is the first time electrophoretic manipulation of complex droplets, both oil-in-water-in-oil (core-shell droplets) and water-in-oil-in-water-in-oil droplets, has been presented. Water shells were created, which allowed the electrophoretic manipulation of oil droplets in a continuous oil phase. It was found that the inner droplet did not affect electrophoretic motion, regardless of size and composition. This is advantageous in a variety of applications. For example, oil droplets of varying types and sizes could accurately be transported and manipulated at the same speed using monodisperse water shells, which can be either thick or ultrathin. This method could be exploited for the manipulation of materials that would otherwise be damaged by an

electrical field [29-31], such as enzymes, which could be transported and manipulated using a complex (W/O/W)/O droplet system.

5.7 References

[1] A. D. Griffiths and D. S. Tawfik, "Miniaturising the laboratory in emulsion droplets," *Trends in Biotechnology*, vol. 24, pp. 395-402, 2006.

[2] A. Huebner, S. Sharma, M. Srisa-Art, F. Hollfelder, J. B. Edel, and A. J. deMello, "Microdroplets: A sea of applications?," *Lab on a Chip*, vol. 8, pp. 1244-1254, 2008.

[3] S. Y. Teh, R. Lin, L. H. Hung, and A. P. Lee, "Droplet microfluidics," *Lab on a Chip*, vol. 8, pp. 198-220, 2008.

[4] G. S. Fiorini and D. T. Chiu, "Disposable microfluidic devices: fabrication, function, and application," *Biotechniques*, vol. 38, pp. 429-446, Mar 2005.

[5] H. Song, J. D. Tice, and R. F. Ismagilov, "A microfluidic system for controlling reaction networks in time," *Angewandte Chemie-International Edition*, vol. 42, pp. 768-772, 2003.

[6] E. M. B. a. P. Mesquida, "Microdroplets as a tool for 'soft' patterning," *Nanoengineering and Nanosystems*, vol. 223, pp. 113-119, 2010.

[7] J. R. Millman, K. H. Bhatt, B. G. Prevo, and O. D. Velev, "Anisotropic particle synthesis in dielectrophoretically controlled microdroplet reactors," *Nature Materials*, vol. 4, pp. 98-102, Jan 2005.

[8] C. G. Lima, A. R. Pianovski, A. F. G. Vilela, K. K. da Silva, V. F. M. Carvalho, C. R. De Musis, S. R. P. Machado, and M. Ferrari, "O/W/O Multiple Emulsions Containing Amazon Oil: Babassu Oil (Orbignya oleifera)," *Journal of Dispersion Science and Technology*, vol. 31, pp. 622-626, 2010.

[9] R. Filho, "PRELIMINARY COMMUNICATION Occlusive power evaluation of O/W/O multiple emulsions on gelatin support cells," *International Journal of Cosmetic Science*, vol. 19, pp. 65-73, 1997.

[10] P. Simon, "Stable O/W/O emulsion and its use as a cosmetic and/or dermatological composition," US 6346256, 2002.

[11] F. Serdoz, D. Voinovich, B. Perissutti, L. Magarotto, and F. Carli, "Design, development and bioavailability assessment of oxytetracycline hydrochloride double o/w/o microemulsion formulation," *Journal of Drug Delivery Science and Technology*, vol. 18, pp. 404-409, Nov-Dec 2008.

[12] K. Choi, M. Im, J. M. Choi, and Y. K. Choi, "Droplet transportation using a pre-charging method for digital microfluidics," *Microfluidics and Nanofluidics*, vol. 12, pp. 821-827, Mar 2012.

[13] D. J. Im, J. Noh, D. Moon, and I. S. Kang, "Electrophoresis of a Charged Droplet in a Dielectric Liquid for Droplet Actuation," *Analytical Chemistry*, vol. 83, pp. 5168-5174, Jul 1 2011.

[14] M. Hase, S. N. Watanabe, and K. Yoshikawa, "Rhythmic motion of a droplet under a DC electric field," *Physical Review E*, vol. 74, p. 046301, Oct 2006.

[15] Y.-M. Jung, H.-C. Oh, and I. S. Kang, "Electrical charging of a conducting water droplet in a dielectric fluid on the electrode surface," *Journal of Colloid and Interface Science*, vol. 322, pp. 617-623, 2008.

[16] M. Takinoue, Y. Atsumi, and K. Yoshikawa, "Rotary motion driven by a direct current electric field," *Applied Physics Letters*, vol. 96, p. 104105, Mar 2010.

[17] M. Jalaal, B. Khorshidi, and E. Esmaeilzadeh, "An experimental study on the motion, deformation and electrical charging of water drops falling in oil in the presence of high voltage DC electric field," *Experimental Thermal and Fluid Science*, vol. 34, pp. 1498-1506, Nov 2010.

[18] D. J. Im, M. M. Ahn, B. S. Yoo, D. Moon, D. W. Lee, and I. S. Kang, "Discrete Electrostatic Charge Transfer by the Electrophoresis of a Charged Droplet in a Dielectric Liquid," *Langmuir,* vol. 28, pp. 11656-11661, Aug 14 2012.
[19] B. Vajdi Hokmabad, B. Sadri, M. R. Charan, and E. Esmaeilzadeh, "An experimental investigation on hydrodynamics of charged water droplets in dielectric liquid medium in the presence of electric field," *Colloids and Surfaces A: Physicochemical and Engineering Aspects,* vol. 401, pp. 17-28, 2012.
[20] D. W. Lee, D. J. Im, and I. S. Kang, "Electrophoretic motion of a charged water droplet near an oil-air interface," *Applied Physics Letters,* vol. 100, p. 221602, May 28 2012.
[21] C. P. Lee, H. C. Chang, and Z. H. Wei, "Charged droplet transportation under direct current electric fields as a cell carrier," *Applied Physics Letters,* vol. 101, p. 014103, Jul 2 2012.
[22] P. J. Bailes, J. G. M. Lee, and A. R. Parsons, "An experimental investigation into the motion of a single drop in a pulsed DC electric field," *Chemical Engineering Research & Design,* vol. 78, pp. 499-505, Apr 2000.
[23] K. G. Marinova, R. G. Alargova, N. D. Denkov, O. D. Velev, D. N. Petsev, I. B. Ivanov, and R. P. Borwankar, "Charging of oil-water interfaces due to spontaneous adsorption of hydroxyl ions," *Langmuir,* vol. 12, pp. 2045-2051, Apr 17 1996.
[24] Structure-Probe-Inc. (2013). *Parafilm M*. Available: http://www.2spi.com/catalog/supp/parafilm.php
[25] J. W. Ha and S. M. Yang, "Fluid dynamics of a double emulsion droplet in an electric field," *Physics of Fluids,* vol. 11, pp. 1029-1041, May 1999.
[26] W. Rybczynski, "Über die fortschreitende Bewegung einer flüssigen Kugel in einem zähen Medium (German)," *Bulletin International de l'Academie des Sciences de Cracovie,* pp. 40–46, 1911.
[27] R. Clift, J. R. Grace, and E. Weber, *Bubbles, Drops, and Particles*: Dover Publications, 2005.
[28] S. Ma, "Routes to controlled microenviroments for cell culture using Droplet-based Microfluidics," Doctor of Philosophy, Routes to controlled microenviroments for cell culture using Droplet-based Microfluidics, Ph.D. thesis, Cambridge, Cambridge, 2013.
[29] A. Van Loey, B. Verachtert, and M. Hendrickx, "Effects of high electric field pulses on enzymes," *Trends in Food Science & Technology,* vol. 12, pp. 94-102, 2001.
[30] T. Grahl and H. Märkl, "Killing of microorganisms by pulsed electric fields," *Applied Microbiology and Biotechnology,* vol. 45, pp. 148-157, 1996/03/01 1996.
[31] A. J. H. Sale and W. A. Hamilton, "Effects of high electric fields on microorganisms: I. Killing of bacteria and yeasts," *Biochimica et Biophysica Acta (BBA) - General Subjects,* vol. 148, pp. 781-788, 1967.

Chapter 6 Conclusions, Limitations and Future Work

The interest in water droplet electrophoresis and its uses as tiny compartments inside microfluidic, lab-on-a-chip devices, has been growing [1-15]. The focus of this thesis was to investigate the electrophoretic mobility of water droplets dispersed in two non-polar oils (silicone and paraffin oil) and the factors that influence this mobility. It was found that deionised water droplets show positive electrophoretic mobility before contact with a biased electrode. This would agree with Im [2, 16] and others [17], who also observed an initial, positive electrophoretic motion of water droplets, but stands in contrast to Hase [3], who observed both positive and negative electrophoretic motion and Lee [10], who found that a water droplet would first move towards the positively charged electrode. Molecular dynamic simulations suggest that the initial charge of a water droplet is positive [18]. This is in agreement with the experimental results presented in chapters 3, 4 and 5, i.e. water droplets dispersed in a non-polar oil, initially, have a positive surface charge. The simulations also suggest that the droplet charge is predominantly located at the droplet's surface. This is consistent with the other observation that the presence of electrolyte ions in the droplets had no significant effect on the surface charge, even over a wide range of concentrations (pH and ion concentrations ranging from pH4 to pH10 and from 0.01 mmol/l to 1.5 mol/l, respectively). The reason for this surface-predominance could be that ions deep inside the droplets are screened and, thus, are "invisible" outside of the droplets. The Debye screening length, $\kappa^{-1} = (3.29\sqrt{I})^{-1}$ nm, of the water in the droplets lies between approximately 1 µm for deionised water and 0.2 nm for maximum KCl concentration. That is, the Debye length is much smaller than the typical droplet radius of above

100 µm. This suggests that the whole concept of preferential adsorption of ions at the water-oil interface, as proposed by Marinova et al. [19], is not applicable for water-in-oil emulsions. The fact that the surface charge density of water droplets in silicone oil can be reduced by the addition of a chaotropic agent and the results of molecular dynamic simulation lead to the more likely conclusion that anisotropic orientation of water molecules at the interface (rather than selective adsorption of ions) is responsible for the initial water droplet charge. Nevertheless, one has to be careful not to over-interpret the results, as the general hydrophobicity of siloxanes and silicones speaks against an overall high affinity of water to silicone. It also does not explain the positive electrophoretic mobility in paraffin oil, as paraffin molecules do not contain any hydrogen bond acceptors or donors. One way of addressing this issue would be to conduct a larger, electrophoretic study with a variety of oils. Furthermore, from a fundamental perspective, it would be interesting to perform future experiments with much smaller droplets in order to learn more about the location of droplet charge.

Although it has been possible to produce meaningful results, using the single-droplet-electrophoresis experimental set-up (as presented in the Methodology chapter) has its limitations. Microchannels restrict the droplet size, especially in surfactant-free emulsions, due to the high interfacial tension between the water and the pipette tip. The only way in which the droplet size could be reduced would be by increasing the flow rate of water through the microchannel. The consequence of this would be that multiple droplets would enter the electrophoretic cell at once. The systematic experimental error of 35% was also extremely high. There is, of course, the possibility to use more sophisticated equipment, which would reduce the error of the radii. However, the large spectrum of standard deviation within the droplet velocities and the error within the hydrodynamic coefficients would remain.

When a pure water droplet makes contact with an electrode, the surface charge density is increased by a factor of 10 and acquires the same polarity as the electrode. It essentially behaves like a perfectly conducting metal sphere. A case can be made for further investigations into the perfect conductor theory and the role of the viscosity of the continuous phase. Metal spheres of similar density and varying in size should be investigated in a highly viscous, non-polar oil, in an attempt to validate the perfect conducting sphere theory. If shown to be applicable, it would enable investigators to deduce information about the viscosity of the continuous phase, only with prior knowledge of the velocity of the sphere.

By adding increasing amounts of the anionic surfactant SDS to the water phase, the initial surface charge density of the water droplets changes from positive to negative. No change in surface charge density was observed when the cationic surfactant CTAB was added to the water phase. It was also found that any surfactant charge effects were overridden once the droplet made contact with a biased electrode. The possibility of easily adjusting the droplet charge by chemical as well as physical means permitted flexible electrophoretic manipulation in microfluidic devices. Often a limiting factor that determines the overall resolution of the particular droplet delivery system is the droplet's size. Using surfactant can significantly help in reducing droplet size, stabilising the emulsion and aiding the creation of more complex emulsion systems. The knowledge that any charge properties of the surfactant can be overridden through contact with a biased electrode is of immense benefit. One application that stands to benefit from this discovery is Electric Droplet Lithography (EDL), a method for micro/nanopatterning soft, biological materials on a solid surface. By reducing the size of the droplets, the resolution of the EDL method would be improved.

The electrophoretic manipulation of core-shell droplets (both (O/W)/O and (W/O/W)/O) was presented for the first time. Results suggest that the electrophoretic mobility of the droplets is determined solely by the outer water shell, regardless of size or composition of the inner droplets. Core-shell droplets essentially behave like simple W/O droplets. Although this is a new method of controlling complex emulsions, it is nonetheless a very difficult process to implement. The production of a concentric, glass microcapillary channel system was challenging and time consuming and one ran the risk of blockages within the channels. Once a channel becomes blocked, it destroys the entire set-up and a new device needs to be built. At this stage of development, the size of the outer water shell was controlled optically, which meant that the monodispersity of the shells could not be guaranteed and the production of a (W/O)W droplet was a long and arduous procedure.

It is also currently unclear what caused the apparent motion of the oil core within the outer water shell. It is most likely due to mechanical forces, i.e. internal flow inside the water shell, but the precise nature of this motion needs to be investigated further. Considering that water droplets are not rigid particles, there is likely to be a substantial amount of internal flow, due to viscous stresses at the oil-water interface when an external force drags the droplets through the oil. Particle image velocimetry of this system might give some indication as to what these flows are and could possibly provide further insight into the behaviour of surfactants inside the water phase.

However, this novel droplet manipulation scheme also presents many advantages and could be applied in a variety of applications. For example, oil droplets of varying types, shapes and sizes could be accurately transported at a constant velocity using either thick or ultrathin, monodisperse water shells. Additionally, materials that would otherwise be

damaged by an electrical field [20-22], such as enzymes, could easily be transported, manipulated and protected using a complex (W/O/W)/O droplet system.

6.1 References

[1] K. Choi, M. Im, J. M. Choi, and Y. K. Choi, "Droplet transportation using a pre-charging method for digital microfluidics," *Microfluidics and Nanofluidics,* vol. 12, pp. 821-827, Mar 2012.

[2] D. J. Im, J. Noh, D. Moon, and I. S. Kang, "Electrophoresis of a Charged Droplet in a Dielectric Liquid for Droplet Actuation," *Analytical Chemistry,* vol. 83, pp. 5168-5174, Jul 1 2011.

[3] M. Hase, S. N. Watanabe, and K. Yoshikawa, "Rhythmic motion of a droplet under a DC electric field," *Physical Review E,* vol. 74, p. 046301, Oct 2006.

[4] Y.-M. Jung, H.-C. Oh, and I. S. Kang, "Electrical charging of a conducting water droplet in a dielectric fluid on the electrode surface," *Journal of Colloid and Interface Science,* vol. 322, pp. 617-623, 2008.

[5] M. Takinoue, Y. Atsumi, and K. Yoshikawa, "Rotary motion driven by a direct current electric field," *Applied Physics Letters,* vol. 96, p. 104105, Mar 2010.

[6] M. Jalaal, B. Khorshidi, and E. Esmaeilzadeh, "An experimental study on the motion, deformation and electrical charging of water drops falling in oil in the presence of high voltage DC electric field," *Experimental Thermal and Fluid Science,* vol. 34, pp. 1498-1506, Nov 2010.

[7] D. J. Im, M. M. Ahn, B. S. Yoo, D. Moon, D. W. Lee, and I. S. Kang, "Discrete Electrostatic Charge Transfer by the Electrophoresis of a Charged Droplet in a Dielectric Liquid," *Langmuir,* vol. 28, pp. 11656-11661, Aug 14 2012.

[8] B. Vajdi Hokmabad, B. Sadri, M. R. Charan, and E. Esmaeilzadeh, "An experimental investigation on hydrodynamics of charged water droplets in dielectric liquid medium in the presence of electric field," *Colloids and Surfaces A: Physicochemical and Engineering Aspects,* vol. 401, pp. 17-28, 2012.

[9] D. W. Lee, D. J. Im, and I. S. Kang, "Electrophoretic motion of a charged water droplet near an oil-air interface," *Applied Physics Letters,* vol. 100, p. 221602, May 28 2012.

[10] C. P. Lee, H. C. Chang, and Z. H. Wei, "Charged droplet transportation under direct current electric fields as a cell carrier," *Applied Physics Letters,* vol. 101, p. 014103, Jul 2 2012.

[11] A. D. Griffiths and D. S. Tawfik, "Miniaturising the laboratory in emulsion droplets," *Trends in Biotechnology,* vol. 24, pp. 395-402, 2006.

[12] A. Huebner, S. Sharma, M. Srisa-Art, F. Hollfelder, J. B. Edel, and A. J. deMello, "Microdroplets: A sea of applications?," *Lab on a Chip,* vol. 8, pp. 1244-1254, 2008.

[13] S. Y. Teh, R. Lin, L. H. Hung, and A. P. Lee, "Droplet microfluidics," *Lab on a Chip,* vol. 8, pp. 198-220, 2008.

[14] G. S. Fiorini and D. T. Chiu, "Disposable microfluidic devices: fabrication, function, and application," *Biotechniques,* vol. 38, pp. 429-446, Mar 2005.

[15] E. M. Blanco, S. A. Nesbitt, M. A. Horton, and P. Mesquida, "A Multiprotein Microarray on Silicon Dioxide Fabricated by Using Electric-Droplet Lithography," *Advanced Materials,* vol. 19, pp. 2469-2473, 2007.

[16] D. J. Im, J. Noh, N. W. Yi, J. Park, and I. S. Kang, "Influences of electric field on living cells in a charged water-in-oil droplet under electrophoretic actuation," *Biomicrofluidics,* vol. 5, Dec 2011.

[17] P. J. Bailes, J. G. M. Lee, and A. R. Parsons, "An experimental investigation into the motion of a single drop in a pulsed DC electric field," *Chemical Engineering Research & Design,* vol. 78, pp. 499-505, Apr 2000.

[18] A. M. Schoeler, D. N. Josephides, S. Sajjadi, C. D. Lorenz, and P. Mesquida, "Charge of water droplets in non-polar oils," *Journal of Applied Physics*, vol. 114, p. 144903, 2013.
[19] K. G. Marinova, R. G. Alargova, N. D. Denkov, O. D. Velev, D. N. Petsev, I. B. Ivanov, and R. P. Borwankar, "Charging of oil-water interfaces due to spontaneous adsorption of hydroxyl ions," *Langmuir*, vol. 12, pp. 2045-2051, Apr 17 1996.
[20] A. Van Loey, B. Verachtert, and M. Hendrickx, "Effects of high electric field pulses on enzymes," *Trends in Food Science & Technology*, vol. 12, pp. 94-102, 2001.
[21] T. Grahl and H. Märkl, "Killing of microorganisms by pulsed electric fields," *Applied Microbiology and Biotechnology*, vol. 45, pp. 148-157, 1996/03/01 1996.
[22] A. J. H. Sale and W. A. Hamilton, "Effects of high electric fields on microorganisms: I. Killing of bacteria and yeasts," *Biochimica et Biophysica Acta (BBA) - General Subjects*, vol. 148, pp. 781-788, 1967.

Chapter 7 List of publications arisen from this thesis

A. M. Schoeler, D. N. Josephides, S. Sajjadi, and P. Mesquida, "Controlling the surface charge of water droplets in non-polar oils" **Colloids and Surfaces A: Physicochemical and Engineering Aspects**, vol. 461, pp. 18-21, 2014.

A. M. Schoeler, D. N. Josephides, A. S. Chaurasia, S. Sajjadi, and P. Mesquida, "Electrophoretic manipulation of multiple-emulsion droplets," **Applied Physics Letters**, vol. 104, pp. 074104, 2014.

A. M. Schoeler, D. N. Josephides, S. Sajjadi, C. D. Lorenz, and P. Mesquida, "Charge of water droplets in non-polar oils," **Journal of Applied Physics**, vol. 114, pp. 144903, 2013.

Chapter 8 Fluid Properties

		Water	PFD	FC-40	FC-77	Heptane
Chemical Formula		H_2O	$C_{10}F_{18}$	-	-	$n\text{-}C_7H_{16}$
Electrical resistivity ρ/Ωcm		$18\cdot10^6$	$1\cdot10^{17}$	$4.0\cdot10^{15}$	$1.9\cdot10^{15}$	$1\cdot10^{16}$
Relative dielectric constant ε_r		81	1.863	1.9	1.86	1.924
Density (water=1)		1	1.908	1.855	1.78	0.6837
Surface Tension σ /(10^{-3}N/m)		72.75	17.6		15	20
Dyn. Viscosity η /(10^{-3}Ns/m^2)		1	5.1	4.1	1.4	4.1

		Water	Silicone	Paraffin	Urea
Chemical Formula		H_2O	C_2H_6OSi	C_nH_{2n+2}, n = 16..24	CH_4N_2O
Electrical resistivity ρ/Ωcm		$18\cdot10^6$	$1\cdot10^{15}$	$1\cdot10^{18}$	
Relative dielectric constant ε_r		81	2.43	2.3	
Density (water=1)		1	0.965	0.86	
Surface Tension σ /(10^{-3}N/m)		72.75	38.2	41	
Dyn. Viscosity η /(10^{-3}Ns/m^2)		1	106.2	134.0	
Reynolds number (10^{-3})			0.904	3.85	

Suppliers: PFD = Fluorochem Ltd., Old Glossop, UK. FC-77 and FC-40 = Interelec Electronics AG, Rüschlikon, CH (Manufacturer: 3M Company, St.Paul, USA). Heptane, Siliocne, Urea and Paraffin = Sigma-Aldrich, Dorset, UK, Water = Millipore Direct-Q 3, Ultrapure Water Systems, Watford U

Chapter 9 Appendix

9.1 Appendix A

untitled.m function

```
function varargout = untitled(varargin)
% UNTITLED MATLAB code for untitled.fig
%      UNTITLED, by itself, creates a new UNTITLED or raises the
existing
%      singleton*.
%
%      H = UNTITLED returns the handle to a new UNTITLED or the handle
to
%      the existing singleton*.
%
%      UNTITLED('CALLBACK',hObject,eventData,handles,...) calls the
local
%      function named CALLBACK in UNTITLED.M with the given input
arguments.
%
%      UNTITLED('Property','Value',...) creates a new UNTITLED or
raises the
%      existing singleton*.  Starting from the left, property value
pairs are
%      applied to the GUI before untitled_OpeningFcn gets called.  An
%      unrecognized property name or invalid value makes property
application
%      stop.  All inputs are passed to untitled_OpeningFcn via
varargin.
%
%      *See GUI Options on GUIDE's Tools menu.  Choose "GUI allows
only one
%      instance to run (singleton)".
%
% See also: GUIDE, GUIDATA, GUIHANDLES
% Edit the above text to modify the response to help untitled
% Last Modified by GUIDE v2.5 17-Sep-2012 11:44:18
% Begin initialization code - DO NOT EDIT

gui_Singleton = 1;
gui_State = struct('gui_Name',       mfilename, ...
    'gui_Singleton',  gui_Singleton, ...
    'gui_OpeningFcn', @untitled_OpeningFcn, ...
    'gui_OutputFcn',  @untitled_OutputFcn, ...
    'gui_LayoutFcn',  [] , ...
    'gui_Callback',   []);
if nargin && ischar(varargin{1})
    gui_State.gui_Callback = str2func(varargin{1});
end

if nargout
    [varargout{1:nargout}] = gui_mainfcn(gui_State, varargin{:});
else
```

```
    gui_mainfcn(gui_State, varargin{:});
end
% End initialization code - DO NOT EDIT


% --- Executes just before untitled is made visible.

function untitled_OpeningFcn(hObject, eventdata, handles, varargin)
% This function has no output args, see OutputFcn.
% hObject    handle to figure
% eventdata  reserved - to be defined in a future version of MATLAB
% handles    structure with handles and user data (see GUIDATA)
% varargin   command line arguments to untitled (see VARARGIN)
% Choose default command line output for untitled
handles.output = hObject;
% Update handles structure
guidata(hObject, handles);
axes(handles.axes2);
data=[];
set(handles.uitable1,'data',data);

% UIWAIT makes untitled wait for user response (see UIRESUME)
% uiwait(handles.figure1);

% --- Outputs from this function are returned to the command line.

function varargout = untitled_OutputFcn(hObject, eventdata, handles)
% varargout  cell array for returning output args (see VARARGOUT);
% hObject    handle to figure
% eventdata  reserved - to be defined in a future version of MATLAB
% handles    structure with handles and user data (see GUIDATA)

% Get default command line output from handles structure

varargout{1} = handles.output;

% --- Executes on button press in pushbutton1.

function pushbutton1_Callback(hObject, eventdata, handles)
% hObject    handle to pushbutton1 (see GCBO)
% eventdata  reserved - to be defined in a future version of MATLAB
% handles    structure with handles and user data (see GUIDATA)
experimentdir=uigetdir('F:\Andreas Paraffin\Viscosity Tests\Cell 3
washed\Alternating Field');
set(handles.edit2,'string',experimentdir);

% --- If Enable == 'on', executes on mouse press in 5 pixel border.
% --- Otherwise, executes on mouse press in 5 pixel border or over
pushbutton1.

function pushbutton1_ButtonDownFcn(hObject, ~, handles)

% hObject    handle to pushbutton1 (see GCBO)
% eventdata  reserved - to be defined in a future version of MATLAB
% handles    structure with handles and user data (see GUIDATA)

function edit2_Callback(hObject, eventdata, handles)
```

```
% hObject    handle to edit2 (see GCBO)
% eventdata  reserved - to be defined in a future version of MATLAB
% handles    structure with handles and user data (see GUIDATA)

b=get(hObject,'String');
% Hints: get(hObject,'String') returns contents of edit2 as text
%        str2double(get(hObject,'String')) returns contents of edit2
as a double

% --- Executes during object creation, after setting all properties.

function edit2_CreateFcn(hObject, eventdata, handles)
% hObject    handle to edit2 (see GCBO)
% eventdata  reserved - to be defined in a future version of MATLAB
% handles    empty - handles not created until after all CreateFcns
called
% Hint: edit controls usually have a white background on Windows.
%       See ISPC and COMPUTER.

if ispc && isequal(get(hObject,'BackgroundColor'),
get(0,'defaultUicontrolBackgroundColor'))
    set(hObject,'BackgroundColor','white');
end

% --- Executes on button press in pushbutton2.

function pushbutton2_Callback(hObject, eventdata, handles)
% hObject    handle to pushbutton2 (see GCBO)
% eventdata  reserved - to be defined in a future version of MATLAB
% handles    structure with handles and user data (see GUIDATA)
set(handles.slider5,'value',1);

b=get(handles.edit2,'string');
files = dir(fullfile(b,'*.jpg'));
global filelist;
filelist= struct2cell(files);
filelist=filelist(1,:)';
set(handles.slider3,'max',size(filelist,1));
filenr=ceil(get(handles.slider3,'value'));
img=imread(cell2mat(strcat(b,filesep,filelist(filenr))));

axes(handles.axes2);
imshow(img);

% if exist('temp.mat','file')==2
%     load temp;
% end
%panzoom(handles.axes2)
%zoom(5)
pan on

% --- If Enable == 'on', executes on mouse press in 5 pixel border.
% --- Otherwise, executes on mouse press in 5 pixel border or over
pushbutton2.

function pushbutton2_ButtonDownFcn(hObject, eventdata, handles)
```

```
% hObject    handle to pushbutton2 (see GCBO)
% eventdata  reserved - to be defined in a future version of MATLAB
% handles    structure with handles and user data (see GUIDATA)

function edit3_Callback(hObject, eventdata, handles)
% hObject    handle to edit3 (see GCBO)
% eventdata  reserved - to be defined in a future version of MATLAB
% handles    structure with handles and user data (see GUIDATA)
% Hints: get(hObject,'String') returns contents of edit3 as text
%        str2double(get(hObject,'String')) returns contents of edit3
as a double

% --- Executes during object creation, after setting all properties.

function edit3_CreateFcn(hObject, eventdata, handles)
% hObject    handle to edit3 (see GCBO)
% eventdata  reserved - to be defined in a future version of MATLAB
% handles    empty - handles not created until after all CreateFcns
called

% Hint: edit controls usually have a white background on Windows.
%       See ISPC and COMPUTER.

if ispc && isequal(get(hObject,'BackgroundColor'),
get(0,'defaultUicontrolBackgroundColor'))
    set(hObject,'BackgroundColor','white');
end

% --- Executes on slider movement.

function slider1_Callback(hObject, eventdata, handles)
% hObject    handle to slider1 (see GCBO)
% eventdata  reserved - to be defined in a future version of MATLAB
% handles    structure with handles and user data (see GUIDATA)

a= get(hObject,'Value');
set(handles.edit4,'string',num2str(ceil(a)));

% Hints: get(hObject,'Value') returns position of slider
%        get(hObject,'Min') and get(hObject,'Max') to determine range
of slider
% --- Executes during object creation, after setting all properties.

function slider1_CreateFcn(hObject, eventdata, handles)
% hObject    handle to slider1 (see GCBO)
% eventdata  reserved - to be defined in a future version of MATLAB
% handles    empty - handles not created until after all CreateFcns
called
% Hint: slider controls usually have a light gray background.

if isequal(get(hObject,'BackgroundColor'),
get(0,'defaultUicontrolBackgroundColor'))
    set(hObject,'BackgroundColor',[.9 .9 .9]);
end

% --- Executes on slider movement.
```

```
function slider2_Callback(hObject, eventdata, handles)
% hObject    handle to slider2 (see GCBO)
% eventdata  reserved - to be defined in a future version of MATLAB
% handles    structure with handles and user data (see GUIDATA)
a2= get(hObject,'Value');
set(handles.edit5,'string',num2str(ceil(a2)));
% Hints: get(hObject,'Value') returns position of slider
%        get(hObject,'Min') and get(hObject,'Max') to determine range
of slider
% --- Executes during object creation, after setting all properties.

function slider2_CreateFcn(hObject, eventdata, handles)
% hObject    handle to slider2 (see GCBO)
% eventdata  reserved - to be defined in a future version of MATLAB
% handles    empty - handles not created until after all CreateFcns
called
% Hint: slider controls usually have a light gray background.
if isequal(get(hObject,'BackgroundColor'),
get(0,'defaultUicontrolBackgroundColor'))
    set(hObject,'BackgroundColor',[.9 .9 .9]);
end

function edit4_Callback(hObject, eventdata, handles)
% hObject    handle to edit4 (see GCBO)
% eventdata  reserved - to be defined in a future version of MATLAB
% handles    structure with handles and user data (see GUIDATA)
% Hints: get(hObject,'String') returns contents of edit4 as text
%        str2double(get(hObject,'String')) returns contents of edit4
as a double
% --- Executes during object creation, after setting all properties.

function edit4_CreateFcn(hObject, eventdata, handles)
% hObject    handle to edit4 (see GCBO)
% eventdata  reserved - to be defined in a future version of MATLAB
% handles    empty - handles not created until after all CreateFcns
called
% Hint: edit controls usually have a white background on Windows.
%       See ISPC and COMPUTER.
if ispc && isequal(get(hObject,'BackgroundColor'),
get(0,'defaultUicontrolBackgroundColor'))
    set(hObject,'BackgroundColor','white');
end

function edit5_Callback(hObject, eventdata, handles)
% hObject    handle to edit5 (see GCBO)
% eventdata  reserved - to be defined in a future version of MATLAB
% handles    structure with handles and user data (see GUIDATA)
% Hints: get(hObject,'String') returns contents of edit5 as text
%        str2double(get(hObject,'String')) returns contents of edit5
as a double
% --- Executes during object creation, after setting all properties.

function edit5_CreateFcn(hObject, eventdata, handles)
% hObject    handle to edit5 (see GCBO)
% eventdata  reserved - to be defined in a future version of MATLAB
% handles    empty - handles not created until after all CreateFcns
called
% Hint: edit controls usually have a white background on Windows.
```

```
%       See ISPC and COMPUTER.

if ispc && isequal(get(hObject,'BackgroundColor'),
get(0,'defaultUicontrolBackgroundColor'))
    set(hObject,'BackgroundColor','white');
end

% --- Executes on mouse press over axes background.

function axes2_ButtonDownFcn(hObject, eventdata, handles)
% hObject    handle to axes2 (see GCBO)
% eventdata  reserved - to be defined in a future version of MATLAB
% handles    structure with handles and user data (see GUIDATA)
% point1 = get(gcf,'CurrentPoint') % button down detected
% rect = [point1(1,1) point1(1,2) 100 50]
% [r2] = dragrect(rect)
% --- Executes on slider movement.

function slider3_Callback(hObject, eventdata, handles)
% hObject    handle to slider3 (see GCBO)
% eventdata  reserved - to be defined in a future version of MATLAB
% handles    structure with handles and user data (see GUIDATA)

global filelist;
b=get(handles.edit2,'string');
filenr=ceil(get(handles.slider3,'Value'));
img=imread(cell2mat(strcat(b,filesep,filelist(filenr))));
axes(handles.axes2);
x=xlim;
y=ylim;
imshow(img);

zoom(get(handles.slider5,'Value'));
xlim(x);
ylim(y);

% Hints: get(hObject,'Value') returns position of slider
%        get(hObject,'Min') and get(hObject,'Max') to determine range
of slider
% --- Executes during object creation, after setting all properties.

function slider3_CreateFcn(hObject, eventdata, handles)
% hObject    handle to slider3 (see GCBO)
% eventdata  reserved - to be defined in a future version of MATLAB
% handles    empty - handles not created until after all CreateFcns
called
% Hint: slider controls usually have a light gray background.

if isequal(get(hObject,'BackgroundColor'),
get(0,'defaultUicontrolBackgroundColor'))
    set(hObject,'BackgroundColor',[.9 .9 .9]);
end

% --- Executes on button press in pushbutton4.

function pushbutton4_Callback(hObject, eventdata, handles)
% hObject    handle to pushbutton4 (see GCBO)
% eventdata  reserved - to be defined in a future version of MATLAB
```

```
% handles    structure with handles and user data (see GUIDATA)
%  if exist('temp.mat','file')==2
%     load temp;
%  end

global filelist;
b=get(handles.edit2,'string');
filenr=ceil(get(handles.slider3,'value'));
img2=imread(cell2mat(strcat(b,filesep,filelist(filenr))));
% axes(handles.axes2);
% imshow(img2);
% zoom(get(handles.slider5,'Value'));

axes(handles.axes2)
x=floor(xlim);
y=floor(ylim);
img=img2(y(1)+1:y(2),x(1)+1:x(2),:);
midsize=str2num(get(handles.edit4,'string'));
save temp;
[accum,circen,cirrad]=dimitriscgui(handles,img,[midsize-
5,midsize+5],[x(1),y(1)]);
%set(handles.uitable1,'data',[circen,cirrad]);

% --- Executes on button press in pushbutton5.

function pushbutton5_Callback(hObject, eventdata, handles)
% hObject    handle to pushbutton5 (see GCBO)
% eventdata  reserved - to be defined in a future version of MATLAB
% handles    structure with handles and user data (see GUIDATA)
handles.stop = 1;

% --- Executes on selection change in listbox1.

function listbox1_Callback(hObject, eventdata, handles)
% hObject    handle to listbox1 (see GCBO)
% eventdata  reserved - to be defined in a future version of MATLAB
% handles    structure with handles and user data (see GUIDATA)
% Hints: contents = cellstr(get(hObject,'String')) returns listbox1
contents as cell array
%        contents{get(hObject,'Value')} returns selected item from
listbox1
% --- Executes during object creation, after setting all properties.

function listbox1_CreateFcn(hObject, eventdata, handles)
% hObject    handle to listbox1 (see GCBO)
% eventdata  reserved - to be defined in a future version of MATLAB
% handles    empty - handles not created until after all CreateFcns
called

% Hint: listbox controls usually have a white background on Windows.
%       See ISPC and COMPUTER.

if ispc && isequal(get(hObject,'BackgroundColor'),
get(0,'defaultUicontrolBackgroundColor'))
    set(hObject,'BackgroundColor','white');
end

% --- Executes when selected cell(s) is changed in uitable1.
```

```
function uitable1_CellSelectionCallback(hObject, eventdata, handles)
% hObject    handle to uitable1 (see GCBO)
% eventdata  structure with the following fields (see UITABLE)
%   Indices: row and column indices of the cell(s) currently selecteds
% handles    structure with handles and user data (see GUIDATA)

table = get(hObject,'Data');
set(handles.uitable1, 'UserData', eventdata.Indices)
ud = get(handles.uitable1, 'UserData');

% axes(handles.axes4);
%
% save aaa;
% %if(~isempty(cell2mat(table(ud(1,1)))))
%     prevexp=load([cell2mat(table(ud(1,1))) 'tracked.mat'])
%     plot(prevexp.tracked(:,1),-prevexp.tracked(:,2));
%     hold off;
%end
%hold on;
% --- Executes on button press in pushbutton6.

function pushbutton6_Callback(hObject, eventdata, handles)
% hObject    handle to pushbutton6 (see GCBO)
% eventdata  reserved - to be defined in a future version of MATLAB
% handles    structure with handles and user data (see GUIDATA)
data=get(handles.uitable1,'data');
ud = get(handles.uitable1, 'UserData')
data(ud(1,1),:)=[];
set(handles.uitable1,'data',data);

% --- Executes on slider movement.

function slider5_Callback(hObject, eventdata, handles)
% hObject    handle to slider5 (see GCBO)
% eventdata  reserved - to be defined in a future version of MATLAB
% handles    structure with handles and user data (see GUIDATA)

a2= get(hObject,'Value');
axes(handles.axes2)
zoom(0.000000001);
zoom(a2);
% Hints: get(hObject,'Value') returns position of slider
%        get(hObject,'Min') and get(hObject,'Max') to determine range
of slider
% --- Executes during object creation, after setting all properties.

function slider5_CreateFcn(hObject, eventdata, handles)
% hObject    handle to slider5 (see GCBO)
% eventdata  reserved - to be defined in a future version of MATLAB
% handles    empty - handles not created until after all CreateFcns
called

% Hint: slider controls usually have a light gray background.

if isequal(get(hObject,'BackgroundColor'),
get(0,'defaultUicontrolBackgroundColor'))
    set(hObject,'BackgroundColor',[.9 .9 .9]);
end
```

```
% --- Executes on button press in pushbutton7.

function pushbutton7_Callback(hObject, eventdata, handles)
% hObject    handle to pushbutton7 (see GCBO)
% eventdata  reserved - to be defined in a future version of MATLAB
% handles    structure with handles and user data (see GUIDATA)
midsize=str2num(get(handles.edit4,'string'));
b=get(handles.edit2,'string');
period=str2num(get(handles.edit5,'string'));
axes(handles.axes2)
x=floor(xlim);
y=floor(ylim);
start=[y(1)+1,y(2),x(1)+1,x(2)]

[tracked]=andreasgui2(handles,b,midsize,period,start);

b=strcat(b,filesep);
data=get(handles.uitable1,'data');
data=[data;mat2cell(b)
,false,num2cell(0),num2cell(0),num2cell(tracked(1,3)),num2cell(period)
,num2cell(0),num2cell(0),num2cell(0),num2cell(0),num2cell(0),num2cell(
0),num2cell(0),num2cell(0)];
set(handles.uitable1,'data',data)

%eval(['save ''' strcat(b,filesep,'aaa') ''''])

function edit7_Callback(hObject, eventdata, handles)
% hObject    handle to edit7 (see GCBO)
% eventdata  reserved - to be defined in a future version of MATLAB
% handles    structure with handles and user data (see GUIDATA)
% Hints: get(hObject,'String') returns contents of edit7 as text
%        str2double(get(hObject,'String')) returns contents of edit7
as a double
% --- Executes during object creation, after setting all properties.

function edit7_CreateFcn(hObject, eventdata, handles)
% hObject    handle to edit7 (see GCBO)
% eventdata  reserved - to be defined in a future version of MATLAB
% handles    empty - handles not created until after all CreateFcns
called
% Hint: edit controls usually have a white background on Windows.
%       See ISPC and COMPUTER.

if ispc && isequal(get(hObject,'BackgroundColor'),
get(0,'defaultUicontrolBackgroundColor'))
    set(hObject,'BackgroundColor','white');
end

% --- Executes on button press in pushbutton8.

function pushbutton8_Callback(hObject, eventdata, handles)
% hObject    handle to pushbutton8 (see GCBO)
% eventdata  reserved - to be defined in a future version of MATLAB
% handles    structure with handles and user data (see GUIDATA)
[matfile,path]=uigetfile('tracked.mat','Load tracking file');
if ~isempty(matfile)
```

```
    prevexp=load([path matfile]);
    data=get(handles.uitable1,'data');
    data=[data;mat2cell(path)
,false,num2cell(0.1),num2cell(30),num2cell(prevexp.tracked(1,3)),num2c
ell(prevexp.period),num2cell(0),num2cell(0),num2cell(0),num2cell(0),nu
m2cell(0),num2cell(0),num2cell(0)];
    set(handles.uitable1,'data',data);
end

% --- Executes on button press in pushbutton9.

function pushbutton9_Callback(hObject, eventdata, handles)
% hObject    handle to pushbutton9 (see GCBO)
% eventdata  reserved - to be defined in a future version of MATLAB
% handles    structure with handles and user data (see GUIDATA)

data=get(handles.uitable1,'data');
ud = get(handles.uitable1, 'UserData');
b=data(ud(1,1),1);

if(cell2mat(data(ud(1,1),7))==0)
    V=750;
    data(ud(1,1),7)=num2cell(V);
else
    V=cell2mat(data(ud(1,1),7));
end

if(cell2mat(data(ud(1,1),4))==0)
    freq=30;
    data(ud(1,1),4)=num2cell(freq);
else
    freq=cell2mat(data(ud(1,1),4));
end

r=cell2mat(data(ud(1,1),5));
T=cell2mat(data(ud(1,1),6));



if(cell2mat(data(ud(1,1),3))==0)
    scalepm=0.096;
    data(ud(1,1),4)=num2cell(scalepm);
else
    scalepm=cell2mat(data(ud(1,1),3));
end

[ang,vel,Q,radius,vel2,Q2,vel3,Q3] =
andreascompute2(handles,b,V,scalepm,r,freq,T)

data(ud(1,1),8)=num2cell(ang);
data(ud(1,1),9)=num2cell(vel);
data(ud(1,1),10)=num2cell(Q);
data(ud(1,1),11)=num2cell(vel2);
data(ud(1,1),12)=num2cell(Q2);
data(ud(1,1),13)=num2cell(vel3);
data(ud(1,1),14)=num2cell(Q3);
data(ud(1,1),5)=num2cell(radius);
set(handles.uitable1,'data',data);
```

```
% --- Executes on button press in pushbutton10.

function pushbutton10_Callback(hObject, eventdata, handles)
% hObject    handle to pushbutton10 (see GCBO)
% eventdata  reserved - to be defined in a future version of MATLAB
% handles    structure with handles and user data (see GUIDATA)

data=get(handles.uitable1,'data');
axes(handles.axes4);
selected=find(cell2mat(data(:,2))==true);
save aaa;
plotRQ(handles,data(selected,:));
%plot(cell2mat(data(selected,5)),cell2mat(data(selected,10)),'bx');
% --- Executes on button press in pushbutton11.

function pushbutton11_Callback(hObject, eventdata, handles)
% hObject    handle to pushbutton11 (see GCBO)
% eventdata  reserved - to be defined in a future version of MATLAB
% handles    structure with handles and user data (see GUIDATA)

data=get(handles.uitable1,'data');
ud = get(handles.uitable1, 'UserData');
b=data(ud(1,1),1);
prevexp=load([cell2mat(b) 'tracked.mat']);
plot(prevexp.tracked(:,1),-prevexp.tracked(:,2));

% --- Executes on button press in pushbutton12.

function pushbutton12_Callback(hObject, eventdata, handles)
% hObject    handle to pushbutton12 (see GCBO)
% eventdata  reserved - to be defined in a future version of MATLAB
% handles    structure with handles and user data (see GUIDATA)
data=get(handles.uitable1,'data');
ud = get(handles.uitable1, 'UserData');
b=data(ud(1,1),1);
prevexp=load([cell2mat(b) 'tracked.mat']);
plot(prevexp.tracked(:,1:2));

% --- Executes on button press in pushbutton13.

function pushbutton13_Callback(hObject, eventdata, handles)
% hObject    handle to pushbutton13 (see GCBO)
% eventdata  reserved - to be defined in a future version of MATLAB
% handles    structure with handles and user data (see GUIDATA)

alldir=uigetdir('/media/FreeAgent GoFlex
Drive/Office/Documents/Documents/Work/MACH 4 JOINT WORK/New set up/Day
16/Mono');
if alldir~=0
    disp(['getting all the saved trackings in dir ' , alldir]);
    completed=subdir([alldir,filesep,'*tracked.mat']);
    save bbb;
    disp('done');
    for i=1:size(completed,1)
        load(completed(i).name);
        data=get(handles.uitable1,'data');
```

```
data=[data;mat2cell(completed(i).name(1:size(completed(i).name,2)-11))
,false,num2cell(0.1),num2cell(30),num2cell(tracked(1,3)),num2cell(peri
od),num2cell(0),num2cell(0),num2cell(0),num2cell(0),num2cell(0),num2ce
ll(0),num2cell(0),num2cell(0)];
        set(handles.uitable1,'data',data);
    end
end

% --- Executes during object creation, after setting all properties.

function pushbutton13_CreateFcn(hObject, eventdata, handles)
% hObject    handle to pushbutton13 (see GCBO)
% eventdata  reserved - to be defined in a future version of MATLAB
% handles    empty - handles not created until after all CreateFcns
called
% --- Executes on button press in pushbutton14.

function pushbutton14_Callback(hObject, eventdata, handles)
% hObject    handle to pushbutton14 (see GCBO)
% eventdata  reserved - to be defined in a future version of MATLAB
% handles    structure with handles and user data (see GUIDATA)

data=get(handles.uitable1,'data');
save('table.mat','data');
% --- Executes on button press in pushbutton15.

function pushbutton15_Callback(hObject, eventdata, handles)
% hObject    handle to pushbutton15 (see GCBO)
% eventdata  reserved - to be defined in a future version of MATLAB
% handles    structure with handles and user data (see GUIDATA)

load table.mat
set(handles.uitable1,'data',data);

% --- Executes on button press in pushbutton17.

function pushbutton17_Callback(hObject, eventdata, handles)
% hObject    handle to pushbutton17 (see GCBO)
% eventdata  reserved - to be defined in a future version of MATLAB
% handles    structure with handles and user data (see GUIDATA)

data=get(handles.uitable1,'data');
axes(handles.axes4);
selected=find(cell2mat(data(:,2))==true);
save aaa;
plotRQ2(handles,data(selected,:));
%plot(cell2mat(data(selected,5)),cell2mat(data(selected,10)),'bx');
% --- Executes on button press in pushbutton18.

function pushbutton18_Callback(hObject, eventdata, handles)
% hObject    handle to pushbutton18 (see GCBO)
% eventdata  reserved - to be defined in a future version of MATLAB
% handles    structure with handles and user data (see GUIDATA)

data=get(handles.uitable1,'data');
ud = get(handles.uitable1, 'UserData');
b=data(ud(1,1),1);
```

```
b=cell2mat(b);
smoothop(handles,b)
```

9.2 Appendix B

andreasgui2.m function

```
function [tracked] = andreasgui2(handles,exppath,radius,period,start)

time1 = cputime;
start

global filelist;
prm_LM_LoBndRa=0.1;
fltr4accum = [1 2 11; 12 16 12; 1 12 1];
fltr4accum = fltr4accum / sum(fltr4accum(:));
i=1
nr=1;

rawimg=imread(cell2mat(strcat(exppath,filesep,filelist(nr))));
totsize=size(rawimg);
if ~isempty(start)
rawimg=rawimg(start(1):start(2),start(3):start(4));
end
eps=0;
circen=[];
while (isempty(circen) || size(circen,1)>1)
    circen=[];
    [accum, circen, cirrad] = CircularHough_Grd(rawimg,[radius-
eps,radius+eps], 10, 4, 0.8, fltr4accum);
    eps=eps+1;
    disp('.')
    if eps>4
        [r,c] = find(accum==max(accum(:)));
        circen=[c,r];
        cirrad=radius;
    end
end
tracked(1,:)=[circen(1,:)+[start(3),start(1)],cirrad(1)];

for nr=2:period:size(filelist,1)
        disp([num2str(ceil(nr/size(filelist,1)*100)) ' % , '
num2str(cputime-time1) ' secs']);

    time1 = cputime;
    i=i+1;
    rawimg=imread(cell2mat(strcat(exppath,filesep,filelist(nr))));

    eps=0;
    circen=[];

    areaofi=[tracked(i-1,2)-200,tracked(i-1,2)+200;tracked(i-1,1)-
300,tracked(i-1,1)+300];
    areaofi=ceil(areaofi);
%     areaofi(find(areaofi<1))=1;
%     areaofi(find(areaofi>size(rawimg,2)))=size(rawimg,2);
%     areaofi(find(areaofi>size(rawimg,1)))=size(rawimg,1);

if areaofi(1,1)<1 areaofi(1,:)=[1,400]; end
```

```
        if areaofi(2,1)<1 areaofi(2,:)=[1,600]; end
        if areaofi(1,2)>size(rawimg,1) areaofi(1,:)=[size(rawimg,1)-
400,size(rawimg,1)]; end
        if areaofi(2,2)>size(rawimg,2) areaofi(2,:)=[size(rawimg,2)-
600,size(rawimg,2)]; end

rawimg=rawimg(areaofi(1,1):areaofi(1,2),areaofi(2,1):areaofi(2,2));

    while (isempty(circen) || size(circen,1)>1)
        circen=[];
        [accum, circen, cirrad] = CircularHough_Grd(rawimg,[radius-
eps,radius+eps], 10, 4, 0.8, fltr4accum);
        eps=eps+1;
        if eps>2
            [r,c] = find(accum==max(accum(:)));

[a,b]=min(sum([abs(circen(:,1:2)-repmat([c,r],size(circen,1),1))]'));

circen=circen(b,:);
cirrad=cirrad(b);

    %        circen=[c,r];
     %       cirrad=tracked(i-1,3);
        end
    end

    axes(handles.axes5);
    imshow(rawimg);
    hold on;
    DrawCircle(circen(1),circen(2),cirrad,32,'g-');
    %drawnow;

tracked(i,:)=[circen(1)+areaofi(2,1),circen(2)+areaofi(1,1),cirrad];
    if tracked(i,2)>0.9*totsize(1)
        break
    end
end
hold off;
axes(handles.axes4);
plot(tracked)
save aaa;

%put data in uitable

eval(['save ''' exppath filesep '''tracked period tracked']);
%fopen(fileID,'done.txt','a');
%fprintf(fileID,[
```

9.3 Appendix C

andreascompute2.m function

```
function [ang,vel,Q,radius,vel2,Q2,vel3,Q3] =
andreascompute2(handles,b,V,scalepm,r,freq,T)

file='tracked.mat'
if exist([cell2mat(b) 'tracked2.mat'])
       disp([]);
   reply = input('Tracked2 exists, to use press 2:  ','s');
   reply = str2num(reply)
   if reply == 2
       file='tracked2.mat'
   end
end
load([cell2mat(b) file])

scaler=1/(scalepm*10^6);
radius=mean(tracked(:,3));
r=radius*scaler;
s=6500e-6;
viscosity=0.10615;
rcyl=0.00325;
h=0.045;

% i=1;
% while( abs(tracked(i,1)-tracked(1,1)<20))
%     i=i+1;
% end
% start=i
%
% while(tracked(i,1)<0.95*max(tracked(:,1)) &&
tracked(i,1)>1.05*min(tracked(:,1)))
%     i=i+1;
% end
%
% finish=i

start = 2;
i=1;
while(tracked(i,1)<0.95*max(tracked(:,1)) &&
tracked(i,1)>1.05*min(tracked(:,1)))
    i=i+1;
end

finish=i

while((tracked(i,1)>0.95*max(tracked(:,1)) ||
tracked(i,1)<1.05*min(tracked(:,1)))&& (i<size(tracked,1)-1))
    i=i+1;
end

start2=i;
```

```
while((tracked(i,1)<0.95*max(tracked(:,1)) &&
tracked(i,1)>1.05*min(tracked(:,1)))&& (i<size(tracked,1)-1))
    i=i+1;
end
finish2=i;

while((tracked(i,1)>0.95*max(tracked(:,1)) ||
tracked(i,1)<1.05*min(tracked(:,1)))&& (i<size(tracked,1)-1))
    i=i+1;
end

start3=i;

while((tracked(i,1)<0.95*max(tracked(:,1)) &&
tracked(i,1)>1.05*min(tracked(:,1))) && (i<size(tracked,1)-1))
    i=i+1;
end

finish3=i;

vtx=scenes(handles,tracked,T,freq,start,finish);
vtx=vtx.*scaler

disp(['error in velocities:' num2str(std(vtx)/mean(vtx)*100) '%']);
vel=vtx(1); % Calculated fitting line to velocity
if abs(std(vtx(1:2))/mean(vtx(1:2))) > 0.10
   disp(['Terminal velocity might be wrong!']);
   reply = input('Choose 1) Velocity (green) 2) Position (fuchsia) 3)
Max(velocity) (cyan) :  ','s');
   reply = str2num(reply)

   if isempty(reply) || reply>3 || reply < 1
    reply=1
   end
   vel=vtx(reply);
end
Q=(6*pi*viscosity*vel*r*s)/V*(1+(2.4*r)/rcyl)*(1+(3.3*r)/h)

vtx2=scenes(handles,tracked,T,freq,start2,finish2);
vtx2=vtx2.*scaler

ang=0;

set(handles.edit7,'string',['Size in um
',num2str(mean(tracked(:,3))*scaler*10^6),'um'])

edit([cell2mat(b) '../Details.txt'])

vel2=vtx2(1); % Calculated fitting line to velocity
if abs(std(vtx2(1:2))/mean(vtx2(1:2))) > 0.10
   disp(['Terminal velocity might be wrong! -- second bit']);
   reply = input('Choose 1) Velocity (green) 2) Position (fuchsia) 3)
Max(velocity) (cyan) :  ','s');
   reply = str2num(reply)

   if isempty(reply) || reply>3 || reply < 1
```

```
    reply=1
   end
   vel2=vtx2(reply);
end

Q2=(6*pi*viscosity*vel2*r*s)/V*(1+(2.4*r)/rcyl)*(1+(3.3*r)/h)
vtx3=scenes(handles,tracked,T,freq,start3,finish3);
vtx3=vtx3.*scaler

ang=0;

set(handles.edit7,'string',['Size in um
',num2str(mean(tracked(:,3))*scaler*10^6),'um'])

edit([cell2mat(b) '../Details.txt'])

vel3=vtx3(1); % Calculated fitting line to velocity
if abs(std(vtx3(1:2))/mean(vtx3(1:2))) > 0.10
   disp(['Terminal velocity might be wrong! -- second bit']);
   reply = input('Choose 1) Velocity (green) 2) Position (fuchsia) 3)
Max(velocity) (cyan) :  ','s');
   reply = str2num(reply)

   if isempty(reply) || reply>3 || reply < 1
    reply=1
   end
   vel3=vtx3(reply);
end

Q3=(6*pi*viscosity*vel3*r*s)/V*(1+(2.4*r)/rcyl)*(1+(3.3*r)/h)

axes(handles.axes4);
hold off

axes(handles.axes5);
hold off

end
```

9.4 Appendix D

Experimental set-up

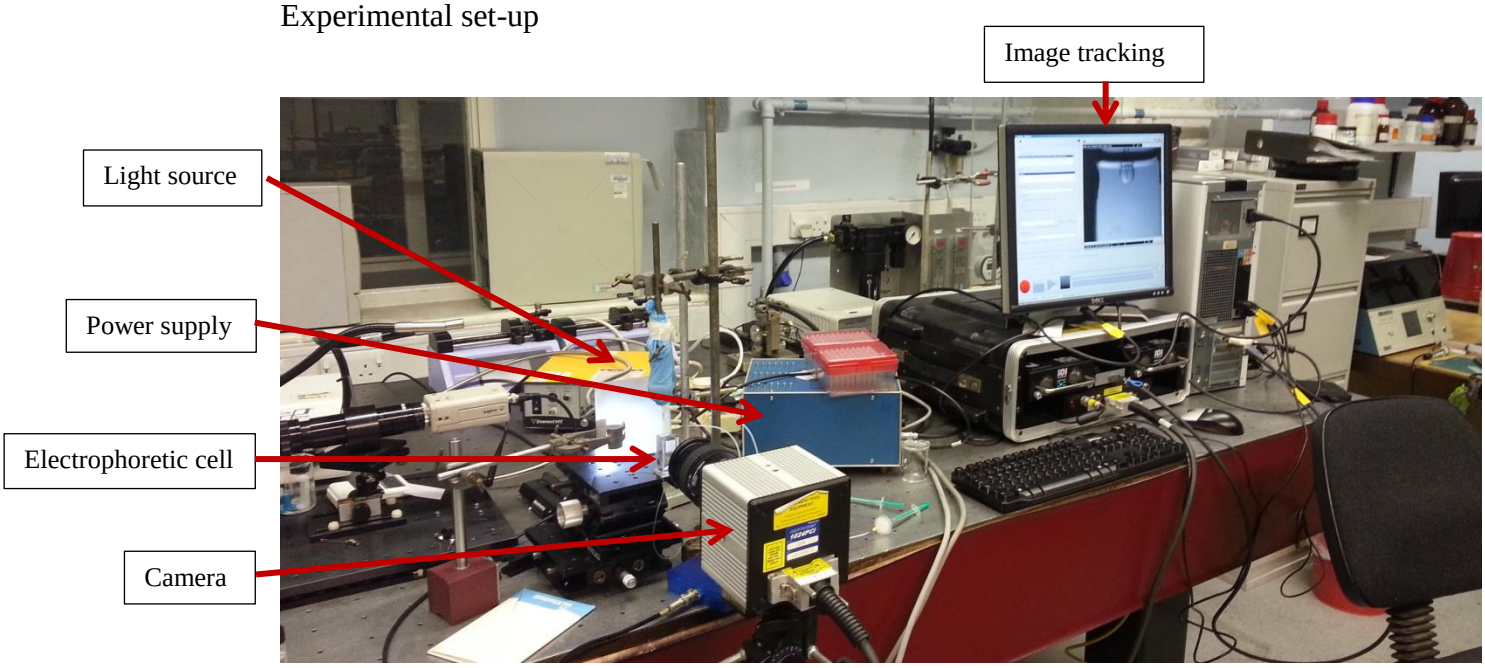

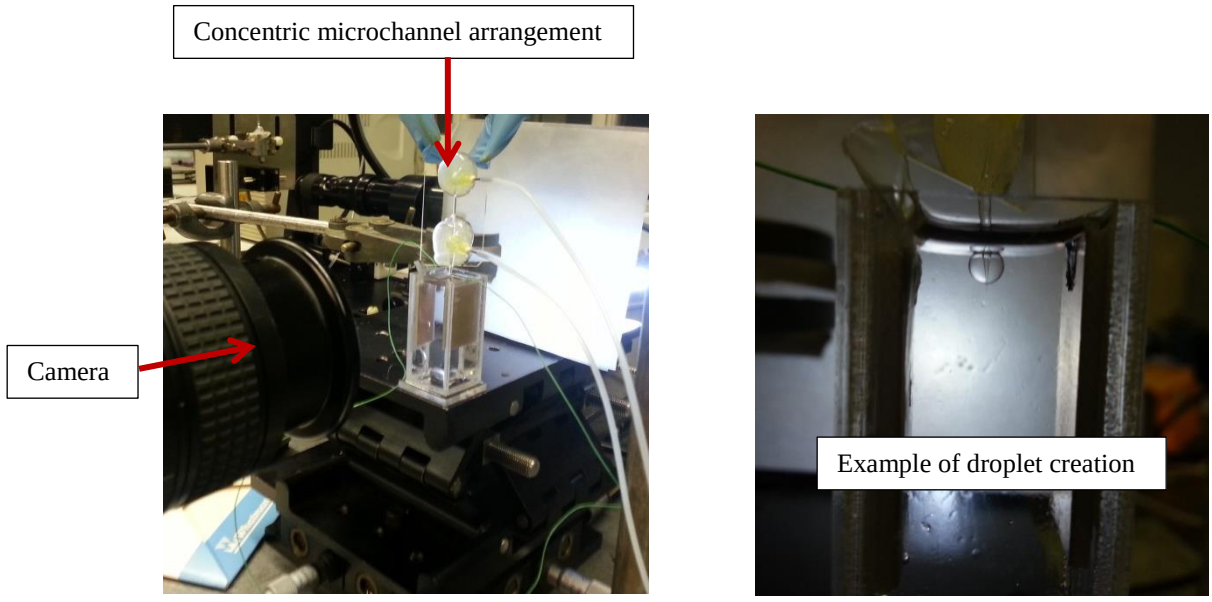

9.5 Appendix E

Block Diagram of the experimental set-up